REGULATORS OF STREAM ECOSYSTEM RECOVERY FROM DISTURBANCE

by

JUSTIN N MURDOCK

B.S., University of Kansas, 1998

M.S., Texas A&M University, 2002

AN ABSTRACT OF A DISSERTATION

submitted in partial fulfillment of the requirements for the degree

DOCTOR OF PHILOSOPHY

Division of Biology
College of Arts and Sciences

KANSAS STATE UNIVERSITY
Manhattan, Kansas

2008

ABSTRACT

Streams exist in a state of dynamic equilibrium with frequent floods and drought. The frequency and intensity of stream disturbances are projected to increase with greater water withdrawal for agriculture and biofuel production, watershed development, and altered climate. Changes in the hydrologic regime may alter stream ecosystems. I studied how stream communities return after disturbances and how nutrients, consumers, and substrata heterogeneity influence recovery trajectories. Large consumers were excluded from pools following a severe drought to assess how community structure and function returned in their absence. Large consumers reduced algal biomass, primary productivity, and nutrient uptake rates, and delayed macroinvertebrate recolonization. However, grazer effects were temporary and their influence weakened after five weeks. In a second experiment, I assessed the relative influence of grazer density and nutrient loadings on algal recovery from flood. Nutrients had a stronger effect on recovery than grazers, but the strength of each varied temporally. Grazer control decreased and nutrient control increased over time. A third experiment addressed the physical properties of stream substrata on algal development. The relationship among algal accumulation and substrata surface topography was assessed by growing algae on substrata with varying orientation and roughness. Total algal biomass decreased on surfaces with angles > 45 degrees, and peaked at an intermediate roughness (pit depth of ~17 μm). Rougher surfaces collected more tightly attached (grazer resistant) forms and less loosely attached (grazer susceptible) forms. Individual algal forms responded differently to grazing pressure, nutrient availability, and surface features. I developed a method using Fourier-transform infrared microspectroscopy to measure single-cell physiological responses in benthic algae. Nutrients and consumers were strong regulators of

ecosystem succession following disturbance, but nutrient influence was stronger. The influence of nutrients and consumers were context dependent, and changed over the course of recovery. Rougher surfaces increase algal growth and shifted algal assemblages to more grazer resistant forms, which may decrease the influence of large consumers on stream function. Altering the severity and frequency of disturbances can change the trajectory of stream recovery and ultimately change community composition and stream metabolic activity, which may alter ecosystem services such as water purification and recreation.

REGULATORS OF STREAM ECOSYSTEM RECOVERY FROM DISTURBANCE

by

JUSTIN N MURDOCK

B.S., University of Kansas, 1998

M.S., Texas A&M University, 2002

A DISSERTATION

submitted in partial fulfillment of the requirements for the degree

DOCTOR OF PHILOSOPHY

Division of Biology
College of Arts and Sciences

KANSAS STATE UNIVERSITY
Manhattan, Kansas

2008

Approved by:

Major Professor
Walter K. Dodds

ABSTRACT

Streams exist in a state of dynamic equilibrium with frequent floods and drought. The frequency and intensity of stream disturbances are projected to increase with greater water withdrawal for agriculture and biofuel production, watershed development, and altered climate. Changes in the hydrologic regime may alter stream ecosystems. I studied how stream communities return after disturbances and how nutrients, consumers, and substrata heterogeneity influence recovery trajectories. Large consumers were excluded from pools following a severe drought to assess how community structure and function returned in their absence. Large consumers reduced algal biomass, primary productivity, and nutrient uptake rates, and delayed macroinvertebrate recolonization. However, grazer effects were temporary and their influence weakened after five weeks. In a second experiment, I assessed the relative influence of grazer density and nutrient loadings on algal recovery from flood. Nutrients had a stronger effect on recovery than grazers, but the strength of each varied temporally. Grazer control decreased and nutrient control increased over time. A third experiment addressed the physical properties of stream substrata on algal development. The relationship among algal accumulation and substrata surface topography was assessed by growing algae on substrata with varying orientation and roughness. Total algal biomass decreased on surfaces with angles > 45 degrees, and peaked at an intermediate roughness (pit depth of ~17 μm). Rougher surfaces collected more tightly attached (grazer resistant) forms and less loosely attached (grazer susceptible) forms. Individual algal forms responded differently to grazing pressure, nutrient availability, and surface features. I developed a method using Fourier-transform infrared microspectroscopy to measure single-cell physiological responses in benthic algae. Nutrients and consumers were strong regulators of

ecosystem succession following disturbance, but nutrient influence was stronger. The influence of nutrients and consumers were context dependent, and changed over the course of recovery. Rougher surfaces increase algal growth and shifted algal assemblages to more grazer resistant forms, which may decrease the influence of large consumers on stream function. Altering the severity and frequency of disturbances can change the trajectory of stream recovery and ultimately change community composition and stream metabolic activity, which may alter ecosystem services such as water purification and recreation.

TABLE OF CONTENTS

LIST OF FIGURES

Chapter 1

Chapter 2

Chapter 3

Chapter 4

LIST OF TABLES

ACKNOWLEDGEMENTS

Although my name is the only one on the title page of this dissertation, the information within this document was the product of many people. I must first thank my wife Jamie for her support and encouragement during our time in Manhattan. Without her I would not have been able to pursue this endeavor, nor would I currently have three toddlers. Which brings up Abby, Peyton, and Camryn. They provide daily inspiration, reminding me of why I continue to work towards lessening our impact on the planet. I also thank them tremendously for letting me sleep through most nights during the final weeks leading up to the completion of this document.

I thank my advisor and mentor Dr. Walter Dodds for guiding me through these hectic years. His leadership has made me a better scientist, teacher, and person. It has been awesome to work with a person that has his knowledge, and the same passion for the small, green, and slimy. I also thank Dr. Keith Gido who spent countless hours helping me with experimental designs, sampling, and data analysis. His unique perspectives on fish and fatherhood have been truly enlightening. I thank my other committee members Dr. Craig Paukert and Dr. Stacy Hutchinson for guidance through the program and for greatly improving the quality of this dissertation, and Dr. Bimal Paul for chairing my dissertation defense committee. Dr. David Wetzel provided valuable insight and instruction with the infrared spectroscopy and was very generous with his time and the use of his laboratory, and Dr. Dan Boyle provided helpful assistance with the confocal microscope.

My friends Jon O'Brien, Kym Wilson, Jessica Eichmiller, Alyssa Standorf (Riley), Katie Bertrand, and all others who I shared time with here were instrumental in shaping my graduate experience (for the better), and I look forward to continuing our friendships in the future. Dolly Gudder provided helpful comments on several of the chapters, and kept Walter from getting too crazy around the lab. I thank Rosemary Ramundo for her abundant help that kept me from damaging the autoanalyzer. The LAB aquatic journal club provided an excellent environment for really getting ideas flowing.

Jennifer Nemec, Justin Bengtson, Tyler Kohler and Charles Krummins helped with sample collection and processing. This work would not have been possible without them. Funding for this research was provided by the Konza Prairie Long-Term Ecological Research Program, and the National Science Foundation Ecology Program (DEB-0416126).

INTRODUCTION

Streams in the Great Plains are often in a state of non-equilibrium due to frequent floods and droughts (Dodds et al 2004). Stream biota have evolved adaptations to these harsh conditions that allow a relatively quick response to these disturbances and an efficient reestablishment of structural and functional integrity (Lytle and Poff 2004). However, humans are further altering the stability of these streams through water withdrawal, dam construction, watershed development, and potentially through climate change. Concurrently, streams in the Great Plains streams are experiencing reduced species diversity, eutrophication, and increased sedimentation rates (Rabeni 1996, Dodds and Whiles 2004), which can further complicate the ability to predict how streams will respond to hydrologic alterations. To understand how these changes are affecting structure and function in an increasingly unstable system, it is necessary to understand the mechanisms that regulate the reorganization of stream communities after a disturbance.

ORGANISM RETURN AFTER DISTURBANCE

Stream responses to disturbances vary with type (e.g. flood or drought) and severity, but both act similarly to reduce organism abundance and function (e.g. primary productivity and nutrient retention) by resetting the successional process (Biggs 1996, Fritz and Dodds 2004). Stream recovery trajectories will depend on the timing and sequence of species return, and available resources. In this dissertation, the term 'recovery' is referring to a process where stream structure and function are retuning to a state that is similar to its pre-disturbance form in

both community composition and distribution. After a severe flood or drought in prairie streams, bacteria and algae typically recover within two to three weeks, macroinvertebrates within two weeks to two months and fish return is variable and can be within days to weeks (Dodds et al 2004). These return times can vary with intensity and timing of disturbance because each group has varying resistance and resilience to each disturbance type and its severity. For example, large mobile organisms such as fish can better deal with floods by occupying low velocity areas along the sides of channels, while algae, bacteria, and other substrata associate biota are washed downstream. Alternatively, smaller microbial and insect species may be able to resist drought better and survive in small isolated pools or wetted subsurface sediments, while larger fish may perish.

The reorganizational process produces rapidly changing biotic and abiotic conditions during recovery due to increased complexity. This can quickly change nutrient availability, producer and consumer biomass, and increase species interactions. One of the main hypotheses relating disturbance to community structure, the dynamic equilibrium model (Huston 1979), suggests that species interactions during a disturbance should differ from steady state conditions because the influence of interactions depends on environmental conditions. As stream conditions change, it is likely that the relative influence of resource limitations or the effect of one functional group on another will also change.

BIOTIC AND ABIOTIC RELATIONSHIPS

Benthic algae are the major autotrophs in prairie streams as they greatly influence stream primary production and nutrient cycling, and are central to energy transfer to higher trophic levels. Thus algal assemblages will have a major effect on the recovery of stream structure and

function. Hundreds of studies (see reviews by Feminella and Hawkins 1995, Hillebrand 2002, Lies and Hillebrand 2004, Gruner et al 2008) have investigated which ecosystem components regulate the growth of stream algae. There is strong evidence that both top down (e.g. removal and consumption) and bottom up (e.g. growth-required resources) effects can regulate algal accumulation and composition during conditions of stable hydrology. The two specific factors that have the strongest influence are nutrient availability that produces positive growth, and grazer consumption/removal, which typically produces negative accumulation. However, high variation among studies in streams suggests that the relative strengths of each of these factors are context dependent, and can vary with nutrient enrichment and grazer density (e.g., Mullholand et al. 1991, DeAngelis 1992, Vanni 2002, Power et al. 2008). Additionally, interactions between these factors have produced positive algal growth. Therefore it is difficult to extrapolate the findings observed during steady state conditions to the non-equilibrium conditions associated with stream recovery.

Adding complexity to the chemical and biological control of benthic algal development are the physical properties of the substratum. Stream substratum characteristics increase habitat complexity and alter algal development by changing the influence of nutrients, grazers, and floods (Dudley and D'Antonio 1991, Burkholder 1996, Bergey 2005). Kings Creek substrata was composed of mainly irregularly shaped limestone cobbles and pebbles that produces a three dimensional matrix of flat and angled surfaces that varied light and water flow paths. Superimposed on these rocks was variation in surface roughness, the geomorphic scale most directly related to microorganisms such as algae. For example, pits and crevices in rocks can provided refuge from grazing and flood scour (Bergey and Weaver 2004), but living in pits may

reduce nutrient and light availability by increasing molecular diffusion distances (Vogel 1994) and potential microtopgraphy shading.

The major questions addressed in this dissertation are 1) what regulates the development of stream structure and function following a disturbance, and 2) what is the temporal variation in the influence of each driver during recovery. These questions were addressed by studying the relationships among nutrient availability, primary producers, primary consumers, and time since disturbance. In chapter one I studied the effects of large consumers on stream recovery following drought in a prairie stream. I also isolated the effect of an abundant vertebrate grazer (a grazing minnow, *Phoxinus erthrogaster*) during drought recovery in large outdoor mesocosms. In chapter two I studied nutrient and grazer regulation of algal development and their interactions after a simulated flood in large mesocosms. I further investigated the conditions needed for grazers to stimulate algal growth by modeling the observed relationships. Chapter three looked at the relationship among benthic algae development and substrata topography. I used tiles placed at varying orientations in a stream to address whole-substratum scale variability in algal accumulation. Confocal laser scanning microscopy was used to image and measure substrata microtopography, and to relate surface properties to algal growth and potential light availability. Findings from these chapters led to realization that species specific algal physiological responses to changes in nutrients, grazing and topography will greatly help to predict algal assemblage succession during recovery. However current methodology limited this type of analysis to whole assemblage scales. Chapter four describes a new method to image and measure nutrient content, as well as the gradual incorporation of nitrogen, into single benthic algal cells using Fourier-transform infrared microspectroscopy.

CHAPTER 1 - Large grazers alter recovery trajectory of prairie stream ecosystem structure and function following drought

Justin N. Murdock, Keith B. Gido, Walter K. Dodds, Katie N. Bertrand, and Matt R. Whiles

ABSTRACT

Aquatic grazers can influence stream structure and function, but this influence is hard to predict in non-equilibrium environments. We studied the temporal influence of large grazers on recovery after a nine-month drought in a prairie stream using grazer exclosure cages. Additionally, large outdoor mesocosms were used to isolate the effect of grazing fish. In the stream, large grazers significantly reduced algal and macroinvertebrate biomass, primary productivity, and nutrient uptake early in recovery. However, grazer influence was transient, as it was strongest during the first 4 to 5 weeks after flow returned and decreased thereafter. Following re-wetting, large grazers first limited growth of desiccation-resistant green filamentous algal growth that otherwise dominated recovering algal assemblages. Grazers later reduced macroinvertebrate colonization upon their return. When stream conditions changed and heavy filament growth was no longer supported, large grazers only decreased macroinvertebrate biomass. By reducing filamentous algal accumulation, grazers substantially altered stream function; benthic gross primary productivity was 45% higher, and nutrient uptake 116% higher when filamentous algae dominated. Similar to field experiments, grazing fish in mesocosms reduced macroinvertebrate colonization, but fish had little effect on algal biomass. Lower fish densities and a less complex grazing community likely influenced the weaker fish effect in mesocosms. However, large grazers did not change the species that colonized grazed areas, but altered the proportion of algal and invertebrate colonizers. We demonstrate that ecosystem structure and function in non-equilibrium systems that are experiencing relatively rapid changes in abiotic and biotic conditions can be regulated by single consumer or producer taxa.

INTRODUCTION

Freshwater grazers such as fish and crayfish can shape stream ecosystem structure and function (Power 1988, Gelwick and Mathews 1992, Evans-White et al. 2001, Flecker et al. 2002). In streams, large grazers commonly reduce algal biomass and shift composition from loosely attached forms such as stalked diatoms and filamentous green algae, to smaller, adnate forms such as pennate diatoms and smaller green algae and cyanobacteria (Pringle and Hamazaki 1998). Grazing of producer biomass can decrease stream productivity and nutrient retention (Whiles et al. 2006, McIntyre et al. 2007). Grazer-algae relationships are well-studied in stream ecology but mainly within periods of relatively stable flow (Feminilla and Hawkins 1995, Stanley et al. 2004) and not following a disturbance such as drought, which is common in streams.

Grazers in streams live in non-equilibrium environments with floods and droughts which cause rapid changes in resource availability and competition. Following disturbances, grazer influence on benthic development should change as stream conditions change. Grazer influence on benthic algae typically depends on nutrient availability (Biggs et al. 1998, Roll et al. 2005), periphyton physical structure and species composition (Steinman 1996), and interactions with other grazers (Vaughn et al. 1993). All of these variables are rapidly shifting during recovery from disturbance as primary producers, macroinvertebrates, and larger grazers recolonize the disturbed area.

Prairie streams are naturally unstable systems (Dodds et al. 2004) and both abiotic and biotic interactions can shape stream communities (Poff and Ward 1989, Murdock et al. 2004, Lytle and Poff 2004, Biggs et al. 2005). Prairie stream biota evolved in conditions of alternating desiccation and inundation. Our understanding of structural and functional reorganization of

streams after drought is less developed than that after flooding, with most studies focusing on the recovery of a specific group, rather than community recovery patterns. Algal biomass typically recovers quickly, between 2 and 4 weeks (Dodds et al. 1996, Peterson and Boulton 1999, Ledger and Hildrew 2001, Robson and Matthews 2004), and metabolic activity of dry biofilms can restart within 3 hours after re-wetting in an intermittent Mediterranean stream (Romani and Sabater 1997) and 10 minutes in a cyanobacterial mat in a polar stream (Hawes et al 1992). Macroinvertebrate recovery is more variable, with most prairie-stream taxa returning within 1-2 weeks, and densities returning to pre-drought levels within 2-10 weeks (Miller and Golladay 1996, Boulton 2003, Fritz and Dodds 2004, Fowler 2004). Fish can arrive within days after flow returns (Magoulick and Kobza 2003, Matthews and Marsh-Matthews 2003). Variations in recovery time for each group greatly depend on drought duration and frequency, distance from refugia, and dispersal and reproductive potential of recolonizing taxa.

Hydrologic regimes of prairie streams are currently threatened by increasing water withdrawal for agricultural needs and biofuel production (de Fraiture et al. 2008, Natural Resource Council 2008), with future instability predicted due to changing precipitation patterns driven by global climate change that could increase the severity of droughts and floods (Groisman et al. 1999, Easterling et al. 2000). Hydrologic changes may accentuate biological effects during disturbance recovery by altering species return patterns, eliminating certain functional feeding groups, or further changing resource availability at the onset of the recovery process (Lake 2003). It is not clear how changes in disturbance frequency and intensity will alter species interactions such as grazing in systems that are already dominated by non-equilibrium conditions because relatively little is known about stream community development and species interactions following drought to provide a baseline for gauging future changes.

Our goal was to provide a multi-trophic level assessment of a dominant consumer group (large bodied grazers such as fish and crayfish), during recovery from complete channel drying. We assessed the impact of these herbivores during the structural and functional recovery of the benthic community with a grazer exclusion experiment in a prairie stream following re-wetting, and isolated the impact of grazing fish in large outdoor mesocosms to understand when and how large grazers alter post disturbance succession. We hypothesized that large grazers would alter benthic structure and function most towards the early to mid recovery when the grazer to algal biomass ratio is greatest, and before grazing-resistant species dominated algal assemblages. We also predicted that the abiotic effects of drying, rather than biotic effects of grazers, would dominate benthic recovery trajectories because early succession species that would likely dominate the colonizer pool would be able to adequately recolonize grazed areas fast enough to avoid total displacement.

METHODS

Kings Creek Field Experiments

Kings Creek is an intermittent prairie stream located on the Konza Prairie Biological Station (KPBS) in the Flint Hills region of northeastern Kansas, USA (see Gray and Dodds 1998 for further description). In March, 2006, during a nine month period with no surface flow, two exclosure cages were constructed in each of 4 consecutive pools in an intermittent reach. Each exclosure had a closed side and a control side that was open on the downstream end (Figure 1-1). Pools had an average surface area of ~74 m^2 and average depth of ~0.6 m during the experiment. The nearest upstream permanent pool of surface water was roughly 3.5 km away, and the nearest

downstream pool was ~100 m away. Cages were made of 5 mm mesh hardware cloth secured to steel poles, and buried 20 cm into the streambed. Twenty-one plastic mesh baskets (10cm x 10cm x 10cm) filled with dried rocks from the stream channel were placed in each half of an exclosure, and buried so basket tops were flush with the stream bottom. Debris that collected on the upstream mesh was removed as needed to maintain a consistent flow through the cage.

On 29-30 April, 2006, after nine months of a dry channel, rainfall recharged groundwater that gradually reintroduced surface flow. Continuous stream discharge measurements were collected from USGS station #06879650 located approximately 0.5 km above the study site. Baskets from exclusion and control sides of each enclosure were sampled during weeks 1 through 5, 7, and 9 after channel re-wetting. Water nutrient concentrations [total nitrogen (TN), total phosphorus (TP), nitrate (NO_3^-), and soluble reactive phosphorus (SRP)] were sampled from each pool during basket collection.

After the week 4 sampling, one enclosure from each pool was reversed (the open half was closed off and the closed half was opened) to assess the scenarios grazers returning after the benthic community has already developed, and that of grazers leaving after influencing benthic development. This created 4 treatments from week 5 through 9; always grazed, always ungrazed, grazed to ungrazed, and ungrazed to grazed.

Population densities of large grazers (fish, crayfish, and tadpoles) were estimated in the study pools during weeks 3 and 9. Single-pass electrofishing was used on week 3 to minimize substrata disturbance in the pools. Three-pass depletion sampling was used to estimate population densities on week 9 following the final sampling. Population densities from single-pass collections in week 3 were extrapolated based on a previous study in Kings Creek that compared catch rates of fish from a single pass to population estimates from three-pass depletion

sampling (Bertrand et al. 2006). Individual lengths were measured and converted to dry-mass (g; hereafter referred to as DM) using equations developed by Kaufman and Byers (1972) for fish, and Benke et al. (1999) for crayfish. Tadpole biomass was estimated from length-mass relationships developed following methods of Benke et al. (1999). Additionally, the small, shallow pools and clear water allowed rough visual estimates of fish from the bank. Estimates were made each week to verify fish presence or absence during periods between large consumer samplings.

Function variables

Benthic metabolism and nutrient uptake potential were measured from rock baskets in recirculating chambers. Three baskets were randomly selected from the open and closed side of each exclosure and returned to the laboratory in moist, sealed plastic containers within 2 hours of collection. Care was taken to minimally disturb the baskets during collection and transport. Baskets were analyzed for benthic metabolism and ammonia (NH_4^+) uptake rates in 22L recirculating chambers (Dodds and Brock 1998) using stream water collected from the study reach and kept at ambient stream temperature. Baskets from each exclosure half were sealed in an airtight chamber with a YSI dissolved oxygen (O_2) probe (Yellow Springs Instruments, Inc., Yellow Springs, OH), and water was circulated at a velocity of ~10 cm s^{-1}, which was similar to stream velocities. Light was excluded from the chambers and respiration (R) was measured as the decline in O_2 over 1.5 hours. Chambers were then exposed to fluorescent lights (approximately 300 μmol quanta m^{-2} s^{-1} PAR) and O_2 was monitored for another 1.5 hours (Wilson 2005). R and net primary production (NPP) rates were calculated as the slope of the change of O_2 concentration over time per the total area of the openings of the three baskets (300

cm^2) and adjusted to mg O_2 m^{-2} hr^{-1}. Gross primary production (GPP) was calculated as NPP + R.

Kings Creek is a low nutrient stream and commonly co-limited by nitrogen (N) and phosphorus (P) (Tank and Dodds 2003). Therefore ammonium (NH_4^+) was used to estimate maximum nutrient uptake rates. Ammonium uptake rates were measured directly following metabolism measurements. An NH_4^+ spike was added to raise the water concentration by approximately 40 µg L^{-1} and filtered water samples were taken at 0, 15, 30, 45, 60, and 90, minutes to monitor the decline in NH_4^+ over time. Samples were analyzed on an OI Analytical Flow Solution IV autoanalyzer using the indophenol blue method (APHA 1998). Ammonium uptake rates were calculated from the slope of the natural log transformed NH_4^+ concentration versus time and adjusted to µg NH_4^+ m^{-2} s^{-1} (Dodds et al. 2002, O'Brien and Dodds 2008).

Structure variables

Following chamber measurements, one of the three baskets was randomly selected to measure benthic algal biomass. All rocks from one basket were placed in an autoclavable bag and submerged in 95% EtOH at 78˚C for 5 minutes, extracted in the dark for 12 hours (Sartory and Grobelaar 1984), and chlorophyll *a* measured on a Turner model 112 fluorometer with a filter set and lamp that does not allow interference from phaeophytin (Welshmeyer 1995). Algae from three rocks from a second basket were brushed into a beaker and homogenized. A 20 mL subsample was preserved with formalin for algal identification. A minimum of 300 cells were counted for each sample and cells were placed into one of nine functional groups; diatoms (single cell pennate, chain forming pennate, single cell centric, chain forming centric), cyanobacteria (filamentous or coccoid), and green (filamentous, single cell, or colonial). Dominant algal cells were identified to genus. Rocks from the third basket were rinsed in a 250

μm mesh sieve. Macroinvertebrates (non-crayfish) in baskets were preserved with formalin, identified to the family level, and assigned functional groups based on Merritt et al. (2007). Algal filament lengths were measured inside exclosures at weeks 4 and 9 by measuring the average filament length at 5 random points in each of 3 transects within each cage. Algal community composition was assessed for weeks 1, 3, 5, and 9, and macroinvertebrate composition was assessed at weeks 3, 5, and 9.

Mesocosm Experiment

Grazing fish were the dominant large consumer during the first two weeks. Eight large outdoor mesocosms located approximately 200 m from Kings Creek were used to isolate the effect of the most abundant fish, *Phoxinus erythrogaster* (southern redbelly dace). Each mesocosm consisted of a 2.54 m^2 pool connected to a 0.84 m^2 riffle. The basic design of these streams is presented in Matthews et al. (2006). Spring water was continuously added to each stream at a rate of approximately 10 L hr^{-1} to offset evaporation losses and provide some nutrient input. Inflowing nutrient concentrations were low (total N 133, total P 2.85 μg L^{-1}). Water was recirculated with an electric motor creating a discharge of 4-6 L s^{-1}, and riffle current velocity of 6-8 cm $s^{-1.}$ Substrata were a mixture of native limestone pebble, gravel, and fine sediment and similar in size and texture to substrata in Kings Creek.

Streams were filled and circulation started two months prior to drying. Algae and aquatic insects emerging from nearby Kings Creek readily colonized these systems. Additionally an experiment immediately preceding this one inoculated all the mesocosms with aliquots of a benthic slurry from Kings Creek. On 20 June 2006, streams were drained and completely dried with no hyporheic refugia. Rock substrata were taken from each pool and

riffle, homogenized, and redistributed to each stream to evenly distribute desiccation resistant taxa. Following a two week drying period, streams were refilled on 4-5 July 2006.

Phoxinus erythrogaster were stocked in four streams at a density of 31 individuals per stream (~9 m^{-2}; ~4.25 g DM m^{-2} , ~9g wet mass m^{-2}), matching typical densities of nearby Kings Creek (Franssen et al. 2006). Dead fish were immediately replaced to maintain initial densities. The remaining four streams served as the fishless control treatment. Streams were sampled on day 6 and then every 12 days for 9 weeks for the same response variables measured in Kings Creek.

Functional response

Whole stream GPP, net ecosystem production (NEP), and community respiration (CR) were estimated by measuring diurnal changes in O_2 concentrations with YSI 600XLM sondes. A single sonde and the open-system single-station approach (Owens 1974) were used for each stream. Aeration was estimated in three streams by the propane injection method (Mulholland et al. 2001) and assumed to be the same across all stream units. Mean daily solar irradiance during GPP measurements were taken from the Konza meteorological station located approximately 0.5 km from the mesocosm.

Nutrient uptake rates (as NH_4^+) were measured with a short-term NH_4^+ addition (Tank et al. 2006) in all streams simultaneously. A plastic flow diffuser was added to the bottom of the riffle to increase pool mixing. A solution containing 0.4 g of NH_4Cl was added at the top of the riffle. Water samples were collected every 15 minutes for 1.5 hours, filtered, and frozen within 2 hours. Photosynthetically active radiation (PAR) was measured during each release and uptake rates were adjusted for ambient light intensity. Uptake rates were calculated as in the chamber method in the field experiment.

Structural response

Algal biomass (mg chlorophyll *a* m^{-2}) was measured for each mesocosm riffle (3 random rocks) and pool (5 random rocks). Rocks were placed on ice and frozen within 4 hours of collection. Chlorophyll *a* was extracted as described earlier. Rock area was measured by tracing the top surface of the rock on paper, digitizing the image, and determining the area of the tracing with SigmaScan 5 (Systat Software Inc. San Jose, CA, USA). Algal filament length was measured at nine points in each riffle; three points along three equally-spaced transects oriented perpendicular to flow and measured at five points in the pool; four around the outer perimeter and one in the center.

Algae and macroinvertebrates were collected with a core sampler that consisted of a 0.018 m^2 tin pipe with an electric pump (0.1 L s^{-1}) attached through the side. Substrata inside the corer were agitated by hand while nine L of water were collected in a bucket. Bucket contents were homogenized and a 20 mL subsample was collected for algal identification and functional group proportions. The remaining material was passed through a 250-µm mesh sieve to collect macroinvertebrates. All samples were preserved with 10% formalin. One core sample was taken from the riffle and one from the pool in each mesocosm. Algal and macroinvertebrate functional group composition were assessed on days 18 and 42.

Algal desiccation resistance was assessed to determine the species pool available upon re-wetting. The day prior to re-wetting, approximately 10 rocks containing dried biofilm were taken from each riffle, placed in a single bucket, and mixed. Eight rocks were placed into each of three autoclaved one L Erlenmeyer flasks, filled with 500 ml of deionized water, capped with cotton, and placed under a fluorescent light (300 um quanta m^{-2} s^{-1} PAR). As a control, additional rocks from the bucket were sterilized by autoclaving for 1 hour and put into 3 flasks

and identical conditions. After 3 weeks algae were brushed into a sample bottle, preserved with formalin and later identified to genus.

DATA ANALYSIS

Kings Creek Field Experiments

A repeated measures analysis of variance (ANOVA), blocked by cage and pool, was used to test treatment differences and treatment by time interactions among response variables (chlorophyll *a*, macroinvertebrate biomass, area and biomass specific GPP, R, and NH_4^+ uptake). We used the proc mixed command in SAS (version 9; SAS Institute Inc., Cary NC, USA) to model the covariance structure of untransformed data, and used AICc (Akaike information criterion adjusted for small sample sizes) values to pick the covariate matrix model that best fit the data (Milliken and Johnson 2002). A priori alpha levels were set = 0.05.

Reversing half the cages created four treatments: always closed, always open, closed to open, and open to closed. A repeated measures ANOVA over weeks 5–9 with *a priori* planned contrasts (comparing closed reversed to open to permanently closed, and comparing open reversed to closed to permanently open) was used to compare response variable differences in these two scenarios.

Algal functional group proportions (arcsine square root transformations) and macroinvertebrate functional group biomass were assessed with analysis of similarity (ANOSIM) of Bray-Curtis similarity matrices. Significant ANOSIM trends were further tested with repeated measures ANOVA on individual algal and macroinvertebrate functional groups. Algal filament lengths at weeks 4 and 9 were tested with a two-way ANOVA with treatment and week as factors.

Mesocosm Experiments

Repeated measures ANOVA was used to detect treatment differences in response variables. Pool and riffle structural variables were analyzed separately. Area- and biomass-specific GPP were significantly correlated to mean daily solar irradiance measurements (r^2 =0.18, P<0.001 and r^2 =0.28, P<0.001 for area and biomass GPP respectively), therefore light was used as a covariate for these variables in the ANOVA. Repeated measures ANOVA was also used to test differences in individual algal and macroinvertebrate functional groups on days 18 and 42.

RESULTS

Kings Creek Field Experiments

Discharge peaked at 0.07 m^3 s^{-1} immediately following the drought, stabilized at 0.04 m^3 s^{-1} after 2 days, and then gradually decreased (Figure 1-2a). The resumption of discharge was not strong enough to be considered a flood and there was no major loss of organic matter from the streambed. Historic mean discharge (1979-2007) for the nearby upstream gauging station was 0.18 m^3 s^{-1} for May, and the mean consecutive flow was 24 weeks (SD 19) (USGS station #06879650). Channel flow continued in the study reach until week 9 when pools became disconnected. An initial pulse of nutrients occurred when flow returned, but dropped by 45 and 38% for TN and TP respectively by week 2 (Figure 1-2b). TN and TP gradually increased back to initial concentrations at week 5. Nitrate followed the same pattern as TN, while SRP steadily decreased by about half from week 1 to week 9. Total N:P ratios following channel re-wetting were < 16 suggesting N limitation.

Large grazer colonization

Large schools of fish were observed in all pools within 2 days after re-wetting, with maximum observed densities occurring during weeks 2 and 3 and few fish visible after week 5. Plains leopard frog (*Rana blairi*) tadpoles were observed in the downstream pool from day 2 through week 9. Crayfish (*Orconectes spp.*) were observed in open cages 9 days after re-wetting through week 9. Electrofishing fish samples at week 3 were dominated by southern redbelly dace (*Phoxinus erythrogaster*) and central stoneroller (*Campostoma anomalum*) (Table 1-1). Other fish species collected at this time included orangethroat darter (*Etheostoma spectabile*), a benthic invertivore, in three pools and creek chub (*Semotilus atromaculatus*), a water column/benthic omnivore, in the downstream pool. No grazing fish were collected during week 9 sampling. Tadpole biomass was four times greater during the week 9 sampling than during week 3 (Table 1-1). Crayfish biomass increased 12-fold in samples from week 3 through week 9 (Table 1-1).

Structural recovery

There was a significant time by grazer interaction effect on algal biomass (repeated measures ANOVA, P=0.028) (Figure 1-2c). Algal biomass increased faster in the ungrazed treatments during the first 5 weeks, acquiring 113% and 70% greater biomass in ungrazed treatments at weeks 2 (P=0.002) and 4 (P=0.017), respectively. Ungrazed biomass peaked during week 5 (227 mg chl m^{-2}), but biomass was 4 times more variable than the previous week, with algal filaments in visibly different stages of senescence. Ungrazed biomass dropped substantially by week 7 (no long filaments observed), and was not significantly different than the grazed treatment through week 9. Algal biomass in the grazed treatments steadily increased, peaking at week 9 at about half the maximum biomass of the ungrazed treatment.

Algal functional group showed a strong temporal successional pattern, with three distinct assemblages over time. Algal functional groups were significantly different at week 1, weeks 3 and 5, and week 9 (ANOSIM: R=0.40, P=0.001). Algal composition differed between grazed and ungrazed treatments (R=0.16, P=0.03), but functional group difference between treatments was most prominent at week 3 (R=0.53, P=0.006). During week 3, grazed substrata were 74% small, single cell (*Navicula* and *Nitzchia spp.*) and chain-forming pennate diatoms (*Meridon sp*), whereas ungrazed substrata were predominantly green filaments (*Ulothrix spp.* 50% of assemblage, Figure 1-3).

Green filament abundance changed with time (significant grazer by time interaction P=0.048). In the ungrazed areas, filament biomass was slowly replaced with pennate diatoms, and by week 5 was similar to grazed areas and dominated by diatoms. Diatoms had shifted from a small, adnate form, to mostly stalked (*Gomphonema sp.*), large (*Synedra* and *Pinnularia spp.*), and chain-forming cells (*Meridon* and *Fragilaria spp*). On week 9, filaments had increased in both treatments, but were now dominated by more grazing resistant forms (i.e., *Stigeoclonium* and the cyanobacterium *Oscillatoria sp.)*. Grazed substrata had a greater proportion of greens and cyanobacteria, but functional groups contained the same species in both treatments. Patterns of filament lengths matched algal counts.

Small macroinvertebrate grazers (non-crayfish) were not abundant until week 5. Assemblages differed temporally by week (ANOSIM, R=0.19, P=0.028), with a strong difference between grazed and ungrazed treatments in week 5 (R=0.73, P=0.001), but not in weeks 3 or 9. During week 5, collector-gather biomass (dominated by Chironomidae) was 6 times greater (repeated measures ANOVA post hoc comparisons, P=0.039), and total biomass was 4.8 times greater (P=0.067) in ungrazed treatments (Figure 1-4). By week 9, scrapers

(mainly *Stenonema spp.* mayflies) dominated invertebrate biomass, and there was no significant difference among treatments.

Functional recovery

GPP increased faster on ungrazed substrata, becoming 45% greater the grazed substrata by week 4 (P=0.034) (Figure 1-2d). However, in week 5, ungrazed GPP dropped 49% and was not significantly different from grazed substrata through week 9. Benthic respiration did not vary (Figure 1-2e), except for a sharp increase during week 2 where respiration was twice as high in the grazed treatment (P=0.078). NPP followed a similar trend as GPP with the ungrazed treatment significantly higher (repeated measures ANOVA) during weeks 2 (P=0.049) and 4 (P=0.044), but no difference from weeks 5 through 9. Biomass-specific productivity did not differ between treatments. Maximum ammonium uptake potential was 1.6 (P=0.015), 1.5 (P=0.006), and 2.2 (P=0.064) times greater on ungrazed substrata during weeks 2, 3, and 4 respectively, but uptake rates fell below those of the grazed substrata by week 5 (significant time by grazer interaction P=0.011) (Figure 1-2f).

Cage reversals

Reversing cages had the strongest impact on macroinvertebrates. Opening up a closed cage to large grazers temporarily decreased total macroinvertebrate biomass 87% at week 5, (2760 vs. 361 mg DM m^{-2}, P=0.042) compared to cages kept closed. This reduction was driven by a 91% decrease in collector-gatherer biomass (P=0.034). Scrapers colonized both of these treatments equally, leading to similar total biomass by week 9. Closing an open cage did not cause immediate changes, and macroinvertebrate assemblages were still similar to the open cages at week 5. By week 9 however, open cages that were closed had 37% more algal biomass

(P=0.018), 55% lower scraper abundance (P=0.034), and 44% higher R (P=0.025) than permanently open cages.

Mesocosm Experiment

Structure

Algal biomass was similar in grazed and ungrazed treatments in the pools or riffles (Figure 1-5a-c). Green filamentous algae dominated early assemblages in both treatments, averaging 84% of algal biomass. Filament length was 9.4 cm (230%) longer in the riffles of the grazed treatment (P=0.011, day 30), but fish had no effect on pool filament length. Maximum filament lengths occurred on day 18 in the pools (7.8 cm) and day 30 in the riffles (12.1 cm), and decreased through day 66. Filament senescence occurred between days 30 and 42, and similar to results from Kings Creek, chlorophyll slightly increased during this time.

Early assemblages in the mesocosms were dominated by desiccation-resilient species. In the laboratory re-wetting experiment, only green algae and cyanobacteria species (mostly filamentous forms) were observed but no living diatoms were found. According to this experiment, the green algal species pool for initial recovery was comprised of the green filaments *Ulothrix* sp., *Spirogyra sp.*, *Microspora sp*., *Cylindrocapa geminella*, and a green colonial coccoid algae. Desiccation-resilient cyanobacteria available to recolonize mesocosms were filamentous *Oscillatoria spp*., *Dichothrix sp.*, *Anabeana sp.*, *Nostoc sp.*, and the coccoid colonial *Aphanothece sp.*

Fish did not change algal assemblage composition at days 18 or 42. *Ulothrix sp.*, a green filamentous alga, became the dominant species after 1 week in both treatments and continued to dominate assemblages on day 18. Senescing *Ulothrix*, was replaced by shorter *Ulothrix*

filaments and *Spirogyra*. Diatoms (*Navicula* and *Synedra spp.*) and cyanobacteria (*Oscillatoria sp.*) rarely made up >10% of the total composition.

Ungrazed treatments had 129% more invertebrate biomass on days 18 and 55% more on day 42 (P=0.024) (Table 1-2). On day 18, biomass was predominantly Chironomidae (78%) in ungrazed treatments, and Chironomidae (42%) and Ostracoda (48%) in grazed treatments. By day 42 both treatments were co-dominated by Chironomidae and Ostracoda, with slight increases in libellulid dragonfly nymphs (predator), Cladocerans (collector-filterer), and snails and baetid mayflies (scrapers).

Function

Grazer effects on stream function were weak in mesocosms. Metabolic activity recovered quickly upon re-wetting. The highest rates of productivity and nutrient uptake occurred during the first week and decreased slightly with time. The main differences in metabolic activity occurred during filament senescence. GPP dropped 59% from day 30 to 42 in the grazed treatment (P<0.001, Figure 1-5d), but was only marginally reduced in the ungrazed treatment (23% reduction, P=0.082). GPP in grazed treatments was approximately half of ungrazed during this decline (P=0.03), but returned to previous rates by day 59. CR followed the same pattern; CR in grazed mesocosms increased 82% from day 30 to 42 (P=0.003) (Figure 1-5e), and was 46% greater than ungrazed treatment on day 42 (P=0.044). Biomass-specific productivity decreased over time, but was not different between treatments. There was no difference in NH_4^+ uptake between treatments. Uptake rates peaked within the first week after re-wetting in ungrazed and grazed treatments respectively (Figure 1-5f). Uptake rates declined by half on day 30 and stayed constant through day 66.

DISCUSSION

Drought recovery

Kings Creek Field Experiment

Large grazers in Kings Creek changed the successional trajectory of the benthic community during drought recovery and, as predicted, grazer influence was temporary. Grazers (fish and tadpoles) had an immediate impact upon their arrival, initiating a divergent trajectory on grazed surfaces that spanned from the beginning to mid recovery, all while benthic communities and water conditions were changing the fastest. Structurally, grazers decreased algal biomass, changed algal composition to more adnate forms, and slowed the recovery of macroinvertebrates. Functionally, grazers reduced GPP and lowered potential nutrient uptake rates. Minimal grazer influence was evident after week 5, when abiotic and biotic conditions stabilized. Significant time by grazer interactions for algal biomass, filament length, and NH_4^+ uptake provided further evidence that the degree and nature of grazer influences on both stream structure and function changed during the course of recovery (Figure 1-6). The effects of grazing during drought recovery observed in Kings Creek are consistent with reported fish effects noted during baseflow conditions (Power 1990, Flecker 1992, Winemiller et al. 2006, Bertrand and Gido 2007), and after floods in streams (Gelwick and Matthews 1992, Pringle and Hamazaki 1997, Bertrand 2007). However, this study shows that the influence of these grazers on structural and functional recovery patterns can be transient and change as biotic and abiotic stream conditions change.

Treatment differences were driven by increased filamentous and loosely attached algae in ungrazed cages, and differences were mediated by the death and displacement of these filaments. Filament senescence coincided with a relatively abrupt change in algal composition and GPP

after week 5. In climax assemblages, green filament-dominated assemblages typically have greater productivity than diatom-dominated assemblages (Steinman et al. 1992, Sabater et al. 2002). However, during drought recovery, GPP (and algal biomass) increased during the switch from filaments to large diatoms in the ungrazed areas. Since diatoms were growing on top of senescing filaments, all loosely attached biomass was lost when filaments detached, and a precipitous drop in productivity followed. After the loss of the loosely attached overstory, no significant algal structural or functional differences in treatments were apparent through week 9. A temporally similar convergent response was found after drying in an intermittent Australian stream where algal communities on rocks that were either initially scrubbed of dry biofilm, or that contained an undisturbed dried biofilm, became similar six weeks after re-wetting (Robson and Matthews 2004).

Recovery patterns of non-crayfish benthic macroinvertebrates in Kings Creek were similar to those in an Oklahoma intermittent stream (Miller and Golladay 1996) and a New Zealand river (Fowler 2004) following re-wetting, with a distinct temporal sequence of early colonization by collector-gathers (mainly chironomids) and scrapers (mainly mayflies) dominant in late-succession communities. In Kings Creek, chironomid re-colonization was slowed in grazed areas by two weeks. Reduced chironomid colonization in grazed areas may have been related to ingestion of chironomids by some of the larger omniovores that feed on invertebrates (e.g., crayfish, stonerollers), displacement by bioturbation, or reduced emigration into grazed areas. Higher macroinvertebrate biomass in ungrazed areas suggests grazers may have restricted dominant macroinvertebrate colonizers to less preferred habitats within a pool. Gresens and Lowe (1994) found chironomids preferred areas similar to our grazed areas (i.e. with lower chlorophyll *a* and algal biovolume).

Consumer groups appeared to have an additive effect on removing algal biomass. For example, grazing fish were the first to arrive and slowed algal accumulation relative to the ungrazed treatments, but could not completely stop accumulation (Figure 1-6). When crayfish and fish were present algal accumulation was halted, but started to increase again at week 5 when fish moved out of the pools. It was not clear if they moved because of a decrease in stream discharge (Warren and Pardew 1998, Schaefer 2001) to find refuge from falling water levels (likely downstream to pools with more permanent water), or in search of areas with more food as algal biomass decreased in the study pools. After small macroinvertebrate grazers colonized, algal accumulation again leveled off. Thus a single group was able to slow down algal accumulation rates, but two groups were needed to stop accumulation altogether.

Cages were reversed when grazed and ungrazed treatments differed the most and as algal filaments were senescing. Thus, trajectories of the newly reversed treatments began at a breakpoint in succession when cages were already on the way to becoming similar through non-grazer mediated effects (i.e. filaments were dying). Reversing cages resulted in modest structural changes, and mostly altered macroinvertebrate composition. Removing grazing pressure after 4 weeks of recovery had a greater, yet more delayed effect than introducing grazing after 4 weeks of exclusion. Closing off open cages to grazing increased algal biomass and benthic respiration, but lowered macroinvertebrate abundance by week 9. Introducing large grazers reduced small grazer biomass and shifted composition to collector-gatherers. However, this change was temporary and only occurred at week 5. By week 9 there was little difference in macroinvertebrate assemblages because late-arriving scrapers entered open and closed cages equally, and high scraper emigration and colonization rates occurred in all treatments.

Mesocosm Experiment

Fish did not change algal communities in mesocosms to the extent seen in Kings Creek likely because densities were too low to keep up with the high algal growth rates. However, some important similarities in algal succession were observed. Filaments senesced at approximately the same time after re-wetting in mesocosms as they did in Kings Creek. Algal biomass was approximately half that of Kings Creek and diatoms did not colonize filament surfaces, suggesting light limitation or algal competition did not initiate death. These factors suggest that nutrient limitation could be the cause of senescence in both systems. Additionally, the drop in GPP in mesocosms after filament death provided further evidence that the loss in filament biomass can significantly reduce whole stream productivity in Kings Creek. Thus, filamentous algae, which are one of the defining components separating grazed and ungrazed substrata, would likely eventually die in the absence of large grazers, producing structurally and functionally similar late-stage benthic communities, regardless of the prior presence of large grazers.

Reduced macroinvertebrates in grazed mesocosms suggests that the grazing fish in Kings Creek were indeed influencing macroinvertebrate colonization in open cages, and reduction was not due entirely to consumption by invertivores. Bertrand (2007) and Bengtson et al. (in press) found low numbers of chironomids in *Phoxinus* guts living in these same mesocosms, suggesting these fish do not rely on them as a food source. Additionally, algal assemblages were not different in mesocosms, suggesting little difference in resource (food and shelter) availability. Displacement or interference with development by grazer bioturbation is possible. Fish may be inadvertently consuming chironomid eggs during grazing, or the physical disruption of the substrata may be interfering with egg or early instar development. Bioturbation can also increase

ostracod abundance (Benzie 1989), as was observed in the grazing treatments, which may increase competition for food.

Grazer community stability and simplicity in mesocosms may have limited grazer effects on algal structure. Fish were stocked at average densities found in Kings Creek (Franssen et al. 2006). After drought, fish clustered into schools containing hundreds of individuals. This may have led to brief, but intense grazing pressure in specific habitats, whereas mesocosms were exposed to constant, but less intense grazing pressure. Lower grazer community complexity (i.e., single-species treatments) in the mesocosms may have also reduced grazer effects, as algal accumulation in Kings Creek was kept in check only when more than one grazer group was present.

Grazer roles in non-equilibrium systems

Disturbance alters the nature and degree of interspecific interactions (Lake 2003, Cardinale et al. 2005), and concepts such as the intermediate disturbance hypothesis (Connell 1978), dynamic equilibrium model (Huston 1979), and habitat matrix concept (Biggs et al. 1998) were developed to explain community dynamics in non-equilibrium systems. Huston's dynamic equilibrium model suggests that the effects of grazing should change as the system progresses from disturbance to a steady state because the influence of species interactions depends on environmental conditions. In Kings Creek, large grazer effects were stronger during early and mid succession when stream conditions were changing relatively fast, than after the stabilization of biotic and abiotic conditions. Modest changes observed when grazing pressure was added or removed after cage reversals also supported a weakening large grazer influence. Gelwick and Matthews (1992) reported rapid grazing effects on algae when fish were introduced into

ungrazed pools 33 days after a flood. However, filamentous algae were still abundant. Our results are consistent with strong but temporary grazing effects observed directly following floods in this stream (Bertrand 2007, Bengtson et al. in press), suggesting the strength and stability of grazing effects may be similar after each of these distinctly different disturbance types.

The successional pattern of algal communities was evident regardless of the presence of grazers in Kings Creek. However, large grazers shifted the trajectory of benthic succession, altering the proportion and abundance of species rather than through a substitution of species. This suggests that resistance to drying determined the colonizer pool, but grazing influenced the abundance of each colonizer. Therefore, grazer influence appeared directly related to the availability of loosely attached algal forms that would otherwise persist in the absence of grazers. Early succession algae are typically small, adnate, and r-selected species (Steinman and McIntire 1990). However, when channel flow returns gradually after drought, desiccation resistant filamentous algae such as *Ulothrix* can respond rapidly to re-wetting (Evans 1959) and take advantage of the initial high nutrient availability (e.g., Steinman et al. 1996).

Fish and crayfish can have different effects on the benthic community, as they can rely on different food sources within the same stream (Evans-White et al. 2001, Bengtson et al. in press). Following re-wetting, both fish and crayfish apparently reduced loosely attached algae, but appeared to only stop total algal accumulation when both were present (Figure 1-6). When only fish were present in Kings Creek, they slowed the rate of algal biomass accrual, but algal accrual stopped only after crayfish colonized. Similarly, once most fish left and crayfish were practically the lone grazer, algal biomass increased again until small macroinvertebrates colonized. We

suggest that late-stage small macroinvertebrate grazing pressure approaches levels exerted by fish and crayfish.

Grazer effects may also depend on stream successional state. In ungrazed areas of Kings Creek, grazers removed loosely attached forms causing adnate diatoms and single cell green algae to dominate. In contrast, Bertrand (2007) found that during steady state conditions in Kings Creek, at a time when K-selected species should be dominant, green filaments grazed by *Phoxinus* were replaced by a different species of green filamentous algae. Peterson (1996) found that algal colonization rates in small open areas in Sycamore Creek, AZ were much faster after a flood than during steady state conditions because algae associated with early succession had higher immigration and reproduction rates. Thus, a freshly grazed spot could have different colonization patterns depending on time since re-wetting. By week 9, basal cells of the green filamentous algal *Stigeoclonium sp.* were abundant in both treatments. It is likely that if these filaments had grown longer, grazer influence on benthic composition would again increase.

CONCLUSIONS

Studies emphasizing the abiotic controls of stream communities are abundant (Poff and Ward 1989, Lake 2000, Dodds et al. 2004). However, reviews and meta-analyses of hundreds of grazing studies by Feminella and Hawkins (1995), Steinman (1996), and Hillebrand (2002), show consistent and overarching biotic controls of community development. Our study emphasizes the context-dependent nature of grazer effects during recovery from a physical disturbance, building on previous work (e.g. Power et al. 1998, 2008, Elmquist et al. 2003) that

stresses the interactive role of biotic and abiotic regulation of stream communities. We also stress the importance of biotic roles at times other than steady state.

Large grazer influence during drought recovery was strongest when biotic and abiotic conditions were changing rapidly. Increased hydrologic instability, including greater frequency and magnitude of drought and floods, is predicted for streams in the Central Plains as a result of climate change and increased water withdrawals. Our results show that increasing instability could amplify the overall effect of large grazers by keeping the stream in an earlier successional stage, which may reduce stream productivity and nutrient retention capacity. However, an increase in primary production and nutrient retention may occur when the change in hydrology is great enough to restrict the recovery of established functional groups such as large grazers. Losses of ecosystem function (productivity and nutrient cycling) resulting from fish and amphibian extirpations has recently been emphasized in tropical streams (Taylor et al. 2006, Whiles et al. 2006, McIntyre et al. 2007, Schindler 2007, Connelly et al. in press). Our results, from a North American prairie stream, show similar functional changes when large grazers are excluded.

Table 1-1 Fish, crayfish, and tadpole densities in Kings Creek experiment.

	Week 3		Week 9	
	Mean (g DM m^{-2})	SD	Mean (g DM m^{-2})	SD
Fish				
Phoxinus erythrogaster	1.21	1.70	0	-
Campostoma anomalum	2.20	1.33	0	-
Etheostoma spectabile	0.19	0.07	0	-
Semotilus atromaculatus	0.18	-	0	-
Pimephales sp.	0.01	-	0	-
Crayfish				
Orconectes nais, O. neglectus	0.42	0.11	4.97	3.51
Tadpole*				
Rana pipiens	0.04	-	1.74	-

Visual estimates of fish densities:
(individual m^{-2} converted to g dry mass m^{-2} using mean weight of individuals from week 3 samples)

Week	Pool 1	Pool 2	Pool 3	Pool 4	Average
1	0	0	0	0	0
3	0.7	0.3	0	0.5	0.4
4	1.1	1.0	0.9	1.9	1.2
10	1.4	0.8	0.6	1.4	1.0
11	1.4	0.8	0.6	1.4	1.0
17	1.4	0.8	0.6	1.4	1.0
24	1.4	0.6	0	1.4	0.9
35	0	0	0	0	0
61	0	0	0	0	0

*Tadpole biomass is in Ash Free Dry Mass

Table 1-2 Mesocosm algal and macroinvertebrate composition.

Algae (percent composition)	Ungrazed		Grazed		Ungrazed		Grazed	
	Day 18				Day 42			
	Average	Standard Deviation	Average	Standard Deviation	Average	Standard Deviation	Average	Standard Deviation
Single-Cell Pennate Diatoms	22.75	27.92	11.59	15.46	3.45	1.95	5.20	4.81
Filamentous Cyanobacteria	1.62	1.95	0.11	0.09	0.18	0.18	0.51	0.69
Coccoid Cyanobacteria	0.17	0.20	0.06	0.07	0.17	0.16	0.04	0.06
Filamentous Green	70.79	25.98	86.03	14.83	88.45	5.16	89.57	6.01
Colonial Coccoid Green	1.45	2.64	0.84	0.95	0.31	0.28	0.24	0.24
Single-Cell Green	3.22	3.88	1.36	0.75	7.45	3.93	4.44	2.22
Macroinvertebrates (g Dry Mass m^{-2})								
Scrapers	0.040	0.080	0.030	0.060	0.029	0.050	0.079	0.149
Predators	0.030	0.047	0.008	0.009	0.133	0.194	0.057	0.067
Collector-gathers	1.052	0.454	0.453	0.255	1.675	0.639	1.030	0.436
Collector-filters	0.043	0.027	0.019	0.025	0.028	0.012	0.039	0.024
Total biomass	1.173	0.489	0.511	0.286	1.867	0.792	1.204	0.334

Figure 1-1 Diagram of cage exclosures with one open and one closed half. Black squares show rock basket placement. Pictures show typical benthic communities in the ungrazed (left column) and grazed (right) throughout the experiment as taken with an underwater camera. The plastic baskets are 10 cm across.

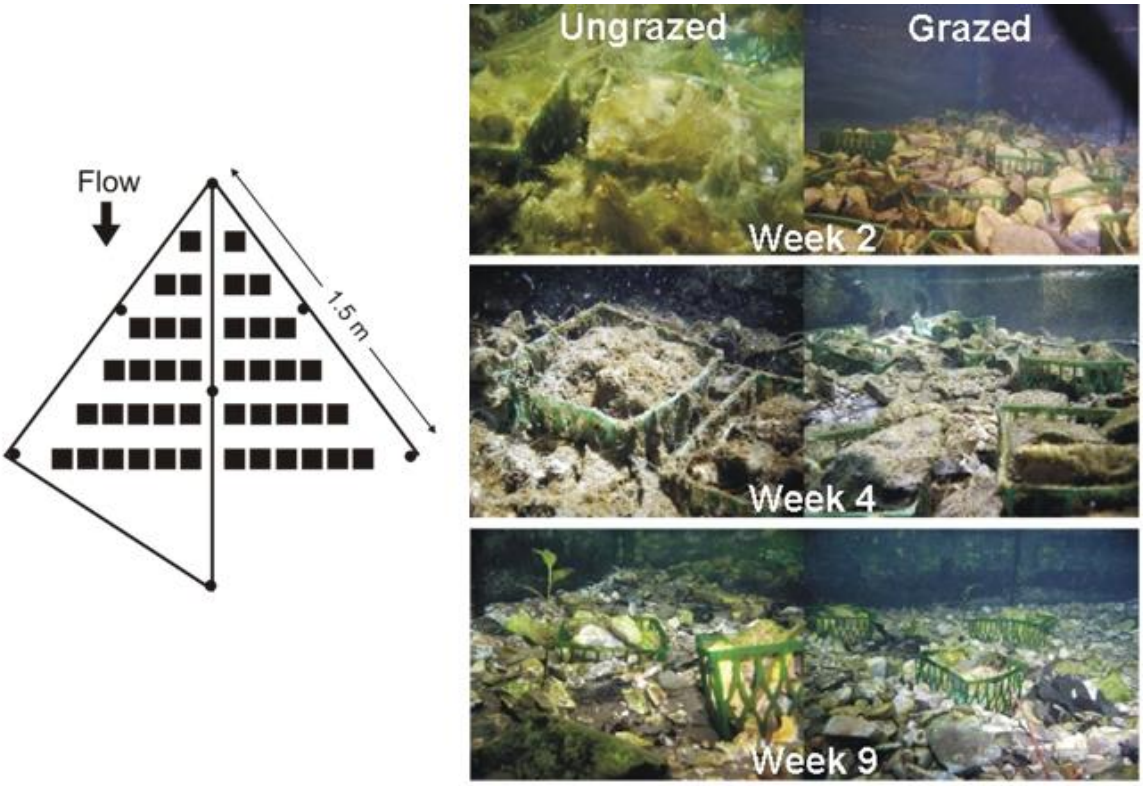

Figure 1-2 Structural and functional responses following re-wetting in Kings Creek. A) Stream discharge after drought and experiment timeline. Arrows show timing of returns of various groups of organisms. Fish returned within days, but large schools were absent following week 5. B) Water nutrient concentrations. C) Algal biomass. D) Gross primary productivity. E) Benthic respiration. F). Ammonium uptake potential. C-F, open circles are ungrazed and filled circles are grazed substrata. Week zero was on 29 April 2006.

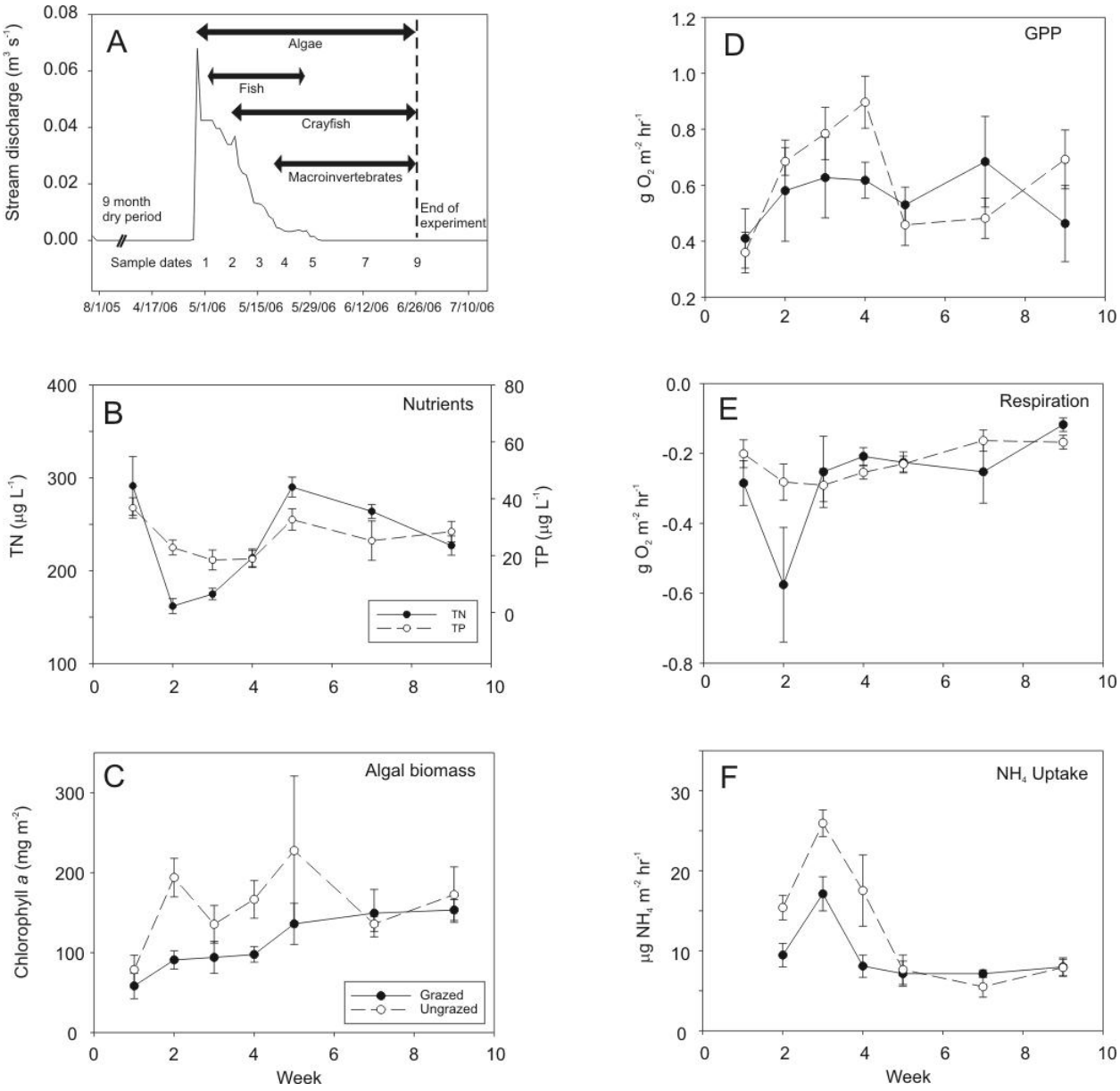

Figure 1-3 Kings Creek algal functional group composition. Closed circles represent grazed treatments and open circles ungrazed treatments. Note different y-axis scales on each row.

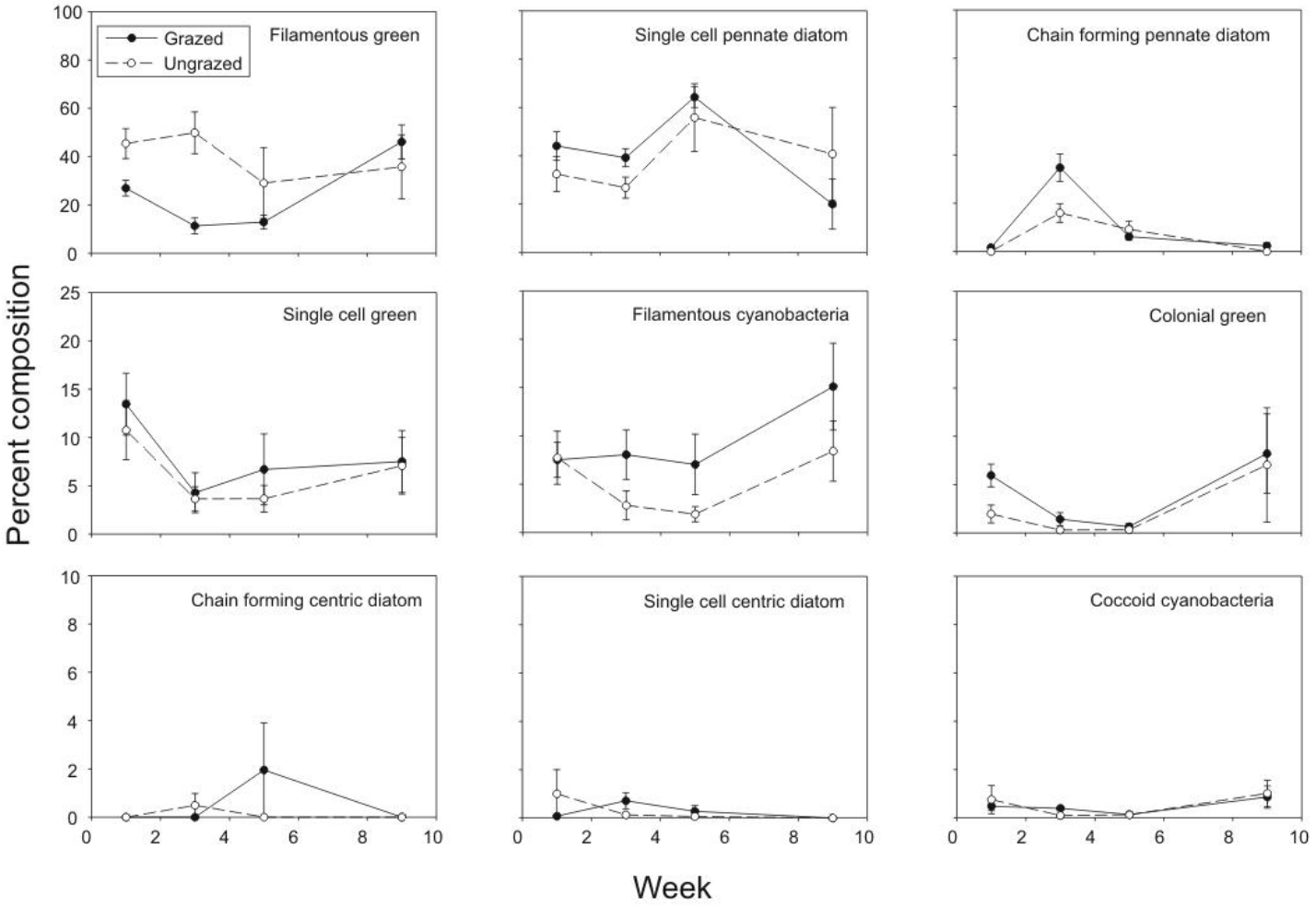

Figure 1-4 Kings Creek macroinvertebrate (non-crayfish) functional group composition. Ungrazed were always closed, grazed were always open, grazed to ungrazed are open cages that were closed at week 4, and ungrazed to grazed are closed cages that were opened.

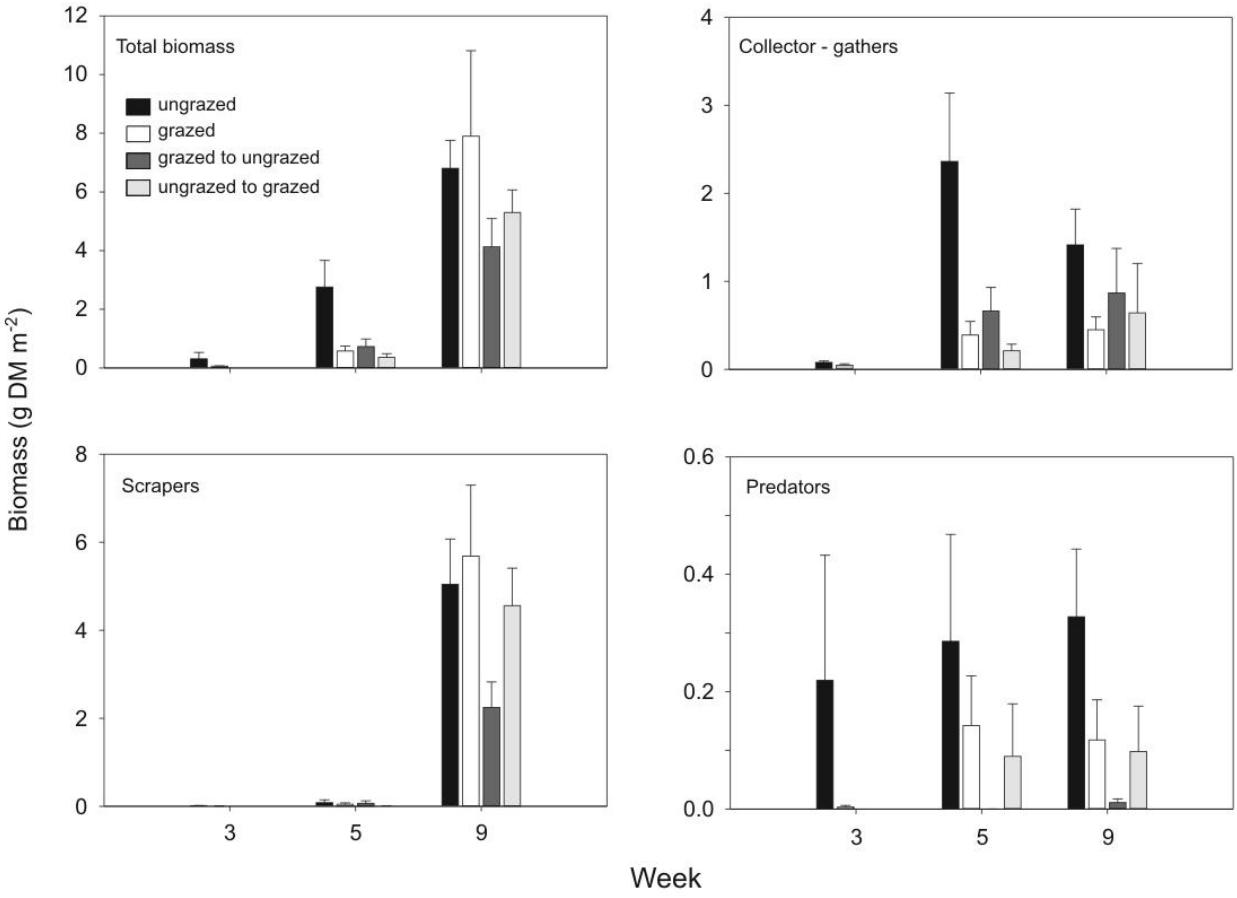

Figure 1-5 Mesocosm experiment structural (A-C) and functional (D-F) response variables.

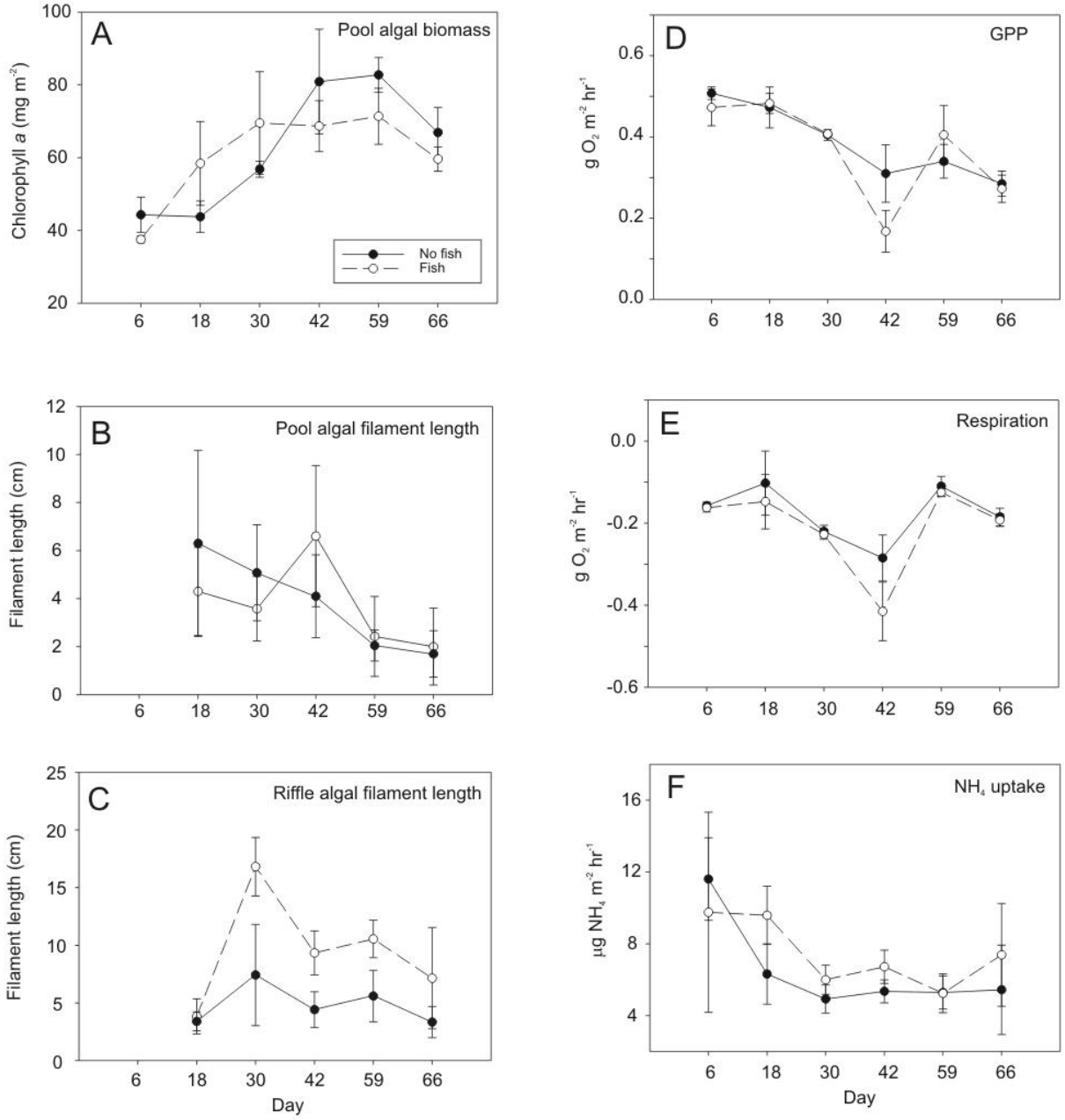

Figure 1-6 Conceptual diagram of recovery in ungrazed and grazed stream pools. Functional responses are on top and structural responses in middle and bottom panels. All functional group biomass has been converted to dry mass (g DM m^{-2}), and stream functional variables are on an arbitrary Y-axis scale.

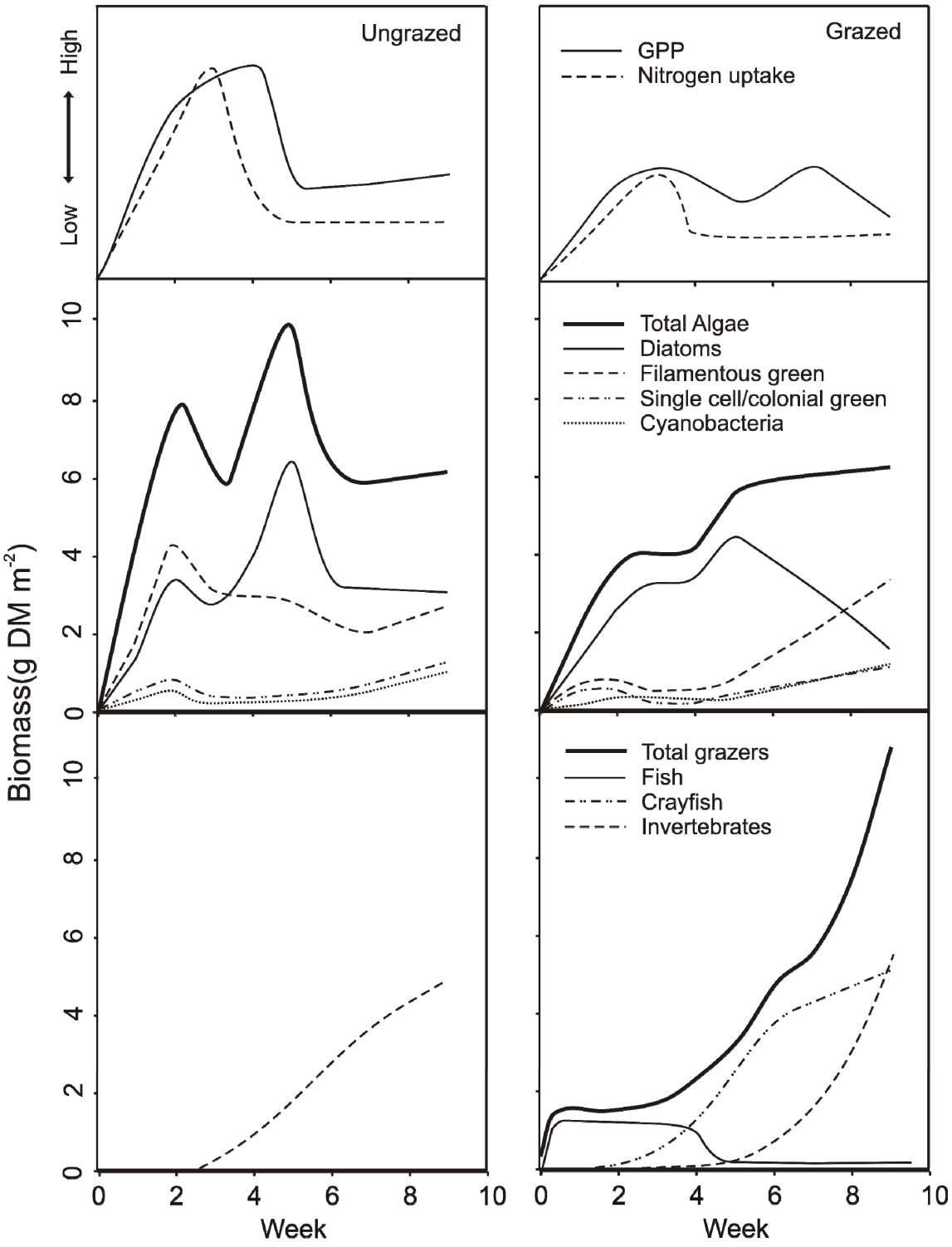

CHAPTER 2 - Nutrient and grazer regulation of algal development is unstable following disturbance

Justin N. Murdock, Walter K. Dodds, Keith B. Gido, and Matt R. Whiles

ABSTRACT

Nutrients and grazers can control algal growth in streams; however the relative strength of these regulators are dependent on nutrient availability and grazing pressure. Biotic and abiotic conditions change rapidly after a flood as the stream recovers, which suggests that nutrient and grazer influences on algal development should also vary temporally as the stream recovers. We measured algal structural and functional development for 35 days after a simulated flood in large outdoor mesocosms under varied nutrient and grazer levels. A gradient of six nutrient loadings were crossed with six grazing fish (*Phoxinus erythrogaster*) densities. During recovery, nutrient regulation was stronger than grazing, and nutrients correlated better with functional than structural aspects of algal accumulation. Fish effects were generally weak, but nonetheless influenced all structural variables and biomass specific gross primary productivity. Grazer control became weaker and nutrient control got stronger with time since flood and as algae switched from a slow to an exponential phase of growth. The only significant nutrient by grazer interaction was with riffle algal biomass, and there was no net positive stimulation of algal growth by grazers. Experimental results were used to parameterize a model of controls of algal growth and nutrient fluxes, as well as grazer/nutrient interactions. Model results support that nutrients have a stronger influence on algal recovery trajectories than grazers, and that ambient nutrient loadings needed to be reduced by approximately half for nutrient remineralization by fish to stimulate algae growth. Producer and consumer relationships after a flood differed from typical interactions during steady state conditions were grazing pressure influences algal growth more than nutrients. In non-equilibrium conditions, resource limitation of algal growth may be more important than grazing losses. Considering streams are defined by disturbances, nutrient

input may play a greater role in determining the basic trajectory of algal growth, but grazers cannot be neglected when predicting stream algal biomass recovery.

INTRODUCTION

Stream algae can be regulated by either top-down or bottom-up factors, and the balance of these processes has been extensively studied over the last two decades (Power et al. 1988, Worm et al. 2002, Hillebrand 2002). In freshwaters, negative grazer effects on algal growth due to direct consumption or physical displacement during grazing are consistently stronger than positive nutrient effects (Feminella and Hawkins 1995, Hillebrand 2002, Lies and Hillebrand 2004, Gruner et al 2008). Despite these strong decreasing patterns, grazers and benthivores can increase primary producer growth across a range of aquatic habitats including tropical streams (Flecker et al. 2002), lakes and reservoirs (Gido 2002, McIntyre et al. 2006), wetlands (Zimmer et al. 2006), and coastal marine systems (Meyer et al. 1983). This algal stimulation response has been most often linked to nutrient remineralization by fish through excretion (Vanni 2002, Hall et al. 2007), but can also occur through the removal of algae with low productivity, and the removal or disruption of other consumers (Power 1990, McIntosh and Townsend 1996). Thus the overall effect of fish on algal growth will vary and should depend on the relative strengths of grazing loss and nutrient availability.

The conditions in which grazers have the strongest effect on algal growth in not certain despite an increasing number of studies on this topic (e.g. Flecker et al. 2002, Vanni et al. 2002, Bertrand and Gido 2007, Gruner et al 2008). Theoretical studies suggest grazer stimulation will

vary with community composition and nutrient availability, but should be strongest when nutrients are limiting and grazer biomass is low to moderate (DeAngelis 1992). It is also not known how fast, or with what magnitude grazer nutrient relationships change when environmental conditions change as few grazer studies in streams have occurred outside of stable flow regimes (Hillebrand 2002, but see Gelwick and Matthews 1992). Due to the context dependent nature of grazer algae interactions it is likely that the influence of grazing fish in streams will depend on ambient abiotic and biotic conditions.

Streams exist in a state of dynamic equilibrium with constant disruptions of biotic and abiotic components (Poff and Ward 1989, Lake 2000). During the recovery process following disturbances such as floods, top-down (i.e. fish) and bottom-up factors (i.e. nutrients) are rapidly changing (Resh et al. 1988), and likely so is their influence on primary producers. Floods often reduce producer and consumer populations disproportionately across a range of disturbance intensities, as larger organism such as fish and crayfish can seek refuge in low velocity habitats, while smaller, more sedentary algae and benthic aquatic insects are scoured (Dodds et al. 1996, 2004). As a result, the algal and grazer biomass ratio can rapidly change following floods due to unequal loss and recovery rates. For example, after a scouring flood in prairie streams algal biomass typically grows exponentially, reaching peak levels within approximately two to four weeks (Dodds et al. 2002, Murdock and Dodds 2007). Macroinvertebrate diversity can recover within 1-2 weeks and pre-flood abundance within 3 to 4 weeks (Fritz and Dodds 2004). Fish communities may be back to pre-flood levels within days (Frannsen et al. 2006). The net effect of grazers on algae will likely change quickly during recovery, and the trajectory of the algal community may vary substantially with nutrient loading and grazer density during recovery.

When stream autotroph biomass is dominated by benthic algae, fish-nutrient interactions can likely also mediate stream function (i.e. primary productivity and nutrient retention).

We studied the influence of grazing minnow densities and nutrient loading on algal structural and functional recovery in large outdoor mesocosms after a simulated flood. We also created a simulation model using algal growth and nutrient mass balance parameters from the experiment to predict how changes in grazer biomass alter algal and nutrient dynamics in different nutrient environments and at different stages of recovery. Our goal was to determine if grazers, nutrients, or their interactions, regulate algal recovery following a flood. We predict that both nutrient loading and fish density will contribute to algal recovery patterns, but these factors will interact to produce non-linear responses in algal development. The strength of both factors will change over time as stream conditions change. Grazer influence on algae should weaken as algal biomass accumulates, and nutrient influence should decrease as mats thicken as nutrient recycling within the algal mat increases. Positive effects of grazers should be strongest in lower nutrient loading treatments and low to intermediate fish densities.

METHODS

Thirty-six large outdoor mesocosms located on the Konza Prairie Biological Station in northeast Kansas were used to test the interactive effect of nutrients and grazing fish on benthic development. Each mesocosm consisted of a 2.54 m^2 pool connected to a 0.84 m^2 riffle. The basic design of these mesocosms is given in Matthews et al. (2006) and shown in Figure 2-1. Water was continuously supplied by a spring, ~1000 L day^{-1} to each mesocosm, and recirculated with an electric trolling motor creating a discharge of 4-6 L s^{-1}, and a current velocity of 6-8 cm s^{-1}in the riffle. Spring water nutrient concentrations were low (~ TN 130, TP 2.8 µg L^{-1}, NO_3^-

30, SRP 1 μg L^{-1}). A shade canopy reduced ambient sunlight by 60%, and water temperature ranged from 18.6-23.7 ^{o}C with a mean of 21.1^{o}C. Substrata were a mixture of pebble, gravel, and fine sediment and similar in size and texture to substrata in nearby streams. Mesocosms were filled on 20 April, 2007 and the benthic community developed for 30 days. On 18 May 2007, substrata were scoured with a high pressure hose to simulate flooding as described by Bertrand (2007). Mesocosms were refilled with water and circulation started within 24 hours. Day zero of the experiment was 23 May, 2007.

A factorial design was used with a gradient of six fish densities and six nutrient concentrations. Mesocosm were arranged in six rows with six units per row. Each nutrient treatment was spread across two adjacent rows so that three mesocosm in each adjacent row had the same nutrient treatment. Treatments had target nitrogen (as dissolved KNO_3^-) inflow concentrations of 30 (ambient), 60, 120, 240, 500, and 1000 μg L^{-1} NO_3^- , and phosphorus (as dissolved PO_4^-) was added in Redfield ratio (16:1). These concentrations produced loading rates ranging from 30 to 1000 mg NO_3^- day^{-1} (160 to 1130 mg total nitrogen [TN]) and 1.9 to 62.5 mg PO_4^- day^{-1}. To add nutrients, A concentrated nutrient solution was continuously pumped into a PVC pipe by a FMI metering pump (model QBG, Fluid Metering Inc., Syosset, NY, USA) at a rate of 5 mL min^{-1} from an 18 L sealed bucket (Figure 2-1). The solution was completely mixed with the incoming spring water prior to entering the first mesocosm. Buckets were cleaned and refilled every two days. Nutrient concentrations were measured from the inflow into each treatment every two days, and measured once per week in each mesocosm pool.

The grazing minnow *Phoxinus erythrogaster* (Southern redbelly dace) was stocked in six densities, 0, 10, 20, 20, 40, and 50 individuals (average 1g wet mass $fish^{-1}$, 0-15g wet mass m^{-2}) per mesocosm. Densities were determined from the range of fish densities that typically occur in

nearby Kings Creek (Franssen et al. 2006, Bertrand 2007), which are similar to other prairie stream *P. erythrogaster* densities (Stasiak 2007). Dead fish were replaced daily to maintain initial densities. Inflow discharges were adjusted daily to maintain equal water volume input in all streams. Daily TN loading rates for each mesocosm were calculated from inflow volume and nutrient measurements.

Mesosocm structural and functional responses were measured on day two and then once per week for five weeks. Structural variables measured in pools and riffles were algal biomass, algal filament length, total benthic organic matter (BOM), and average benthic particle size. Functional response variables measured were areal and biomass specific gross primary productivity (GPP), community respiration (CR), and nutrient retention as TN.

At each sampling date, algal biomass (as mg chlorophyll *a* m^{-2}) was measured from three randomly collected rocks in each riffle, and from five rocks in the pool. Rocks were placed on ice and frozen within four hours of collection. In the laboratory, rocks were put in an autoclavable bag and submerged in 95% EtOH at 78˚C for five minutes, extracted in the dark for 12 hours (Sartory and Grobelaar 1984), and chlorophyll *a* measured on a Turner model 112 fluorometer with a filter set and lamp that does not allow interference from phaeophytin (Welshmeyer 1995). Rock areas were measured by tracing the top surface of the rock on paper, digitizing the image, and determining the area of the tracing with SigmaScan 5 (Systat Software Inc. San Jose, CA, USA). Algal filament length was measured at nine points in each riffle, i.e. three points along three equally spaced transects oriented perpendicular to flow. Filament lengths in the pool were measured at five points, four around the outer perimeter and one in the center. BOM (g AFDM m^{-2}) was collected with a core sampler that consisted of a 0.018 m^2 tin pipe with an electric pump (0.1 L s^{-1}) attached through the side. Substrata inside the corer were

agitated by hand while nine liters of water were collected in a bucket. Bucket contents were homogenized and a 500 mL subsample was collected for analysis.

Whole stream GPP and CR were estimated by measuring diurnal changes in dissolved oxygen (DO) concentrations. Hourly DO and temperature measurements in each mesocosm were taken with a handheld DO meter (YSI model 550a) from one hour before sunrise to one hour after sunset on one day each week. Hourly solar radiation was measured nearby (data available at www.konza.ksu.edu). Aeration estimates for whole-stream metabolism were calculated using a model that corrects the photosynthetic rates following a hyperbolic tangent model of Jassby and Platt (1976) and respiration for temperature using an equation from Parkhill and Gulliver (1999). Due to differences in light availability, daily areal GPP measurements were light corrected and calculated as g O_2 m^{-2} mol $quanta^{-1}$. Biomass specific GPP was calculated as g O_2 m^{-2} mg chl^{-1}. Nutrient retention was calculated each week as the difference in TN in the inflowing nutrient concentration and the ambient water concentrations.

Data analyses:

A quadratic surface response curve was fit to the data from each response variable for each week to compare the relationship of fish density and TN loading over time. Multiple regression analysis was used to further determine which factor, fish density, nutrient loading, time since flood, or a combination of these was the best predictor of structural and functional variation (i.e. explained the most variation in the response variable, R^2). Response variable and nutrient loading data were $\log_{10}$ transformed to achieve constant variances across sampling dates. A cross product term was added to the equation to test for 2-way interactions (i.e. nonlinear relationships) among fish, nutrients, and day since flood. Response variables in each mesocosm

were regressed against the average preceding TN loadings in that mesocosm that was calculated as the average loading rate of all days prior to that sampling time. Using average preceding loadings integrated day to day variations in inflow volumes and nutrient input. An information theoretic approach was used to compare candidate regression models. For each response variable the full model was:

response variable = intercept + days since flood + fish density + nutrient loading + fish*nutrient + fish*day + nutrient*day + error.

Additionally, we used an information theoretic approach to assess which model had the best combination of the factors and their interactions. As recommended by Burnham and Anderson (1998), we used the small sample adjustment of AIC (AICc; Akaike 1973) to rank candidate models by the difference between the AICc value for each candidate model and the model with the lowest AICc value. We then calculated the Akaike weight (w_i; weight of evidence) for each candidate model, which gives the probability that each model is the best model for the data, relative to the highest ranked model. Only candidate models with w_i's greater than 10% of the w_i of the best model were compared, which can be considered as all models within the 90% confidence interval of the best approximating model (Royal 1997). Both the regression and AIC approach was used to assess which factors and interactions were important, but also determine the amount of variation in the response variable explained by the factors in the best model. For each response variable, the relative importance of individual parameters was assessed by summing the Akaike weights of candidate models that contained the parameter of interest (Burnham and Anderson 1998).

A simulation model relating algal growth, fish grazer biomass, and flux of TN through the system was developed using Stella version 5 (Isee Systems, Inc., Lebanon, NH, USA) and

parameterized with data from this experiment. This model was used to further address the relationships among nutrients, algae, and grazers, and investigate the conditions necessary to elicit observable and positive grazer effects on algal growth and nutrient remineralization. The questions investigated were 1) are algae more sensitive to changes in nutrients or grazers during recovery, 2) at what level of grazers is necessary to elicit a strong response in each nutrient treatment, 3) what are the conditions necessary for nutrients and grazers to interact to produce algal stimulation, and how robust is this effect to changes in nutrients and fish density and 4) at what nutrient loadings does grazer nutrient remineralization increase water nutrient concentrations? Equations and model structure are described in the results section.

RESULTS

Nutrient loadings were consistent and only slightly lower than targets throughout the experiment (Table 2-1). Nutrient pumps all failed during days 13 and 14. Response curves for each variable indicated that nutrient loading and day since flood were stronger regulators of recovery than fish density (Figure 2-2). Nutrient loading, fish density, and day since flood explained 17-59% of the variation in structural variables and 16-49% in functional variables. Nutrient loading and day since flood consistently accounted for the majority of the explained variance, were both included in the best model for every response variable except riffle particle size, and consistently had higher Akaike importance weights than fish (Table 2-2). Although fish density was not as strong, fish were included in the best approximating model for all structural variables, and for biomass specific GPP.

Structural recovery:

Nutrient loading, fish density, day since flood, and their interactions explained 53% and 45% of the variation in algal biomass in pools and riffles respectively (Table 2-2). Algal biomass had a much stronger correlation with nutrient loading and day since flood than with fish density (Figures 2-2A and 2-2B). However, Akaike weighting of candidate models suggests that fish were indeed important, as models including fish were 1.7 times (in pools) and 1.9 times (in riffles) more likely to be the best approximating model than the next best candidate models that did not include fish.

Pool biomass accrued in two distinct temporal stages. Days 1 through 14 were characterized by low biomass in all nutrient treatments, while during days 14-35, biomass increased rapidly with rates increasing proportionately with nutrient loading. Riffle biomass accrued in a logarithmic fashion and approached peak biomass on day 14 in treatments below 120 $\mu g\ L^{-1}$, and by day 21 at higher loading rates. A distinct nutrient threshold in algal accrual occurred in both pools and riffles, with loading rates greater than 240 $\mu g\ L^{-1}$ having distinctly more algal accrual. Algal filament lengths in pools or riffles were not strongly related to nutrient loading or day since flood as multivariate models were not significant. Fish significantly reduced filament length at ambient nutrient concentrations in both pools (r^2 =0.20, p=0.01) and riffles (r^2 = 0.20, p=0.01, Figure 2-3), but this trend was not visible at higher nutrient loadings.

There was a strong influence of nutrient loading and day since flood on pool and riffle BOM accumulation (Figures 2-2C and 2-2D). Slightly more of the variance in BOM was explained in pools (59%) than in riffles (43%), with nutrient loading, day since flood, and a nutrient*day interaction significant predictors. Fish density was included in the best model for pools, but not riffles. The best approximating model for pool BOM was 1.6 times more likely to

be the best model than when fish were not included (i.e. the third best model). In contrast, the best riffle BOM model was 2.8 times more likely to be the best model than the same model with fish included (i.e. the second best model) (Table 2-2). Day since flood and fish density were the strongest predictors of benthic particle size in pools and riffles, and nutrients had a reduce role on riffle particle size compared to other variables (Figures 2-2E and 2-2F).

Functional recovery:

Area specific GPP was best explained by nutrient loading (Figure 2-4A), with nutrients accounting for 48% (out of a total of 49%) of the explained variance. Fish density did not significantly influence area specific GPP, but was important in biomass specific GPP (Figure 2-4B). Unlike area specific GPP, nutrient loading explained very little variation in biomass specific GPP (r^2= 0.03, p=0.025), and biomass specific GPP decreased consistently over time while area specific GPP increased. Community respiration was most closely associated with nutrients and day since flood (R^2=0.16 p<0.001) (Figure 2-4C).

TN retention was better correlated with nutrient loading and day since flood than fish density (Figure 2-4D). The best model was 2.8 times more likely than the next model that included fish (i.e. the third best model). The proportion of TN retained increased with increasing TN loading rates and day since flood, but decreased with increasing stream water TN (Figures 2-5A and 2-5B). Mesocosm water TN concentrations did not correlate well with TN loading rates and was mediated by algal biomass. High stream water TN concentrations occurred with high loading rates and low algal biomass, while low stream water TN concentrations were associated with low loading rates with low algal biomass, and high loading rates with high algal biomass (Figure 2-5C). Mesocosms with low nutrient loading rates were net sources of TN for the first three to four weeks.

Interactions:

Factor interactions were present in the best model for every response variable except area specific GPP. A nutrient by day since flood interaction was the most common and was included in the best model for seven of the ten response variables, while there were only three fish by day, and one nutrient by fish interaction. A summary of interactions for all response variables are listed in Table 2-3. The coefficient of variation (r^2) and slope of the regression equation in Table 2-3 can be used as an indicator of the strength of the regulating factor (i.e. nutrients or fish), and gradual increases or decreases in the slope or r^2 can be taken as a change in the influence of the factor over time. For example, nutrient by day interactions were stronger and changed quicker than fish interactions for pool algal biomass, because nutrient relationships changed significantly on a weekly basis, whereas fish effects did not.

Nutrient and fish interactions –

Riffle algal biomass was the only variable with a significant nutrient by fish interaction (Table 2-2). Fish had no decreasing effect at low nutrient loadings, but significantly decreased biomass at high nutrient loadings (Figure 2-2B). In riffles, increasing fish densities caused a decrease in the amount of algae produced per amount of nutrient supplied to the system, i.e. fish density reduced the slope of the relationship between algal biomass and nutrient loading (Figure 2-6A, Table 2-3) through a top-down process.

Nutrient and day since flood interactions –

Structure

Relationships among response variables and nutrients changed during recovery. The nutrient/algaal relationship was weak in pools early, with both low and high loading rates

resulting in similarly low biomass. As succession progressed, nutrients had an increasingly positive effect on algal growth and accrual up to day 28 (Figure 2-6B), and this relationship became stronger with time as the r^2 increased from 0.08 to 0.67 on days 7 and 28 respectively (Table 2-3). Pool and riffle BOM had similar relationships with nutrient loading, with nutrient regulation becoming stronger with time and peaking at day 28 (Figure 2-6C). There was little to no relationship between pool distribution of particle sizes and nutrients (Table 2-3).

Function

Nutrient influences on stream function changed as the stream recovered, but interactions were slightly weaker, or more variable than interactions with structural variables. The CR/nutrient relationship generally became stronger over time (Figure 2-6D, Table 2-3). Changes in biomass specific GPP over time were slower than for other variables and it decreased with increasing nutrient loading from days 21-35 (Figure 2-6E, r^2=0.10, p=<0.001). The TN retention/nutrient relationship was strong at the beginning and end of the experiment, but weakened in the middle (Table 2-3). Negative retention (net loss) was seen in low nutrient loadings at the start of recovery providing the largest variation in retention with nutrient loading early in recovery (Figure 2-6F). Changes in the area specific GPP/nutrient relationship did not change significantly over the course of the experiment. A decrease in CR, GPP and TN retention occurred on day 14 when the nutrient supply pumps malfunctioned and no nutrients were added.

Fish and day since flood interactions-

Fish had the strongest effect (reducing biomass) during days 1-14 when biomass was low, however this influence was weak (r^2=0.03, p=0.064) (Table 2-3). There was no noticeable effect of fish from days 21-35. Fish decreased mean particle size in pools during the first 14 days, but

did not have a significant effect after day 14. In riffles, fish only reduced particle size at day 7, and had no effect after that (Table 2-3).

Algal production/consumption model:

Model parameters-

The production/consumption model (Figure 2-7) contained variables for nutrients, algae, and fish and the equations defining initial values, relationships, and conversions among variables are listed in Table 2-4. The nutrient budget accounted for the mass of nutrient (as g TN) in the water, the flux of nutrients into the water from pump loadings and fish remineralization, and the flux out of the water into algae and outflowing water. Fish grazing rates were modeled as a sigmoid relationship between algae consumed and available algae, with the maximum grazing rate estimated from removal rates of grazers by Cattanneo and Moussuea (1995). Fish nitrogen excretion rates (0.95 mg N day^{-1} g^{-1} wet mass fish) were calculated on day 23 of this experiment from fish from each mesocosm (Kohler et al. unpublished data), and this value was used as a maximum remineralization rate. A hyperbolic relationship between fish remineralization and grazing rate was used to account for a change in excretion with consumption. Algal accumulation was calculated from the relationship of biomass specific algal growth rates and nutrient loading rates. Daily biomass specific algal growth rates were calculated from weekly changes in chlorophyll:

$$\text{biomass specific algal growth} = \ln(chl_2) - \ln(chl_1) / t_2\text{-}t_1 \quad \text{(Stevenson 1996)}$$

where chl is mg chlorophyll *a* m^{-2}, and t is day since flood at 7 day intervals. The average biomass specific growth rates for each nutrient treatment (averaged across fish treatments) were regressed against the average continuous TN loading rates of each nutrient treatment to the

equation relating algal growth to nutrient loading. All mass conversion relationships were calculated from data from this experiment.

Several assumptions were made to reduce the complexity of the model and focus on the variables of interest. These assumptions included no change in fish biomass, remineralization of nutrients was only through grazing, only algae and washout removed TN from water, algal growth was limited only by nutrients, and algal death was only by consumption. Pool algal dynamics were used to construct model relationships.

Model results-

The model predicted that nutrient loadings were a much stronger regulator of ending algal accumulation than grazers, and the effects of grazing were limited to a much smaller range (Figure 2-8). Algal accumulation increased non-linearly with nutrient loading, and did not increase with more nutrients above a loading of 0.5 g TN d^{-1} (~ 500 μg TN L^{-1} inflow concentration). In this model, a grazer effect was observed at all nutrient loading rates with all grazer densities. Grazer effects increased with increasing nutrient loading and were strongest at higher nutrients and later in recovery. For example algal biomass had a 16, 31, and 44% decrease from 0 to 50 g WM fish at 0.07, 0.25, and 1.0 g TN d^{-1} loading respectively.

Interactions between nutrient loading and grazers was only observed at loading rates below ambient mesocosm rates with the highest loading of 0.03 g TN d^{-1} (~30 μg TN L^{-1}) (Figure 2-9). At this level, all grazers stimulate growth, but middle fish densities (30 and 40 g WM) elicited the greatest positive result. At lower loading rates, fish had a consistently positive effect on algal biomass.

Grazer remineralization caused a noticeable increase in stream water TN concentration at ambient nutrient loadings with increasing grazer density from 10-50 g WM (Figure 2-10). This

trend was weak, but noticeable in the next higher nutrient treatment (0.1 g TN d^{-1}), and not evident at higher loading rates. Stream water TN peaked during week 2, with increasing grazer density slightly delaying the peak. This elevated mass of nutrients in the water quickly decreased as algae growth increased and an increasing amount of nutrients were being diverted into the algal nutrient pool.

DISCUSSION

Nutrient loading and fish density both influenced algal recovery after flooding, but in contrast to stable conditions where grazers generally control algal growth (see reviews by Feminella and Hawkins 1995, Hillebrand 2002, Gruner 2008), the influence of nutrients were much stronger. Nutrient loading was better correlated to functional responses than structural responses. Nutrients accounted for at least half of the explained variation in each functional response variable, and 96% of the explained variation in area specific GPP, versus an average of 23% of the variation in structural variables. However structural variables were still more related to nutrients than fish density as end of experiment algal biomass and BOM was consistently higher with increasing nutrient loading.

Nutrient loading may be important after a disturbance because it regulates potential algal metabolic activity, and growth and reproduction rates, which can drive algal recovery trajectories. McCormick and Stevenson (1991) found that algal reproductive potential was the key characteristic determining stream algae succession, and that species succession was driven by which species had the highest per capita reproduction rate under the current stream conditions. Model results also supported nutrient regulation of recovery trajectories, with fish

density, given the partially unknown parameters assigned to it, causing variation within the nutrient controlled trend.

Fish influenced algal structural development, but their impact was weak within the typical range of *Phoxinus* biomass found in nearby Kings Creek and other prairie streams (Stasiak 2007) during baseflow conditions. The direction of fish influence was in line with other studies with decreased algal biomass (Power and Matthews 1983, Power et al. 1988) and filament lengths (Bertrand 2007), and increased biomass specific GPP (Gelwick and Matthews 1992), but the effect was either temporary, weak, or nutrient dependent. Algal biomass reduction and nutrient remineralization by fish was not great enough to indirectly alter algal functional responses such as area specific GPP or nutrient retention.

A weak grazer effect during recovery may be due to an inability to overgraze algae with high algal accumulation rates (Biggs 1996, Peterson 1996). The early fish effect in pools disappeared when exponential algal growth began after day 14. During recovery from drought in nearby Kings Creek, *Phoxinus* consumption was able to slow algal accumulation, but could not stabilize it until an additional grazer (crayfish) also returned (Murdock unpublished data). Physiological differences of early and late succession algae may also reduce fish influence. For example, grazer stimulation of algal growth and biomass specific GPP can occur from the replacement of older, lower quality algae with more productive algae (Lamberti et al. 1989). Following a scouring flood, early arriving algae are typically fast colonizers with high metabolic and reproductive rates (Peterson 1996), therefore both the grazed and replacement algae are likely similar structurally and functionally.

We predicted that nutrient remineralization by fish would stimulate algal growth at low nutrient availability. There was not a net positive effect of fish nutrient remineralization at low

nutrients. Grazer stimulation of algae requires a narrow range of conditions including nutrient imitated algal growth and low to moderate grazer density (Steinman 1996, Vanni 2002), but it was expected that our gradients of fish and nutrients would fall within this range. The only significant interaction between nutrient loading and fish density was in riffle algal biomass, with no net reduction in algae at low nutrients. This suggests that some stimulatory effect of fish on algal growth, albeit weak, was indeed occurring. The model results suggested that ambient nutrients levels were too high for this effect to occur in the mesocosms. At day 35 stream water nutrient concentrations were declining and algal biomass was still increasing. It is possible that when algal growth and nutrient uptake peaks, water nutrient levels may be low enough to observe a positive algal response.

The model was also used to test fish effects on algal recovery, but several key parameters were unknown, such as consumption rates, and excretion changes with food availability. Using literature values and sensitivity analyses for these parameter values, we found that fish consumption was greater than what we observed in the mesocosms and was not as temporally variable. It is likely that consumption rates in the mesocosms may be reduced by factors not accounted for in the model such as temperature, behavioral interactions with other grazers, or differential pool and riffle feeding since our model was based on only pool dynamics. Further delineation of fish consumption and excretion rates is critical for further model development.

Temporal trends:

Days since flood was a strong driver for all structural response variables. Multiple nutrient and fish interactions with day since flood show that there are temporal shifts in both top-down and bottom-up control of algal development during flood recovery, and the strengths of these factors can change over a few days. Temporal changes in algal development responded

much quicker to nutrients than to grazing fish as nutrient/algae relationships changed weekly, and fish/algae relationship changes (where significant) were only evident over the course of several weeks. Generally during recovery, fish influence started weak and got weaker, while nutrient influence stared weak and got stronger.

There is little evidence that nutrients or grazers can stop or start algal succession (Steinman 1996), but macroinvertebrate grazers can change the timing of succession by altering algal colonization sequences. Neither nutrients nor fish significantly changed the timing of algal succession as the lag (initial slow accumulation) and log (exponential growth) period of algal growth (Biggs 1996) occurred at similar times in all treatments. Nutrients mainly changed succession in terms of the rate of growth during the log phase and peak biomass accumulation. Fish appeared to have little influence on the trajectory endpoint as fish had their greatest effect early in recovery, and the changeover in weak grazer to strong nutrient control coincided with the start of exponential algal growth, i.e. when nutrient influence started to strengthen.

Nutrient fluxes:

Nutrient loading regulated algal recovery and uptake rates by algae were consistently high following the flood. The relationship between TN retention and TN loading rates was opposite of what was expected, as streams with higher nutrient content typically have lower proportional retention (e.g., O'Brien et al 2007). The discrepancy between the mass of TN input and mass in the water appeared driven by algal uptake potential. High TN loading led to faster algal growth and higher biomass, and a corresponding greater removal of nutrients from the water. On the other end, low nutrient treatments with low algal biomass were initially net sources of TN, but eventually retained equal proportions of TN as algae developed. The production/ consumption model showed a similar pattern with stream water Tn closely following algal

biomass accrual. Model results suggest that algae were not nutrient limited in ambient nutrient treatments, so the remineralized nutrients may have been going unused and flushed from the system in the outflowing water.

Nutrient budgeting showed that remineralization by fish was 43% of ambient loadings at our highest fish density; however a positive effect on algal biomass was not seen as predicted. We found a neutral effect of grazers in riffles at low nutrients, but grazers reduced biomass at high nutrients (Table 2-3, Figure 2-2B). Since it is not likely that fish only graze in riffles when nutrient loadings are high, this suggests that there is a positive effect on biomass that equals the negative effect of consumption. Nutrient translocation by fish can move nutrients to different part of the system (Vanni 2002, Meyer et al 1983, Hall et al. 2007), and may have made more nutrients available to riffles than pools. During the day, fish were observed spending the majority of the time in the pool water column, moving down periodically to graze substrata. Fish were also observed directly down stream of the riffle consuming material in the current that was dislodged from the riffle. Consequently most dissolved nutrients from their benthic food were probably excreted in the water column and quickly recirculated through the return grate at end of the pool, and back to the head of the riffle. In a natural stream this effect would be seen in the riffle downstream of the pool.

CONCLUSIONS

Resources may be more influential than grazing on algal recovery from disturbance. Following a flood, we observed two major deviations from the common findings of meta-analyses of grazer and nutrient controls of algae (Hillibrand 2002, Leiss and Hillibrand 2004, Gruner et al. 2008). First we found that in this non-equilibrium environment nutrient regulation

of algae was stronger than grazers. Second we found grazer effects decreased as algal biomass increased. This deviation is likely caused by the rapid speed of algal accumulation relative to steady state conditions. One reason grazer influence may be stronger is that consumption losses are immediate, while there is a lag time for algae to take up nutrients and grow. After a disturbance the fast generation time of algae (~ 2 days, Stevenson 1996) may decrease the lag time to use available nutrients, and weaken the relative influence of grazers.

A common thread across the hundreds of studies in freshwater systems is that many of the effects are context dependent. Under certain conditions fish remineralization of nutrients can stimulate algal growth (Flecker et al. 2002, Hargrave et al. 2006). Similarly, it appears nutrients can override grazer effects in the context of disturbance recovery. Bertrand (2007) found that a longitudinal nutrient gradient determined algal recovery after a flood in a prairie stream, and that grazing and water-column feeding minnows had no significant effect.

Why do we see context dependent effects of algal regulation in streams? The basic mechanisms causing fish and nutrient effects do not change. Grazers eat algae and nutrients increase algal growth and metabolic activity. Because streams are inherently non-equilibrium systems, the changing biotic and abiotic conditions continuously alter the relative strength on each factor .We found that the strength of nutrient and grazer regulation of algae can change quickly following disturbance as algal succession progresses, and reproduction rates and nutrient uptake ability change.

Many grazer/nutrient experiments are designed to minimize environmental variability and increase system stability in order to better understand and refine these direct and indirect relationships under very specific conditions. For example, Cattaneo and Mousseau (1995) deliberately excluded early stages when establishing a model of grazer removal rates of algae.

By examining these relationships in changing biotic and abiotic conditions we document richer system dynamic with respect to the boundaries of bottom-up and top-down relationships and how they change as stream communities change, as well as how the relationships contribute to the endpoint stable state community.

Table 2-1 Nutrient daily loading rates. Phosphorus added in 16:1 (NO_3:PO_4) ratio, n=210.

Target NO_3 loading (mg day^{-1})	Nutrient loading rates (mg day^{-1})			
	Average Nitrate	Standard deviation	Average Total nitrogen	Standard deviation
30 (background)	68	15	251	73
60	101	40	275	89
120	133	35	310	89
240	194	90	357	134
500	447	125	633	153
1000	763	268	928	287

Table 2-2 Candidate models and percent variation explained (R^2), and relative importance of each parameter for structural and functional response variables. (all p-values <0.001)

Response variable	Model and parameters*	Adjusted R^2	AICc	Δ_i	w_i	K	Relative importance					
							Day	Nutrient	Fish	dn	df	nf
Structure												
pool chl	day, nutrient, fish, dn, df	0.514	500.639	0	0.355	7	0.981	0.981	0.775	0.981	0.481	0.204
	day, nutrient, fish, dn	0.509	-499.649	0.99	0.216	6						
	day, nutrient, dn	0.507	-499.556	1.083	0.206	5						
	day, nutrient, fish, dn, df, nf	0.512	-498.579	2.06	0.127	8						
	day, nutrient, fish, dn, nf	0.507	-497.589	3.05	0.077	7						
riffle chl	day, nutrient, fish, nf	0.439	-406.512	0	0.28	6	0.982	0.982	0.769	0.367	0.223	0.462
	day, nutrient	0.43	-405.192	1.321	0.145	4						
	day, nutrient, fish, dn, nf	0.438	-404.94	1.572	0.128	7						
	day, nutrient, fish, dn, df	0.438	-404.94	1.572	0.128	7						
	day, nutrient, fish	0.431	-404.346	2.166	0.095	5						
	day, nutrient, dn	0.429	-403.679	2.833	0.068	5						
	day, nutrient, fish, dn, df, nf	0.437	-403.237	3.275	0.054	8						
	Day, nutrient, fish, dn	0.43	-402.814	3.698	0.044	6						
	Day, nutrient, fish, df	0.429	-402.655	3.858	0.041	6						
pool BOM	day, nutrient, fish, dn	0.579	-660.619	0	0.349	6	1.000	1.000	0.784	0.548	0.435	0.316
	day, nutrient, fish, df, nf	0.58	-659.838	0.781	0.236	7						
	day, nutrient, int	0.574	-659.656	0.963	0.216	5						
	day, nutrient, fish, dn, df	0.577	-658.47	2.149	0.119	7						
	day, nutrient, fish, dn, df, nf	0.578	-657.654	2.965	0.079	8						
riffle BOM	day, nutrient, dn	0.417	-699.996	0	0.574	5	0.962	0.962	0.388	0.892	0.182	0.070
	day, nutrient, fish, dn	0.414	-697.951	2.045	0.206	6						
	day, nutrient, fish, dn, df	0.413	-696.724	3.272	0.112	7						
	day, nutrient, fish, df, nf	0.41	-695.786	4.21	0.07	7						

pool particle size	day, nutrient, fish, df, dn	0.399	-414.585	0	0.377	7	0.992	0.992	0.992	0.262	0.865	0.639
	day, nutrient, fish, df	0.395	-414.45	0.135	0.353	6						
	day, nutrient, fish, dn, df, nf	0.396	-412.529	2.056	0.135	8						
	day, nutrient, fish, dn, nf	0.392	-412.405	2.18	0.127	7						
riffle particle size	day, fish, df	0.154	-374.405	0	0.423	5	0.882	0.459	0.882	0.120	0.821	0.288
	day, nutrient, fish, df	0.15	-372.589	1.816	0.171	6						
	day, nutrient, fish, df, nf	0.156	-372.557	1.848	0.168	7						
	day, nutrient, fish, dn, nf	0.146	-370.527	3.878	0.061	7						
	day, nutrient, fish, dn, df, nf	0.151	-370.471	3.934	0.059	8						
Function												
Area specific GPP	day, nutrient	0.485	-614.4	0	0.24	4	0.723	0.989	0.474	0.225	0.082	0.137
	Nutrient	0.479	-613.569	0.83	0.159	3						
	day, nutrient, fish	0.484	-613.072	1.327	0.124	5						
	day, nutrient, dn	0.484	-612.954	1.446	0.117	5						
	nutrient, fish	0.479	-612.003	2.397	0.072	4						
	day, nutrient, fish, dn	0.483	-611.625	2.775	0.06	6						
	day, nutrient, fish, df	0.483	-611.454	2.946	0.055	6						
	day, nutrient, fish, nf	0.483	-611.369	3.03	0.053	6						
	nutrient, fish, nf	0.477	-610.533	3.867	0.035	5						
	day, nutrient, fish, df, nf	0.482	-610.007	4.393	0.027	7						
	day, nutrient, fish, dn, df	0.482	-609.893	4.507	0.025	7						
	day, nutrient, fish, dn, nf	0.481	-609.71	4.69	0.023	7						
CR	day, nutrient, dn	0.141	-870.26	0	0.539	5	0.922	0.922	0.383	0.846	0.164	0.076
	day, nutrient, fish, dn	0.137	-868.466	1.794	0.22	6						
	day, nutrient, fish, dn, df	0.134	-866.627	3.633	0.088	7						
	day, nutrient, fish, df, nf	0.132	-866.342	3.918	0.076	7						

Biomass specific GPP	day, nutrient, fish, dn	0.2	-516.091	0	0.338	6	0.934	0.934	0.696	0.768	0.325	0.186
	day, nutrient, dn	0.192	-515.395	0.696	0.238	5						
	day, nutrient, fish, dn, df	0.198	-514.317	1.774	0.139	7						
	day, nutrient, fish, df, nf	0.197	-514.222	1.869	0.133	7						
	day, nutrient, fish, dn, df, nf	0.194	-512.409	3.682	0.054	8						
	day, nutrient, fish	0.174	-511.461	4.63	0.033	5						
TN retention	day, nutrient, dn	0.305	-326.56	0	0.377	5	0.909	0.909	0.318	0.511	0.105	0.050
	day, nutrient	0.298	-325.437	1.122	0.215	4						
	day, nutrient, fish, dn	0.302	-324.502	2.057	0.135	6						
	day, nutrient, fish	0.295	-323.402	3.157	0.078	5						
	day, nutrient, fish, dn, df	0.3	-322.727	3.832	0.055	7						
	day, nutrient, fish, df, nf	0.299	-322.513	4.046	0.05	7						

* Intercept and error terms also included in all models

dn = day by nutrient interaction, df = day by fish interaction, nf = nutrient by fish interaction, w_i = Akaike weighting, K = number of parameters in model, Δ_i = difference in AICc of model from the 'best' model

Table 2-3 Summary of nutrient, fish density, and day since flood interactions for each response variable.

Response variable	Interaction	Boundary of change	Relationship direction	Regression equation (y = response variable)						x in equation	r^2	P-value
Pool algal biomass	fish x day	days 1-14	Fish slightly decreased biomass	y	=	3.55	-	0.009	x	per fish	0.03	0.064
(mg chl m^{-2})		days 21-35	through day 14, and then no effect	y	=	4.29	+	0.002	x	per fish	0.00	0.725
	nutrient x day	day 1	Increasing algal biomass with	y	=	3.30	+	0.429	x	g TN loaded	0.08	0.101
		day 7	increasing nutrients	y	=	4.46	+	0.611	x	g TN loaded	0.40	<0.001
		day 14		y	=	4.04	+	0.842	x	g TN loaded	0.20	0.006
		day 21		y	=	4.94	+	1.516	x	g TN loaded	0.61	<0.001
		day 28		y	=	5.37	+	1.234	x	g TN loaded	0.67	<0.001
		day 35		y	=	5.99	+	1.203	x	g TN loaded	0.57	<0.001
Riffle algal biomass	nutrient x fish	fish = 0	Higher fish densities reduce	y	=	5.54	+	1.347	x	g TN loaded	0.34	<0.001
(mg chl m^{-2})		fish = 10	maximum biomass at high	y	=	5.06	+	1.020	x	g TN loaded	0.23	0.003
		fish = 20	nutrient loading	y	=	5.56	+	1.235	x	g TN loaded	0.35	<0.001
		fish = 30		y	=	5.26	+	1.058	x	g TN loaded	0.22	0.004
		fish = 40		y	=	4.84	+	0.683	x	g TN loaded	0.10	0.054
		fish = 50		y	=	4.62	+	0.664	x	g TN loaded	0.10	0.061
Pool BPOM	nutrient x day	day 7	Increasing OM with increasing	y	=	-4.28	-	0.176	x	g TN loaded	0.07	0.121
(g AFDM m^{-2})		day 14	nutrient loading to day 28	y	=	-3.44	+	0.347	x	g TN loaded	0.20	0.006
		day 21	then decrease in relationship	y	=	-3.12	+	0.593	x	g TN loaded	0.36	<0.001
		day 28		y	=	-2.53	+	0.821	x	g TN loaded	0.59	<0.001
		day 35		y	=	-2.67	+	0.452	x	g TN loaded	0.39	<0.001

Riffle BPOM	nutrient x day	day 7	Increasing OM with increasing	y	=	-4.35	-	0.219	x	g TN loaded	0.19	0.008
(g AFDM m^{-2})		day 14	nutrient loading to day 28	y	=	-3.40	+	0.275	x	g TN loaded	0.14	0.027
		day 21	then decrease in relationship	y	=	-3.38	+	0.303	x	g TN loaded	0.14	0.023
		day 28		y	=	-2.95	+	0.486	x	g TN loaded	0.44	<0.001
		day 35		y	=	-3.20	+	0.283	x	g TN loaded	0.25	0.002
Pool particle size	nutrient x day	day 7	Increasing mean particle size	y	=	3.02	+	0.037	x	g TN loaded	0.00	0.887
(µm)		day 14	with increasing nutrient loading	y	=	4.18	+	0.580	x	g TN loaded	0.08	0.096
		day 21	to day 28 then decrease	y	=	4.34	+	0.597	x	g TN loaded	0.13	0.030
		day 28		y	=	4.70	+	0.661	x	g TN loaded	0.24	0.003
		day 35		y	=	4.96	+	0.518	x	g TN loaded	0.17	0.012
	fish x day	day 7	fish decreased mean	y	=	1.56	-	0.011	x	per fish	0.24	0.003
		day 14	particle size over time, but	y	=	1.83	-	0.010	x	per fish	0.20	0.007
		day 21	only significant before day 14	y	=	1.70	+	0.001	x	per fish	0.00	0.881
		day 28		y	=	1.88	-	0.003	x	per fish	0.03	0.326
		day 35		y	=	1.84	+	0.003	x	per fish	0.02	0.435
Riffle particle size	fish x day	day 7	fish decreased mean	y	=	1.61	-	0.009	x	per fish	0.16	0.015
(µm)		day 14	particle size over time, but	y	=	1.82	-	0.007	x	per fish	0.08	0.107
		day 21	only significant on days 7	y	=	1.59	-	0.004	x	per fish	0.14	0.026
		day 28	and 21	y	=	1.80	-	0.002	x	per fish	0.03	0.320
		day 35		y	=	1.71	+	0.003	x	per fish	0.03	0.279
Community respiration	nutrient x day	day 7	Increasing respiration with	y	=	1.13	+	0.048	x	g TN loaded	0.52	<0.001

(g O_2 m-2 day-1)		day 14	nutrient loading to day 28	y	=	1.06	-	0.135	x	g TN loaded	0.22	0.004
		day 21	then decrease in relationship	y	=	1.10	+	0.129	x	g TN loaded	0.80	<0.001
		day 28		y	=	1.20	+	0.252	x	g TN loaded	0.64	<0.001
		day 35		y	=	1.09	+	0.056	x	g TN loaded	0.53	<0.001
TN retention	nutrient x day	day 1	Decreasing TN retention with	y	=	0.45	+	0.826	x	g TN loaded	0.50	<0.001
(proportion)		day 7	time, with strongest relationships	y	=	0.72	+	0.433	x	g TN loaded	0.21	0.005
		day 14	early and late	y	=	-0.22	-	0.164	x	g TN loaded	0.07	0.127
		day 21		y	=	0.65	+	0.494	x	g TN loaded	0.16	0.016
		day 28		y	=	0.66	+	0.554	x	g TN loaded	0.31	0.001
		day 35		y	=	0.73	+	0.209	x	g TN loaded	0.43	<0.001
Biomass specific GPP ($g O_2 mol^{-1} day^{-1} mg chl^{-1}$)	nutrient x day	days 1-14	no effect	y	=	0.002	+	0.0001	x	g TN loaded	0.00	0.720
		days 21-35	BioGPP decreased with increasing nutrient loading	y	=	0.001	-	0.0002	x	g TN loaded	0.10	0.001

Table 2-4 Equations used in algal production/consumption model.

Variable	Equation or value	Units	Notes
Algae biomass =	Algae biomass (t - dt) + (Algae accumulation - Algae loss) * dt	mg chlorophyll a m^{-2} day^{-1}	All values in model change on a per day time scale
INITIAL Algae =	15	mg chlorophyll a m^{-2}	
INFLOWS:			
Algae accumulation =	(.018*LOGN(Mass nutrient input)+.08)*Algae	mg chlorophyll a per mg chlorophyll a day^{-1}	Biomass specific growth per g total nitrogen input
OUTFLOWS:			
Algae loss =	((Grazing rate*(Grazer biomass*.25))*3.5)/2.54	mg chl m^{-2} consumed day^{-1}	Grazer biomass converted to DM (1g WM = .25g DM), multiplied by rate 3.5 mg chl per g DM algae, 2.54 m^{-2} in mesocosm
Grazer biomass =	Grazer biomass(t - dt)	g WM	Average fish was 1 g WM
INITITIAL Grazer biomass =	0 to 50	g WM	Variable in model
Grazing rate =	Sigmoidal grazing equation	g DM algae consumed per mg chl m^{-2} available day^{-1}	Food dependent grazing. Maximum grazing rate = .24 g DM algal per g DM fish day^{-1}. Max rate calculated from Cattaneo and Mousseau 1995.
Remineralization rate	saturating equation		consumption dependent remineraliztion rate,

			Max rate = .95 mg N per g DM fish day^{-1}. Max rate calculated from fish at day 23, Kohler et al ., unpublished data.
Mass nutrients in water =	Mass nutrients in water (t - dt) + (Mass nutrient input - Mass nutrient into algae - Mass nutrient in outflow) * dt	g total nitrogen	Nutrient = total nitrogen
INITIAL Mass nutrients in water =	0.068	g total nitrogen	Ambient loading
INFLOWS:			
Mass nutrient input =	Mass nutrient loading + Mass nutrient remineralized	g total nitrogen day^{-1}	
Mass nutrient loading =	0.03 to 1	g total nitrogen day^{-1}	Variable in model
Mass nutrient remineralized =	(Remineralization rate/1000)*Grazer biomass	g total nitrogen day^{-1}	Converted mg N to g N. Multiplied by total fish biomass
OUTFLOWS:			
Mass nutrient into algae =	(0.217*LN(Algae biomass)-0.660)*Mass nutrients in water	g total nitrogen day^{-1}	Relationship between algal chlorophyll and total nitrogen retention
Mass nutrient in outflow =	(Mass nutrients in water/1500)*1000	g total nitrogen day^{-1}	Mesocosm holds ~1500 L, Inflow/outflow was ~ 1000 L per day

Figure 2-1 Diagram of mesocosms and nutrient addition apparatus.

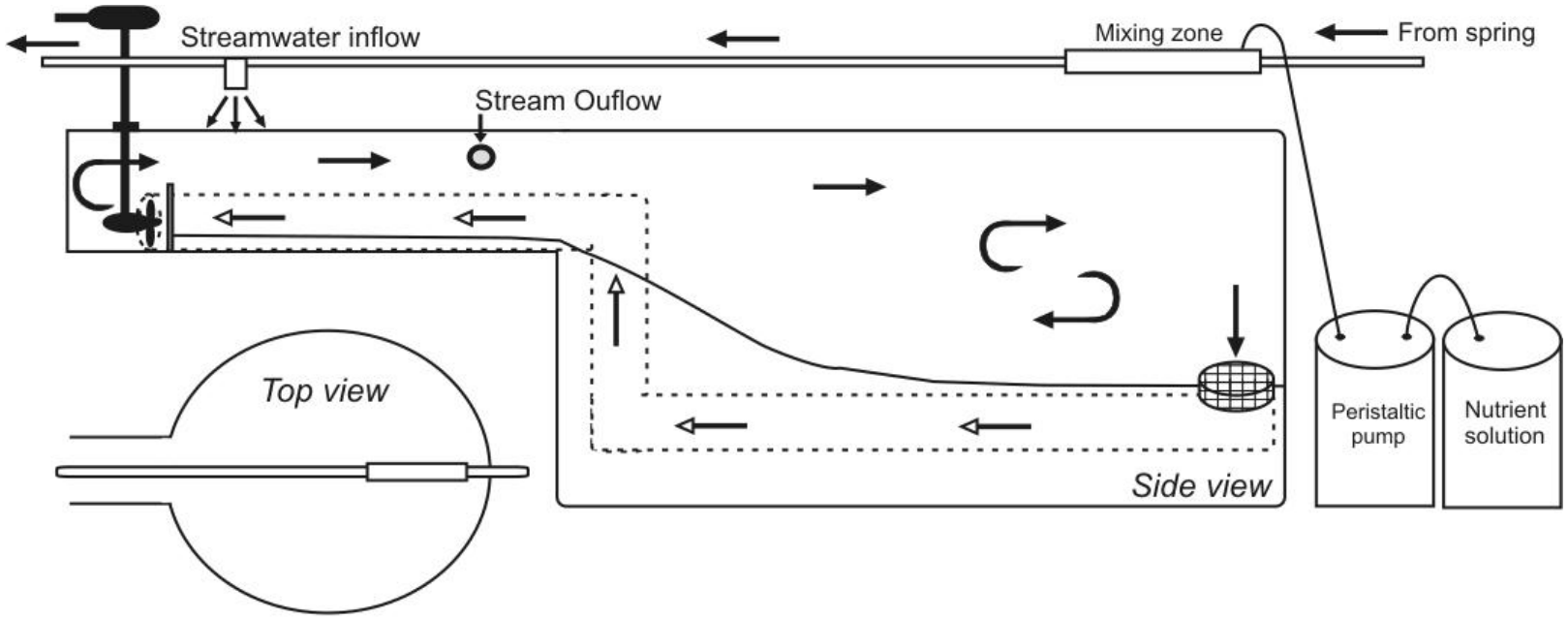

Figure 2-2 Structural response variables vs. nutrient loading and grazing fish density. Data were fit with a quadratic surface to visualize overall trends. Two sampling dates, one early recovery (day 7) and one mid-late recovery (day 28) are displayed for each variable to show temporal shifts in nutrient and fish influence on the response variable.

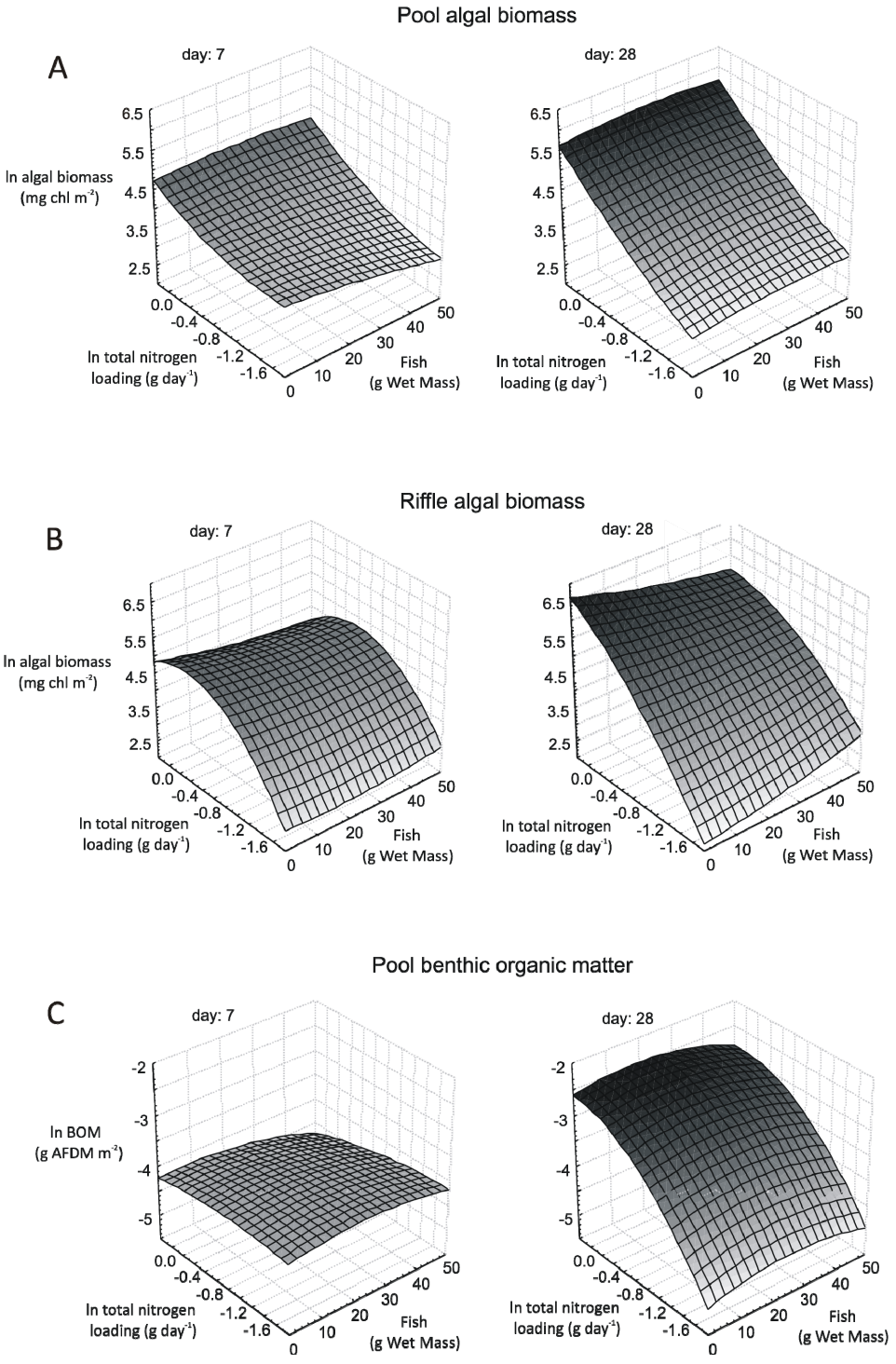

Figure 2-2 continued. Note mean particle size graphs are from days are 14 and 35.

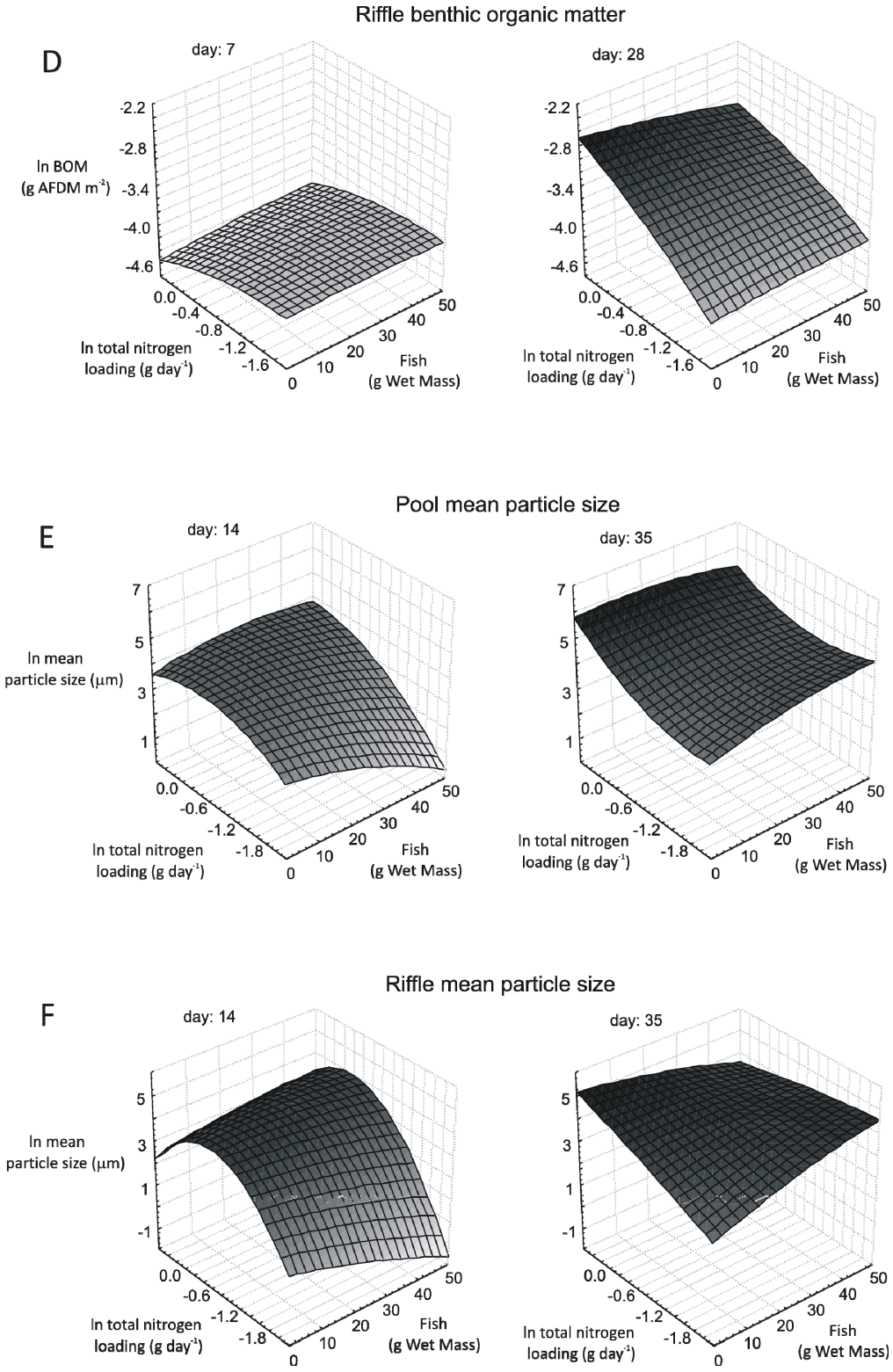

Figure 2-3 Algal filament length and fish density relationship at ambient nutrient concentrations across all weeks for A) pools and B) riffles.

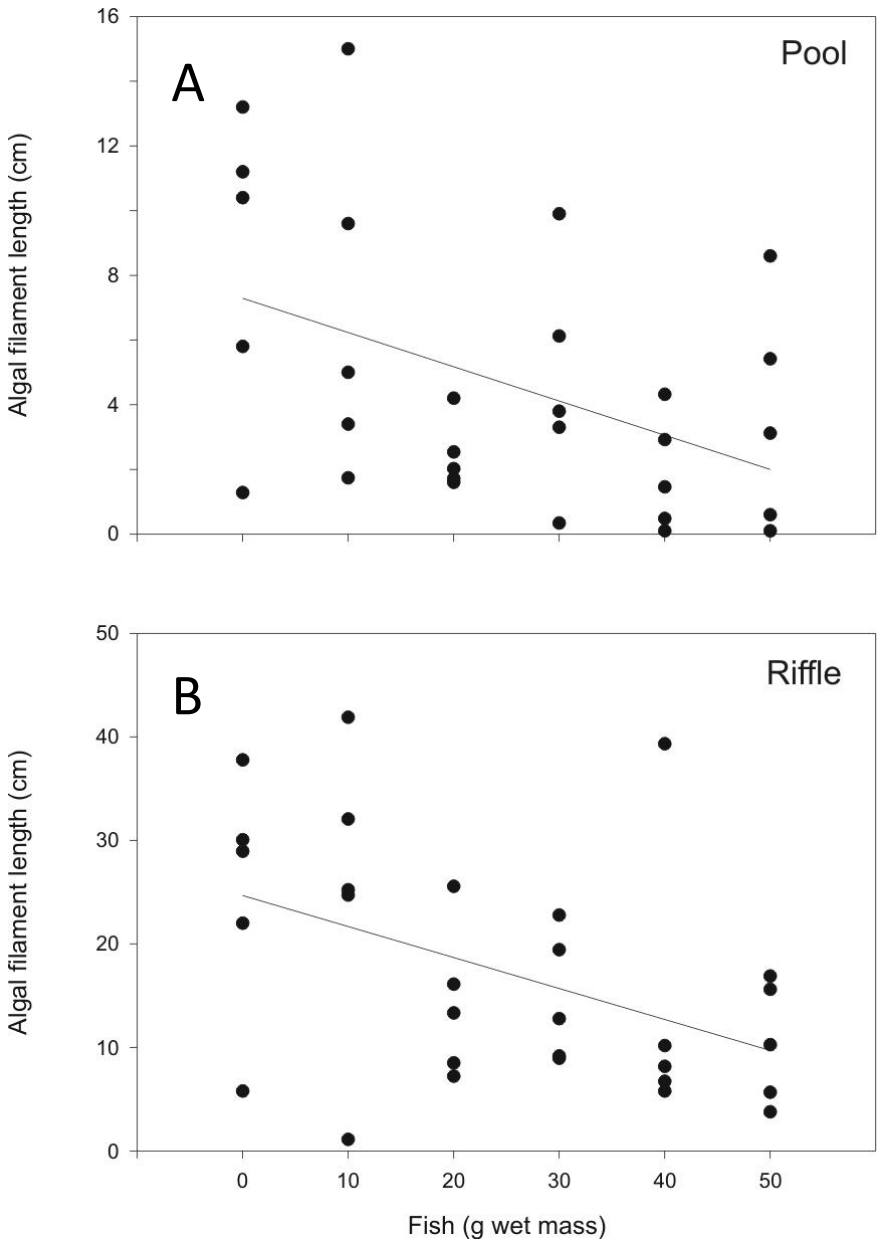

Figure 2-4 Structural response variables vs. nutrient loading and grazing fish density. Data were fit with a quadratic surface to visualize overall trends. Two sampling dates, one early recovery (day 7) and one mid-late recovery (day 28) are displayed for each variable to show temporal shifts in nutrient and fish influence on the response variable.

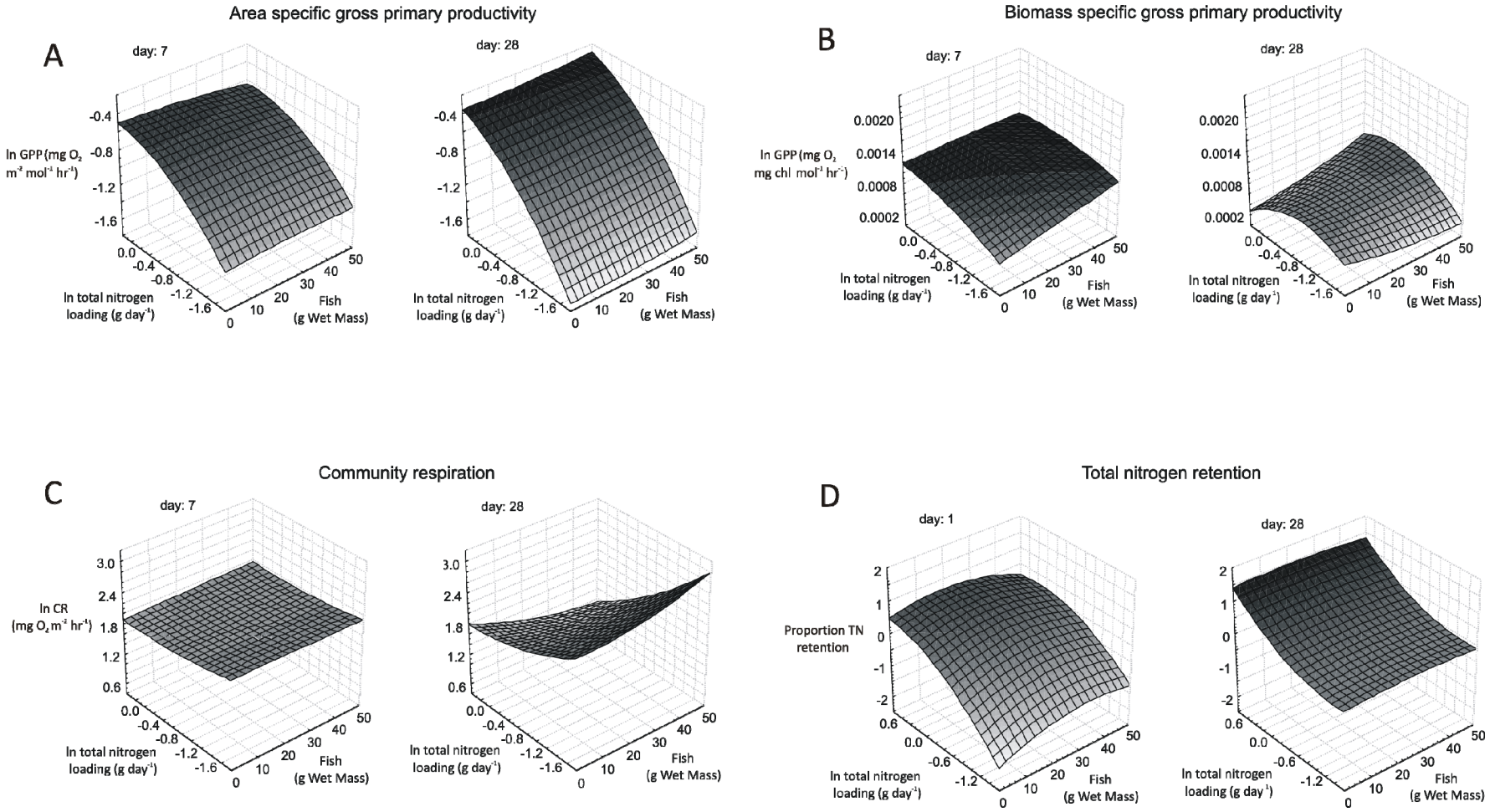

Figure 2-5 Relationship among total nitrogen loading and retention across all weeks. A) TN loading vs. water TN, B) Water TN vs. TN retention, and C) Algae and TN relationship.

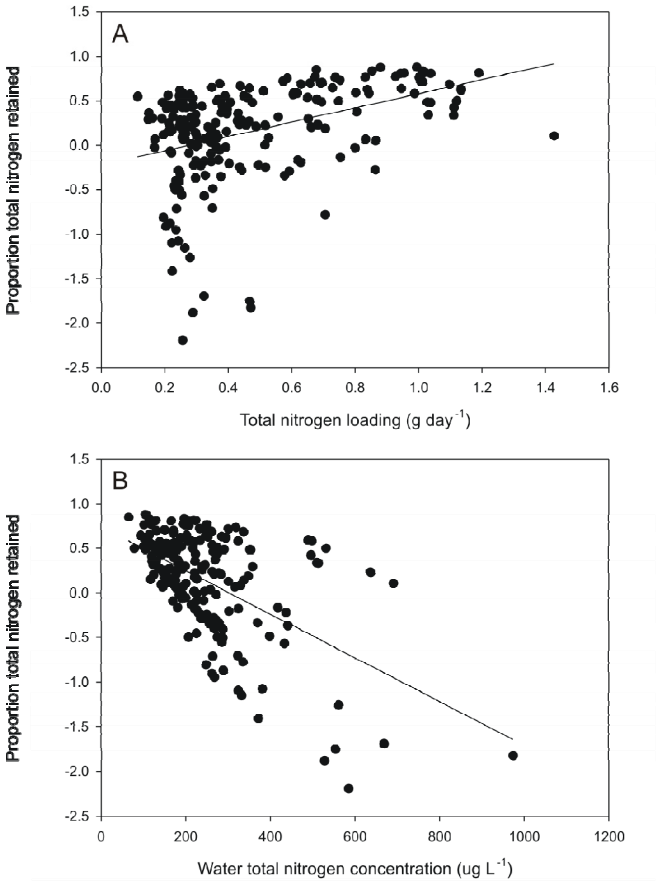

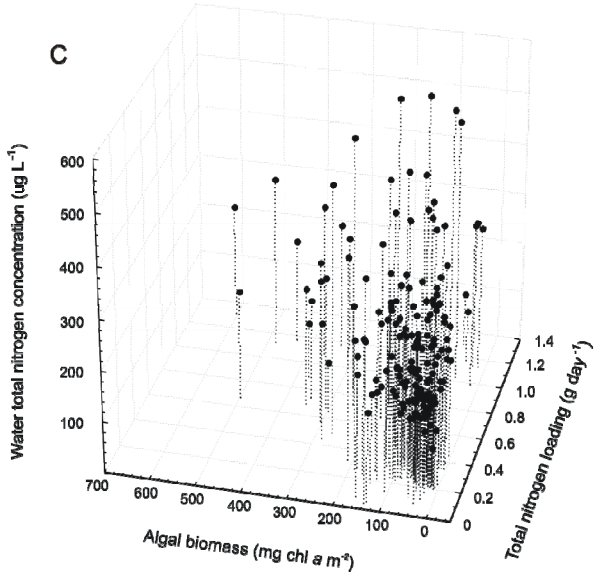

Figure 2-6 Changes in response variables with fish density or day since flood for nutrient by fish (A) and nutrient by day (B-F). Points are the relationships (i.e. slopes of the linear regressions in Table 2-3) among the interacting factors. See text and Table 2-3 for further explanation.

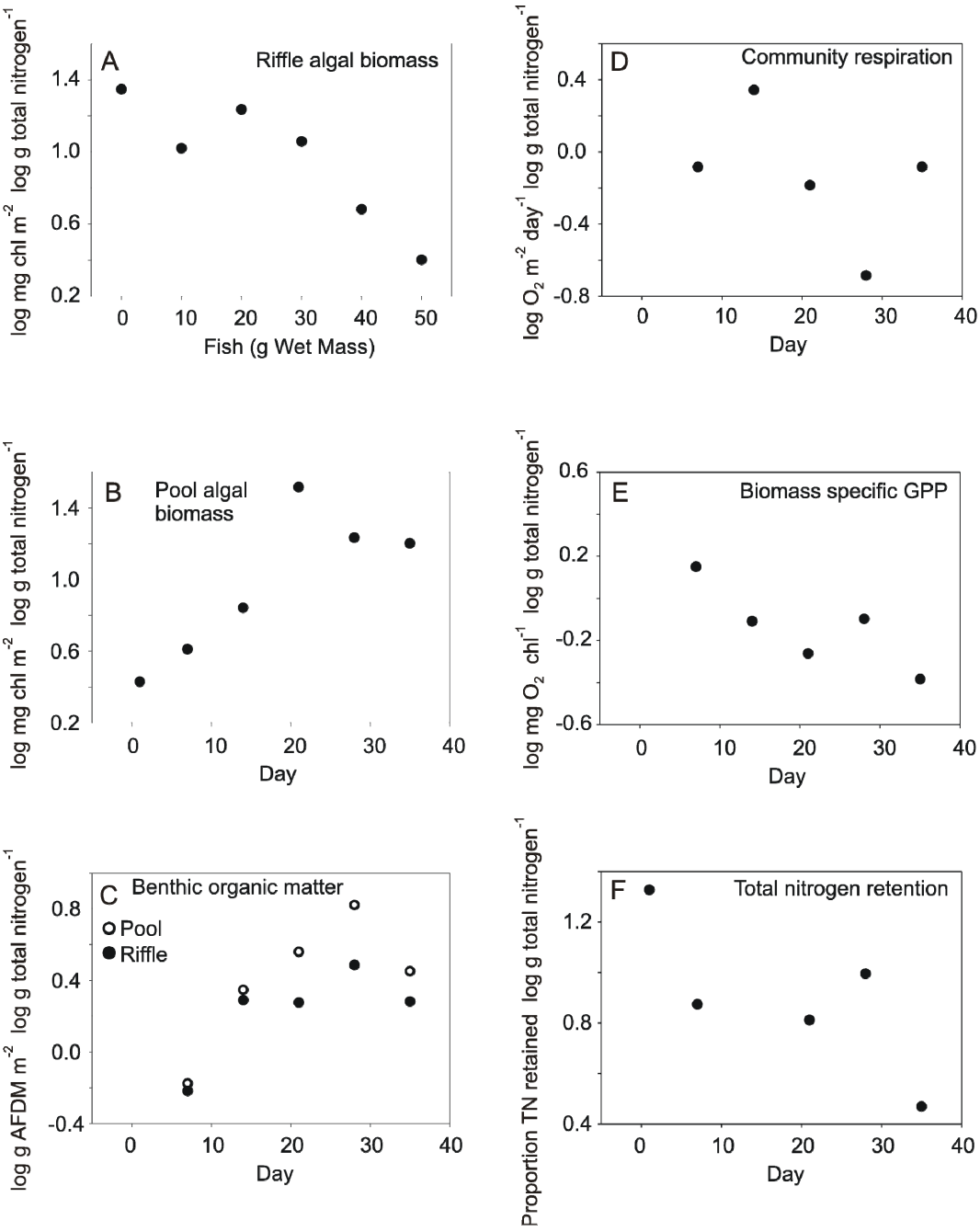

Figure 2-7 Model of nutrient, algal, and grazer relationships parameterized by relationships derived from this experiment.

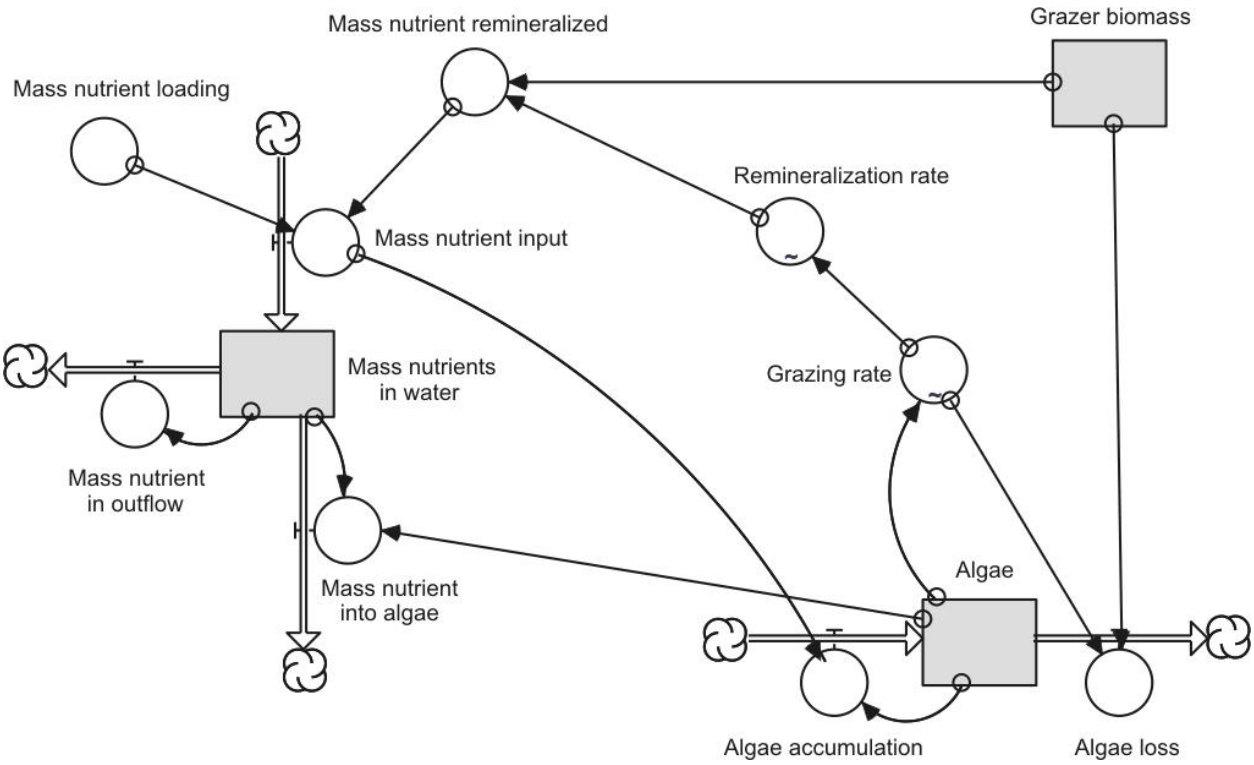

Figure 2-8 Model results. Algal biomass accumulation over 35 days for six grazing fish densities (0, 10, 20, 30, 40, and 50 g wet mass fish), at three nutrient loading rates (0.07 [ambient], 0.25, and 1.0 g Total Nitrogen day^{-1}).

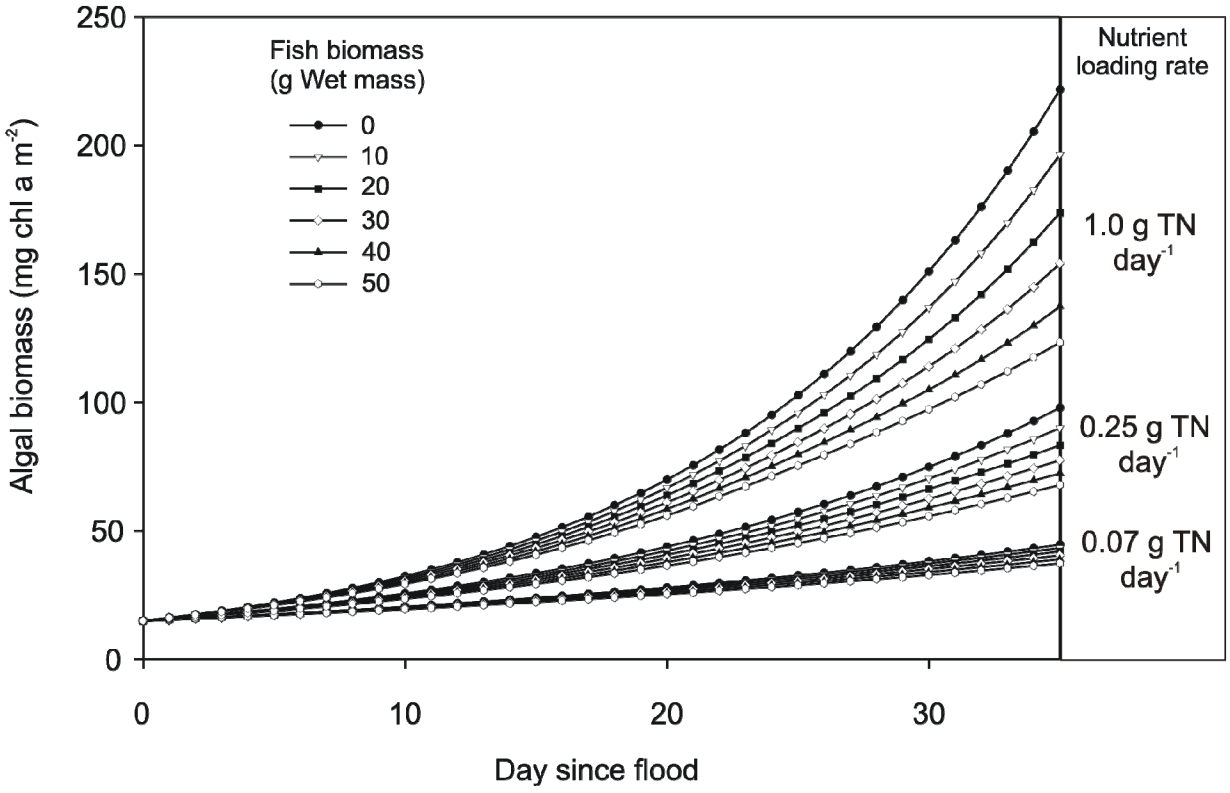

Figure 2-9 Model results. Nutrient by grazer interaction at low nutrient laodings. Algal accumulation for 0-50 g wet mass fish at 0.03 g Total Nitrogen day^{-1}, i.e. the highest loading rate algal stimulation is observed, and 0.02 g Total Nitrogen day^{-1}.

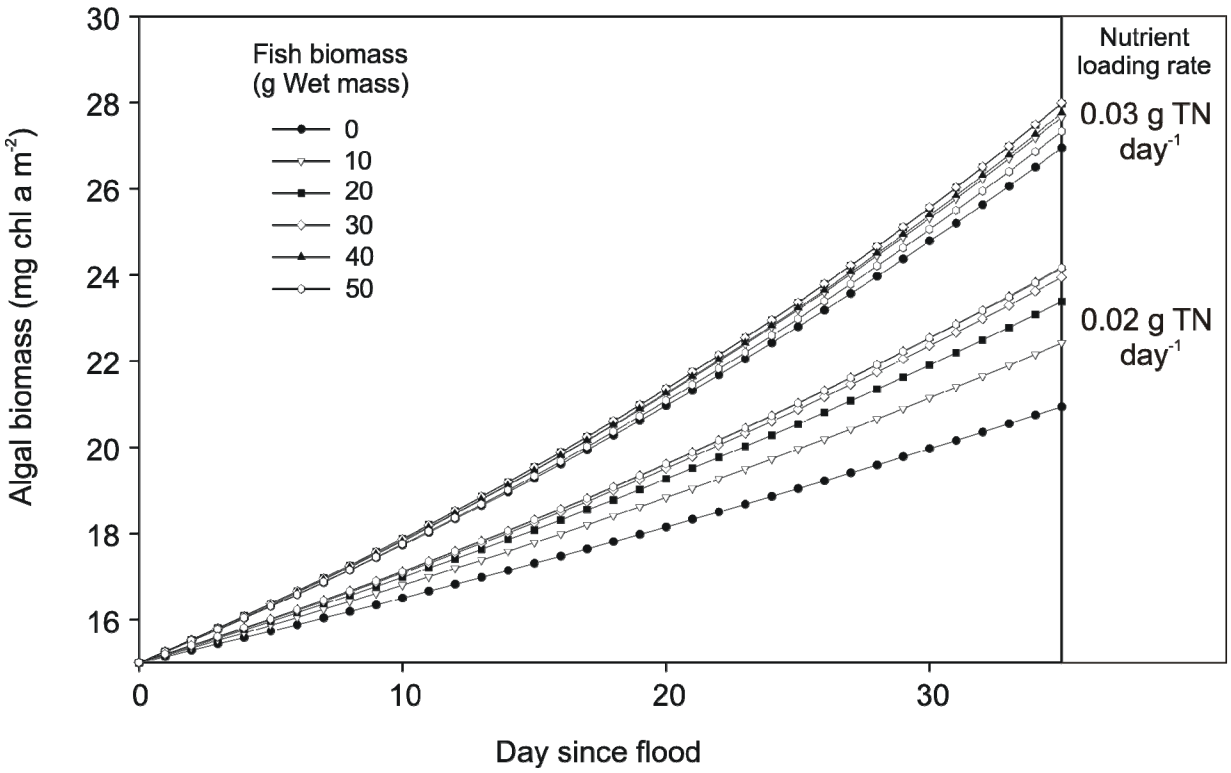

Figure 2-10 Model results. An example of Total Nitrogen flux rates through a mesocosm for ambient nutrient loading (0.07 g Total Nitrogen day^{-1}) and mid fish density (40 g Wet mass). Fish cause nutrients to accumulate above the loading concentration, but peak is mediated by increasing algal growth and nutrient incorporation.

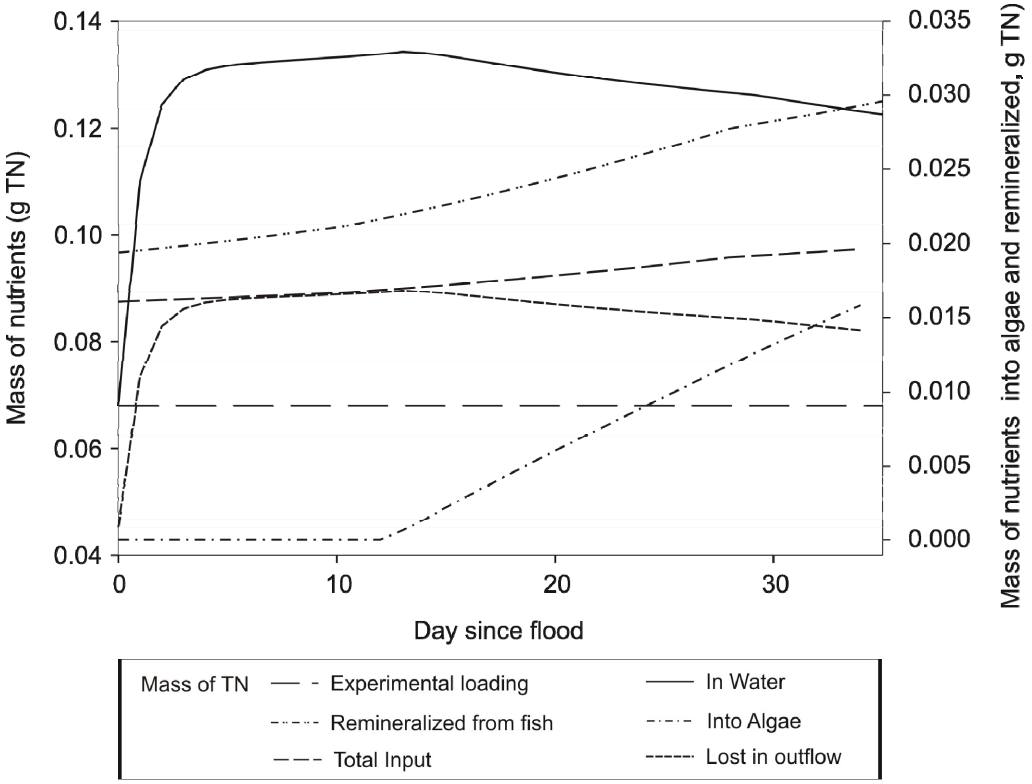

CHAPTER 3 - Linking benthic algal biomass to stream substratum topography[1]

Justin N. Murdock and Walter K. Dodds

[1] Reprinted with permission from "Linking Bethic Algal Biomass to Stream Substratum Topography" by Justin N. Murdock and Walter K. Dodds, 2007. Journal of Phycology, 43, 449-460. © 2007 Phycological Society of America

.

ABSTRACT

The physical properties of substrata significantly influence benthic algal development. We explored the relationships among substratum surface texture and orientation with epilithic microphytobenthic biomass accumulation at the whole-substratum and micrometer scales. Unglazed clay tiles set at three orientations (horizontal, vertical, and 45^{o}), and six substrata of varying surface roughness were deployed in a prairie stream for 3 weeks. Substrata were analyzed for loosely attached, adnate, and total benthic algal biomass as chlorophyll a, and confocal laser scanning microscopy was used to measure substrata microtopography (i.e., roughness, microscale slope angles, and three-dimensional surface area). At the whole-substratum level, vertical substrata collected significantly ($P < 0.05$) less algal biomass, averaging 34% and 36% less than horizontal and 45~ substrata, respectively. Benthic algal biomass was also significantly less on smoother surfaces; glass averaged 29% less biomass than stream rocks. At the microscale level, benthic algal biomass was the greatest at intermediate values, peaking at a mean roughness of approximately 17 μm, a mean microscale slope of 50^{o}, and a projected/areal surface area ratio of 2:1. The proportion of adnate algae increased with surface roughness (26% and 67% for glass and brick, respectively), suggesting that substratum type changes the efficiency of algal removal by brushing. Individual substrata and microsubstrata characteristics can have a strong effect on benthic algae development and potentially affect reach scale algal variability as mediated by geomorphology.

INTRODUCTION

Stream bottoms are often thought of and studied as two-dimensional (2-D) planes. A 2-D approach is evident by many measurements quantified and reported in areal units (e.g., mg chl a m^{-2}, Dodds et al. 2002). When examined at a smaller scale, such as that experienced by microorganisms (i.e., benthic algae), a stream bottom becomes a complex three dimensional (3-D) terrain (Bott et al. 1997), and to algae, edges and pits on a substratum may represent "mountains and valleys" during assemblage development. As a result of the small scale in which microorganisms grow, relatively minor changes in the physical environment affect colonization processes and assemblage structure (Burkholder 1996, Bergey 2005). Determining the relationships between benthic algal accumulation and substrata physical properties at the pit/crevice (microscale) level, in addition to the whole-substratum (macroscale) level, could further elucidate the heterogeneous nature of benthic communities (Robson and Barmuta 1998) and improve sampling efficiency and standardization. The most prominent physical differences among substrata are surface texture and orientation, and these properties potentially have a large effect on benthic algal development.

Considerable research has been conducted on the effects of the overlying abiotic environment on benthic algae (Stevenson et al. 1996, Wetzel 2001, Murdock et al. 2004); yet, the physical attributes of the underlying substratum have been studied much less frequently. Substratum research has focused mainly on qualitative measurements (Dudley and D'Antonio 1991, Clifford et al. 1992, Johnson 1994, Cattaneo et al. 1997) because of technical limitations of microscale measurement (but see Sanson et al. 1995, Bergey and Weaver 2004, Bergey 2006). Although confocal laser scanning microscopy (CLSM) is used to assess aquatic biofilms (Lawrence et al. 2002, 2004, Larson and Passy 2005, Leis et al. 2005), to our knowledge there

have been few attempts to use it to quantify the characteristics of the substrata on which benthic algae grow.

Whole-substratum surface properties affect benthic algal development. Algal accumulation is consistently greater on horizontal surfaces than on vertical surfaces (Vandermeulen and DeWreede 1982, Baynes 1999, Kralj et al. 2006) and on rougher, textured surfaces (Clifford et al. 1992, Sanson et al. 1995). Reasons cited for the greater biomass with texture include increased sedimentation efficiency (Johnson 1994) and cell adhesion (Sekar et al. 2004, Scardino et al. 2006), protection from disturbances, such as scour and grazing (Dudley and D'Antonio 1991, Bergey and Weaver 2004), and alteration of flow around a substratum (DeNicola 1 and McIntire 1990, Jørgenson 2001). As a result of the fractal nature of surface topography, it is likely that the surface characteristics evident at the whole substratum level, such as texture, are influenced by the microscale surface properties of that substratum.

Micrometer-scale surface irregularities such as pits, crevices, and protrusions can also reduce algal susceptibility to grazing and scouring (Lubchenco 1983, Bergey 1999, Bergey and Weaver 2004) and alter diffusion boundary layer thickness (Vogel 1994, Dade et al. 2001, Dodds and Biggs 2002). Additionally, as texture changes the physical dimensions of substratum surfaces, it should also change the availability of resources regulated by these dimensions, such as colonization area and light. Ultimately, though, the assemblage itself will change surface topography during development, providing substrata for further colonization and reducing light and nutrient availability near the substratum surface (Dodds 1991). Thus, surface influence should change during the successional sequence.

The physical properties of texture at the micrometer (i.e., individual algal) scale can create heterogeneous microhabitats across a single substratum, which may lead adjacent algal

assemblages to become dominated by species with different adaptive traits. For example, small adnate species can obtain refuge from disturbances in pits (Bergey 2005), but this environment may decrease nutrient and light availability. Larger, loosely attached species can acquire more light and nutrients through vertical growth, but this strategy makes them more susceptible to loss from grazing or scouring (Biggs and Thomsen 1995, Biggs et al. 1998). As a result, physically diverse benthic algal assemblages may develop on different areas of the same or adjacent substrata, markedly increasing local assemblage heterogeneity. Amplified heterogeneity in substrata physical properties due to texture should therefore increase benthic algae microscale, and macroscale, heterogeneity (Downes et al. 1998).

Understanding the basic ecology of colonization and accumulation of benthic algae in streams is vital because of the nonequilibrium nature of most lotic habitats. Scouring floods and inundation/drying oscillations regularly reduce algal biomass and reset successional processes. We hypothesize that changes in micrometer-scale physical properties of a substratum's surface will affect the physical properties (i.e., growth forms) of the accumulating benthic algal assemblage. Our objective was to assess the relationships among surface characteristics and epipelic algal biomass based on coarse, physical groupings of loose and adnate forms. Confocal laser scanning microscopy was used to measure 3-D substratum microtopography, and algal/substratum relationships were evaluated at both micrometer and whole-substratum levels. Microscale quantification also allowed us to address two possible physically based factors that may regulate accumulation (i.e., increased surface area due to texture, and reduced light availability due to 3-D sloping and shading). We also briefly assessed the percentage of algal biomass left behind after brushing in relation to its roughness and discuss implications for collection.

MATERIALS AND METHODS

Study site

Experiments were conducted in lower Kings Creek on the Konza Prairie Biological Station, located in the Flint Hills region of the Great Plains, approximately 10 km south of Manhattan, Kansas, USA (39^{o} 6.34' N, 96^{o} 36.31' W). Kings Creek is a headwater stream with an upper watershed of pristine tallgrass prairie and a lower watershed containing a mixture of prairie and agricultural land with oak woodland as the riparian vegetation (Gray et al. 1998, Gray and Dodds 1998). Three successive runs (<30 m between runs) were used to achieve similar current velocities (20–30 cm s^{-1}), depth (15–30 cm), and light regimes (~60% shade duration) among all substrata used in the experiments. The runs were physically similar, with a mean depth of 0.3 m, mean width of 2.5 m, and mean length of 7 m. Stream substratum in the study reach was primarily limestone cobble (5–10 cm).

Substratum deployment and algal collection

Benthic algal chl a levels were monitored in the study reach after a severe flood (165 m^3 s^{-1}) 3 months prior to the experiment to assess the accumulation rate of loosely attached algae and determine the duration of the substrata colonization experiment. The flood scoured all visible algae from the reach. Beginning 5 d after the flood, five rocks were randomly collected every 2 d for the first 2 weeks and then every 4 d for the next 3 weeks. Algae were brushed into a bottle and processed as described below for the natural rock substrata. Algal biomass accumulation began to level off at ~30 d (Fig. 1); therefore, a 3-week colonization period was chosen to

achieve a benthic algal mat with both a developed understory and overstory while minimizing sloughing losses.

Thirty 6.5 cm x 20.5 cm unglazed clay tiles (133.3 cm^2) were deployed in the middle run from 18 October to 10 November 2004. A stream reach was used that positioned the tiles in an east–west orientation to ensure a similar daily light regime for all tiles [~11:13 light:dark (L:D)]. During the study period, the sun was in the southern half of the sky, with an average declination of 25.4~ and maximum declination of 40.4~. Tiles were placed in one of three orientations: horizontal (0^o), vertical (90^o from horizontal, facing north, because of heavy sunlight interception shading from south bank vegetation), or 45^o from horizontal (facing north) with a total of 10 replicates per orientation. A block design was used, placing five 5.1 cm diameter poly-vinyl chloride (PVC) pipe frames into rows, with each row containing six systematically oriented tiles with two angle replicates per row. The frames were positioned lengthwise across the stream, approximately 50 cm apart, and placed in similar current velocities, depth, and light conditions to reduce environmental variability.

Five additional substrata types of varying roughness (glass slides, two glazed tile types, bricks, and sterilized rocks taken from the site) were tested, for a total of six roughness values with the horizontal unglazed tile. Ten replicate PVC sheets, each containing one of each substrata type were deployed in the adjacent runs. Substrata were randomly positioned on each sheet, and all substrata in this experiment were positioned horizontally.

All substrata were removed after 23 d, and individual tile contents were divided into loosely attached and adnate benthic algae. Loose algae are defined as those relatively easily removed by brushing, and adnate as those tightly attached to the substrata (most likely some adnate algae were removed by brushing). Algae were brushed from the top

surface of each tile with a stiff nylon brush and rinsed into a bottle (loose algae). Brushing consisted of short strokes (approximately 4 cm per stroke) with moderate pressure over the entire top surface, with each particular area receiving approximately 10 strokes. During substrata brushing, the loosened content was rinsed into the bottle after each third of the surface was brushed. The ‘‘loose algae’’ bottle was placed on ice in the field. The brushed substrata, containing the remaining ‘‘adnate algae,’’ were placed in individual plastic bags and put on ice.

Samples were analyzed for chl a in the laboratory within 4 h of collection. Each bottle of loosely attached algae was homogenized for 1 min with a hand blender, and a subsample filtered onto a GFF filter (Whatman, Middlesex, UK). Filters and brushed tiles were frozen until chl analysis could be performed. For chl a extraction, filters and tiles were immersed in 95% ethanol:water and placed into a hot water bath at 78^{o}C for 5 min (Sartory and Grobbelaar 1984). Samples were then placed in the dark at 4^{o}C for 12 h. Extracts were analyzed for chl a with a Turner Model 112 fluorometer (Turner Designs Inc., Sunnyvale, CA, USA) using an optical configuration optimized for the analysis of chl a without phaeophyton interference (Welschmeyer 1995). Benthic algae growing on the sides of the substrata were removed as much as possible with brushing, wiping, and rinsing before whole-substratum extraction.

Substratum microscale measurement

Substratum surfaces were analyzed using CLSM (Zeiss Axioplan 2 LSM 500 CLSM; Carl Zeiss, Jena, Germany). Images were collected with a 10x planneofluar objective (x100, 0.85 mm^2 per image), with a 488 nm laser, recording all wavelengths of the reflected light. Measurements were taken from five areas on each substrata type of the more homogeneous manufactured substrata, and three areas on five rocks. Each measurement consisted of a series of images of incrementing depth (Z-stack) with vertical resolution ranging from 0.9 μm for glass to

10 µm for brick. Slice thickness was set to optimize vertical resolution while still maintaining a practical scanning time. For example, scanning time for glass with a peak-to-pit distance of 4 µm with an incrementing thickness of 0.9 µm would be similar to scanning a brick with a peak-to-pit distance of 400 µm at a thickness of 10 µm (~10 min).

Z-stacks were analyzed with Image J digital image analysis software (Abramoff et al. 2004; U. S. National Institute of Health, Bethesda, MD, USA, http://rsb.info.nih.gov/ij/) and an associated plugin, SurfCharJ (Chinga et al. 2003), for mean surface roughness (the average distance from the bottom of all pits, and the top of all peaks to a middle plane that is equidistant from the deepest pit and highest peak), mean microscale orientation (the angle of pit walls and sides of peaks), and increased surface area resulting from increased texture. Fractal dimensions (D) of each surface type were calculated from the CLSM images with ImageJ and the MapFractalCount plugin (http://rsb.info.nih.gov/ij/plugins/ index.html), which calculates fractals for 3-D topography, to assess scale-independent surface characteristics among substrata.

In addition to CLSM surface area measurement, surface area was measured using the soapy water method (Harrod and Hall 1962) to compare it with a currently used and more readily conducted technique. Ten replicates of each substratum were weighed, the top surface dipped in soapy water for 20 s, allowed to drip for 20 s, and then reweighed. The weight of the water was then correlated to the 3-D surface area. Projected (2-D) surface areas for each substratum were determined by measuring the length and width of the top surface of the substratum. Areal rock surface area was measured by scanning the outline of a rock into a computer to produce a digital image and then calculating the planar surface area using SigmaScan 5.0 (Systat Software Inc., Richmond, CA, USA). The glass surface was used as the reference value (i.e., 1 mm_2 of 2-D

glass equals 1 mm^2 of 3-D area). All other surfaces were set to a proportional increase in mass of soapy water retained relative to glass.

Minimum microscale determination.

Confocal microscopy allows microtopography measurements at a submicron scale; thus, it is possible to focus on a scale smaller than is relevant to benthic algae. For instance, the slope of a 3.2 μm segment on a rock (two pixel widths in our images) would most likely be irrelevant to a 50 lm alga. Finding and applying the most relevant lower scale for image analysis is necessary because changes in this scale can alter microscale measurements. Different minimum scales were evaluated to determine their impact on the resulting microtopography measurements by using a fast Fourier transform (FFT) band-pass filter on the image prior to analysis. This filter enables the user to set a lower and upper limit of a given linear segment used for measurement. We used a minimum segment length of 15 μm and no maximum limit on segment length to analyze substrata images.

We obtained the relevant linear segment length by estimating the median algal size accumulating on the experimental substrata. The smoothest (glass), roughest (brick), and a midroughness (red tile) substrata were redeployed in the same reach, for the same colonization time, during the same month in the following year. Algal cell length was measured from cells growing directly on each substratum with CLSM. Images of algal fluorescence (excitation 488 nm and emission > 650 nm) were collected from three areas on each substratum (20x planneofluar objective, 0.21 mm^2 per area), and 600–900 cells/colonies/filaments were measured per substratum type. The minimum cell length measurable with this method was ~2 μm.

Data analysis.

At the whole-substratum scale, two-way analysis of variance (ANOVA) was used to compare benthic algae biomass among surface orientations and row placement, and among surface texture and run placement using SPSS 11 (SPSS Inc., Chicago, IL, USA). Multiple comparisons were performed using Tukey's HSD post hoc procedures when significant differences were determined among algal biomass and substrata type or orientation. Linear and nonlinear regression analyses were used to correlate the microscale characteristics of surface roughness, microscale slope, and 3-D surface area to accumulated algal chl using SigmaPlot8 (Systat Software Inc.). Note that the same chl measurements (i.e., loosely attached, adnate, and total chl from each substratum type) are used for comparison at both whole-substratum and microscopic scales.

Chlorophyll values were adjusted to the 3-D area available for colonization for each substratum type to assess the effects of increased surface area on benthic algae accrual. For example, if a tile had an areal surface area of 100 cm2, but its roughness increased the 3-D area to 150 cm2, the chl content was calculated as mg chl per 150 cm^2 and then adjusted to m^{-2}. Changes in the intensity of direct light hitting a given point due to texture (i.e., changing angles of incidence on substrata) were calculated using Lambert's Law, E = cos (F), where (E) is the proportion of illumination hitting a surface, which varies as the cosine of the angle of incidence (F, in radians).

RESULTS

Minimum scale determination.

Confocal microscopy revealed substantial physical differences among substrata at an algal-relevant micrometer scale. Figure 3-2 illustrates these differences, showing 3-D surface plots and a random profile of each surface. Values for surface roughness, microslope orientation, surface area, and D of each substratum increased with surface texture and are listed in Table 3-1. Detailed trends for each physical component will be discussed below. Microscale measurement differed depending on the minimum segment length used to base the image analysis. As a finer scale is used, mean roughness decreases, mean microslope orientation gets closer to 90^{o}, and surface area greatly increases (Table 3-2).

Algal cell/filament/colony lengths were similar among glass, red tile, and brick substrata. Across substrata, algal cells had a median length of 13 μm, a mean of 21 μm, a standard deviation of 34, and a range of 546 μm. As CLSM analysis identifies algal chloroplasts, some cell lengths may have been underestimated—especially pennate diatoms, which dominated assemblages during both deployments. Therefore, we adjusted for the underestimation of the dominant cell type and used a minimum substrata segment length of 15 μm for image analysis. The diatom genera *Achnanthes* and *Cocconeis* dominated adnate forms, while loosely attached forms were dominated by stalked diatoms from the genera *Gomphonema* and *Cymbella*, the filamentous green alga *Cladophora*, and filamentous cyanobacterium *Oscillatoria*.

Orientation

Benthic algal chl a concentrations were significantly different among whole-substratum orientations ($a = 0.05$, $P = 0.001$ for loose, adnate, and total algae), but not different between

rows (P = 0.465, P = 0.879, and P = 0.490 for loose, adnate, and total algae, respectively). No significant orientation by row interaction effects was observed for any algal form (P > 0.05 for all forms). The 0^o and 45^o tiles accumulated significantly greater loose and adnate algae than the 90~ tiles but were not significantlydifferent from each other (Fig. 3a). Total chl variability was also greater within the 0^o and 45^o tile eplicates than in the 90^o replicates (Levene test of constant variance, P = 0.011). Although differences were observed in biomass and variability, the proportion of loose versus adnate forms was not significantly different among orientations (P = 0.363). Loosely attached algae averaged 53%, 57%, and 54% of the total algae for 0^o, 45^o, and 90^o tiles, respectively.

Microslope orientation varied from a 1~ mean slope for glass, to 63^o for brick (Table 3-1). Adnate, loose, and total benthic algae biomass increased in a Gaussian pattern with increasing microscale slope (adnate: $r^2 = 0.84$, $P < 0.0001$; loose: $r^2 = 0.42$, $P < 0.0001$; total: $r^2 = 0.77$, $P < 0.0001$; Fig. 4), and peak biomass occurred at a slope of ~50^o. Above 50^o, adnate chl did not change (ANOVA, Tukey's post hoc comparisons, P = 0.42), but loose and total chl decreased (Tukey's post hoc, P = 0.002 and P = 0.001, respectively). The greatest change in chl with microslope angle occurred at an intermediate orientation (16^o –50^o mean slope). In this portion of the curve, adnate chl increased linearly at roughly twice the rate (1.3 mg chl a m^{-2} $degree^{-1}$) as loose chl (0.55 mg chl a m^{-2} $degree^{-1}$), and these trends were stronger for adnate ($r^2 = 0.72$, $P < 0.001$) than loosely attached forms ($r^2 = 0.24$, $P < 0.001$). The mean proportion of loose to adnate algae decreased linearly ($r^2 = 0.96$, $P < 0.0001$) with increased microscale slope at a rate of 0.7% per degree, and assemblages switched from a dominance of loose forms to adnate forms at a mean microslope angle of ~50^o.

Surface roughness

At a qualitative whole-substratum level, texture significantly influenced the accumulation of both growth forms ($P < 0.001$ for adnate, loose, and total algae; Fig. 3b). Loosely attached algae differed between runs ($P = 0.001$), but adnate and total algae did not ($P = 0.379$ and $P = 0.056$, respectively). There were no substrata-by-run interaction effects ($P > 0.05$ for all types). Smoother substrata (i.e., glass and glazed tiles) collected less adnate and total algae than the rougher unglazed tile, natural rock, and brick. Maximum loosely attached chl was observed on an intermediate roughness, but no strong pattern was exhibited. The proportion of loose to adnate algae decreased on increasingly rougher surfaces, with loose forms comprising 78%, 71%, 65%, 53%, 45%, and 33% on glass, white tile, red tile, unglazed tile, rock, and brick, respectively.

Microscale surface roughness differed by two orders of magnitude between the smoothest surface, glass (0.87 μm), and the roughest surface, brick (53.8 μm; Table 3-1). Benthic algal biomass exhibited a right-skewed peak (best fit with a Weibull distribution, SigmaPlot 8, Systat Software Inc.) over the range of roughness used (adnate: $r^2 = 0.85$, $P < 0.0001$; loose: $r^2 = 0.42$, $P < 0.0001$; total: $r^2 = 0.74$, $P < 0.0001$; Fig. 5). Algal biomass increased linearly with increasing surface roughness, up to a mean roughness of ~17 μm. In the linear portion of the curve, adnate algae increased at twice the rate as loose algae, increasing at 3.9 and 1.8 mg chl a m^{-2} μm^{-1} roughness, respectively. This trend was stronger for adnate forms ($r2 = 0.84$, $P = 0.001$) but was still significant for loose algae ($r^2 = 0.31$, $P = 0.001$). The proportion of loosely attached forms decreased linearly at a rate of 0.8% ($r^2 = 0.81$, $P = 0.001$) with each μm increase in mean roughness. Loosely attached dominance gave way to adnate dominance at ~17 μm.

Substrata with greater heterogeneity in surface roughness (coefficient of variation, CV) collected more total chl (linear regression, $r^2 = 0.91$, $P = 0.03$; Fig. 6). However, chl

heterogeneity (CV) on a particular substratum type decreased linearly ($r^2 = 0.71$, $P = 0.04$) with increasing heterogeneity in surface roughness. Substrata D generally increased with increasing roughness (Table 3-1), but no significant trends were found with D and benthic algal chl.

Surface area and light intensity.

Both the CLSM method and the soapy water method showed an increase in the 3-D surface area with increasing roughness; however, the soapy water measurements were consistently greater than the CLSM results (Table 3-1). Regression analysis of surface roughness versus CLSM measured area increase showed a linear gain in surface area of approximately 0.047 mm^2 μm^{-1} average roughness ($r^2 = 0.89$, $P < 0.001$). The soapy water method showed a linear gain in surface area of 0.098 mm2 μm^{-1} increase in average roughness ($r^2 = 0.69$, $P = 0.05$). Confocal microscopy results were used for further comparative analysis for consistency in the method used to collect substrata measurements.

Surface-area-adjusted chl differed significantly across substratum types for adnate and total algae ($P < 0.001$ and $P < 0.001$, respectively; Fig. 7), showing a similar trend to the non-adjusted values, and peaked at a 3-D to 2-D area ratio of 2:1. Loosely attached chl, though, was only significantly different on the roughest surface.

Increasing surface area enlarged the angle and length of pit walls. Table 3-3 shows the calculated availability of direct light on the smoothest, an intermediate, and the roughest substratum used in this experiment with varying substratum and microscale slopes, and incoming light directions. Direct light intensity on a given area of substrata was reduced 45% from glass to brick.

DISCUSSION

Algal biomass

Algal biomass was significantly affected by substratum texture. At the whole-substratum scale, our results generally support the previous findings that rougher (Clifford et al. 1992, Johnson 1994, Sanson et al. 1995) and more horizontal surfaces (Knott et al. 2004, Kralj et al. 2006) collect more algae. Yet our results differed in that biomass peaked at an intermediate roughness, suggesting that the stimulatory effects of increased texture on algal biomass accrual decrease as roughness increases past a certain point. Confocal microscopy measurements identified this peak at about 17 μm, which was similar to the roughness of the natural rocks found in this stream. It is tempting to speculate that more algal species were adapted to the surface roughness of the rocks, and that is why the peak biomass accrual occurred at a roughness approximately equal to natural rock roughness. The true biomass peak though, may lie in the roughness range between unglazed tiles and bricks, as there was a large gap between these roughness values. Algal biomass has been linked to other physical substratum characteristics, such as size (Watermann et al. 1999) and stability (Cattaneo et al. 1997), and it is likely that roughness is equally important in regulating a substratum's physical effect in streams.

Surface roughness is fractal in nature, and microscale roughness affects whole-substratum roughness. Thus, similar mechanisms may be regulating algal growth at both macro- and microscales. For example, edges of substrata tend to accumulate more algae than the interior surface (Comte et al. 2005), and rougher textured substrata (i.e., those with more microscale edges) tend to collect more algae (Clifford et al. 1992, Sanson et al. 1995). Additionally, algal cell attachment efficiency has been observed to increase with roughness at scales ranging from 1 to 14 μm (Scardino et al. 2006), from 0.1 to 1.2 mm (Johnson 1994), and from 2.0 to 4.0 mm

(Sanson et al. 1995). Therefore, our focus on roughness was not necessarily a comparison between scales, but an illumination and quantification of roughness that can be applied to both scales. Our data support the theory that in addition to macroscale texture (i.e., stream bed roughness, Quinn et al. 1996), microscale roughness has significant effects on algal accumulation. Additionally, we conclude that qualitatively assigning texture as smooth and rough decreases the accuracy of cross site comparisons of substrata effects as these classifications are subjective and scale dependent.

More algal accrual on horizontal than vertical surfaces in our study was consistent with findings in other systems and on varying substrata, such as glass slides in a Croatian lake (Kralj et al. 2006); asbestos plates in a British Columbian bay (Vandermeulen and DeWreede 1982); and pontoons, concrete breakwalls, and rocky reefs in Sydney bays (Glasby and Connell 2001, Knott et al. 2004). Studies looking at surface angles between 0 and 90^{o} are rare; however, the accumulation of the green macroalga Cladophora in Tosa Bay, Japan, on 0^{o}, 45^{o}, and 90^{o} acrylic tiles (Somsueb et al. 2001) followed very similar accumulation patterns to loosely attached algal growth on the angled tiles in Kings Creek.

Surface orientation is distinct at both the substratum and microscale levels and can be quantified independently at both scales. Unlike chl and orientation at the substratum scale, which was only significantly different at 90^{o}, chl at the microscale orientation peaked at an intermediate level. However, comparison with whole-substratum orientation is limited because none of the substrata had a mean microscale slope close to 90^{o}; but it is unlikely that many natural substrata have a mean microscale slope close to 90^{o}. A larger gradient of orientations at the substratum scale may have made microscale differences more apparent. Nevertheless, significant differences between 0^{o} and 45^{o} at the microscale level suggest that effects of orientation may change with

scale. Determining whether surface angles have more influence at the scale of an individual alga, or if substratum orientation overrides the effect of microscale angles, will require further study.

Consistent patterns at the scale of individual algal cells showed that microtopography differences can structure assemblages during development at the coarse separation of loose and adnate forms, and this may be partially a result of differential grazer removal abilities with texture (Dudley and D'Antonio 1991, Bergey and Weaver 2004, Hutchinson et al. 2006). Rougher surfaces appear to benefit both forms but favor the accumulation of tightly attached forms. There also appeared to be an optimal roughness and orientation range for both forms, with a wider optimal range for adnate forms, as shown by their smaller decline from the unglazed tile to the brick. All trends were consistently the strongest for adnate benthic algae, which is logical because this group is more closely associated with the surface.

The mechanisms behind changes in algal biomass and form with varying texture are not well understood. Microtopography measurements allow us to further examine three aspects of surface texture that may regulate resource availability and therefore influence algal accumulation: (i) overall surface heterogeneity, (ii) surface area available for colonization, and (iii) light availability on the surface.

Microscale heterogeneity

Habitat heterogeneity is a major driver of community diversity in lotic ecosystems and has been observed at the scale of watersheds (Vannote et al. 1980, Griffith et al. 2002), pools and riffles (Stevenson 1997), and substrata (Taniguchi and Tokeshi 2004). As long as the environment varies on a scale relevant to the organism in question, we should expect a biological response to changing physical conditions, even at a microscopic scale. The positive correlation of algal biomass with substratum roughness (CV) conforms to this presumption. Decreased

variability in algal biomass with increasing variability in substratum roughness was unexpected and deserves additional study. The decrease in variability in algal biomass may be the result of grazer/cell immigration/roughness interactions. At the riffle scale, Poff and Nelson- Baker (1997) observed no effect of substratum surface heterogeneity on algal biomass (CV) in an ungrazed system, but different (albeit increased) biomass variability in snail-grazed systems. Biofilm abundance patchiness also increased with individual substratum roughness in marine rocky intertidal biofilms because of grazing and algal recruitment efficiency (Hutchinson et al. 2006).

Rougher surfaces have deeper and steeper sloped pits, resulting in portions of the ''extra'' area becoming partially or completely shaded. This shading creates a mosaic of light intensities across a small area, possibly allowing species with different light requirements to coexist and increase overall assemblage variability and diversity (Steinman 1992). Also, light heterogeneity increases as the sun moves across the sky and regions that were shaded become lit and vice versa. Deeper pits also increase the distance of the diffusion boundary layer between a resident algal cell and the overlying water (Jørgenson 2001). As a result, living in a pit may reduce nutrient availability and slow waste removal (Hart and Finelli 1999). Still, deep pits are not completely uninhabitable by benthic algae and may provide benefits. Motile algae such as pennate diatoms and flagellates can move vertically, maximizing resource availability and protection from the substrata (Consalvey et al. 2004, Underwood et al. 2005). Fish grazers, such as *Campostoma anomalum*, which were common during the study, have mouthparts that scrape the substratum's surface but may not be able to get into the smaller crevices (Matthews et al. 1986, Bergey and Weaver 2004). Increased roughness traps more detritus (Bergey 1999, Taniguchi and Tokeshi 2004), which could serve as a nutrient source for colonizing algal cells

when mineralized by heterotrophic microorganisms. Finally, greater algal cell deposition on a rougher substratum may provide a larger initial base of cells to start reproducing, and increased sediments may provide additional nutrients to feed benthic algae growth.

Surface area

As surface roughness increased, surface area increased. If the increase in algal biomass was solely because of the increased area, then the adjusted chl values would be the same for each substratum type. This was generally true for loosely attached algae. Adjusted values were only different for the roughest surface, suggesting surface area availability is important for loose forms. Adnate forms (as well as total algae), though, were not strongly regulated by surface area. For tightly attached forms, it appears that after a certain 3-D increase (2:1 in this study) other factors appear to negate the positive effects of more surface area. A similar trend of decreasing algal biomass per area with increasing surface complexity at a centimeter scale was observed by Robson and Barmuta (1998). This trend was attributed to the added area creating lower quality attachment sites through less nutrient availability and more shading.

Light

Light often limits benthic algae growth (Hill et al. 1995, Roberts et al. 2004), and substrata texture changes light availability. Microscale texture increases surface area but decreases the intensity of light across that surface area (Table 3-3) because the same amount of light energy is distributed across a larger area (Lambert's Law). Additionally, direct light intensity changes with whole-substratum orientation and light direction because of microscale slope angle. For example, when the substratum (mean microscale slope of 63^{o}) is horizontal and the light is directly overhead, all surfaces receive approximately the same amount of light, which

is 45% of the incoming intensity. If that surface is rotated 90 degrees and the light source changes to a 45 degree incident angle, surfaces facing the light source receive almost 100% of the incoming intensity, while surfaces facing away from the light receive no direct light. The influence of whole-substratum tilting is greater on rougher surfaces, as increasing roughness increases the mean microscale slope of a surface. Our model is simplistic and does not take into consideration other factors that affect light availability to benthic phototrophs, such as light that is scattered, refracted, or absorbed by organism pigments (Kuhl et al. 1996), or differential properties related to variation in wavelength (DeNicola et al. 1992, Kelly et al. 2003). The model is presented to highlight the potential heterogeneity in light imparted by surface roughness characteristics.

We assume that chl content is equally related to algal biomass for both loose and adnate forms. When light becomes limiting, benthic algae can increase chl content (Thomas et al. 2006), and adnate biomass may be overestimated. In the future, CLSM methods could be used to measure algal biovolume relationships with surface texture, which would address this limitation. The above influence of texture might also be limited to adnate forms and/or early to midsuccessional assemblages. Once benthic algal mats become thicker and grow further from the substratum's surface, surface influence should diminish, with other factors dominating growth and loss dynamics.

Implications for collection

Artificial substrata are frequently used to assess stream benthic algae assemblages (Aloi 1990, Cattaneo and Amireault 1992) and have advantages over sampling natural substrata, such as reduction in algal variability and known time of colonization (Meier et al. 1983), and some (e.g., glass slides) can allow direct examination of benthic algal structure. Our study divided

algae into loosely attached (mostly green filaments) and adnate (mostly diatoms) categories, and our data are concordant with the previous findings that artificial substrata can produce different green algae, cyanobacteria (Cattaneo and Amireault 1992), and diatom abundances (Barbiero 2000). We show that gross growth forms can also be significantly affected by substrata, and a component of this difference may be the result of microscale texture.

The adnate portion of benthic algae in this study is analogous to that left behind after algae are removed during collection. A common collection technique is to brush or scrape rocks rather than extracting the entire rock for chl. On all surfaces, adnate forms were a large proportion of total biomass and exhibited more variability among substrata types than loose forms. Several studies have looked at the efficiency of brushing or scraping rock (Jones 1974, Cattaneo and Roberge 1991) and have also observed that significant amounts of algae can be left after scrubbing. This collection bias can potentially underestimate biomass as well as alter the proportion of adnate algae during identification.

To get more accurate estimates of benthic algae biomass, we recommend using substrata that are similar in texture and orientation to that of the natural stream and to extract the entire substratum for chl measurements, when possible. Ideally, it would be best to identify algal species on the surfaces they grow, and this has been suggested for some time (Jones 1974). However, currently this is neither easily done nor economically feasible for most researchers. Scraping and brushing substrata can leave behind significant amounts of adnate algae, which may differ with substrata type and brushing effort. Benthic algal data should therefore be collected, analyzed, and interpreted with knowledge of this limitation.

Table 3-1 Substratum surface characteristics for the six substrata used in the experiment.

Substratum	Mean roughness (μm)	Surface area increase		Mean microslope orientation (degrees)	% of microslopes < 45 deg.	Fractal dimension (D)
		Soapy water	Confocal			
Glass	0.87 (0.05)	1.00	1.00	1.05 (0.12)	99.8 (0.48)	1.983 (.035)
White tile	3.19 (0.45)	2.80	1.07	16.4 (2.28)	97.8 (1.10)	2.478 (.085)
Red tile	5.99 (1.36)	1.41	1.25	31.5 (2.85)	80.6 (6.77)	2.250 (.068)
Unglazed tile	15.2 (9.53)	4.14	1.88	43.6 (16.0)	51.6 (33.1)	2.419 (.168)
Rock	17.1 (9.62)	6.52	2.00	49.7 (10.0)	37.4 (21.2)	2.047 (.163)
Brick	53.8 (25.0)	5.93	3.53	63.1 (6.94)	15.6 (8.71)	2.445 (.167)

Table 3-2 Changes in microscale measurements with increasing lower limit resolutions on a single surface image (brick).

Smallest segment length measured (μm)	Mean roughness (μm)	Mean microslope orientation (degrees.)	Surface area (mm^2)
1.8 μm	61.8	84.1	15.2
5 μm	40.2	75.9	5.4
10 μm	36.5	63.8	2.7
15 μm	34.7	54.6	1.9
20 μm	33.9	48.3	1.6
50 μm	28.5	29.5	1.1
100 μm	23.2	18.6	0.9

Table 3-3 Example of how direct light intensity on a given point on a surface changes with whole substratum orientation and microslope angle.

Substratum (mean microslope angle)	Whole substratum orientation	Light hitting surface (% of full intensity)		
		Incident light directly above (all surfaces)	Incident light at 45° angle	
			Surfaces facing towards	Surfaces facing away
Glass (1.1°)	Horizontal	99.9	72.0	69.4
	Vertical	0.0	69.4	0.0
Unglazed tile (44°)	Horizontal	72.4	99.9	2.4
	Vertical	0.0	2.4	0.0
Brick (63°)	Horizontal	45.2	95.1	0.0
	Vertical	0.0	0.0	0.0

Calculated values (from Lambert's cosine law) are given for a substratum horizontal to the stream bottom and one rotated 90° (vertical), for situations where the light is coming from directly overhead, and from a 45° angle in the same direction as the 90º tilt.

Figure 3-1 Benthic algal accumulation in the study reaches following a scouring flood. A second-order sigmoidal curve fit (r2 = 0.87, P = 0.001), versus a linear fit (r2 = 0.78, P = <0.001), suggests algal biomass began to level off at ~4 weeks after the flood.

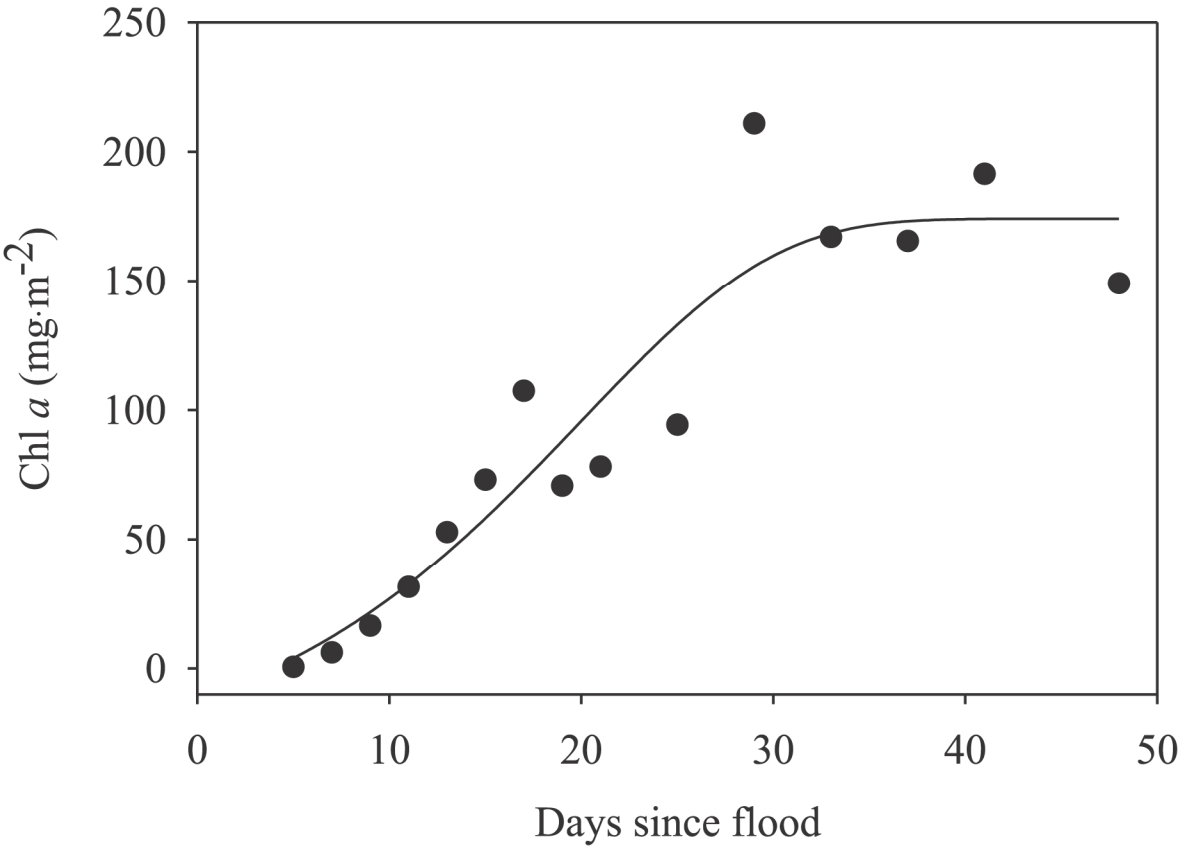

Figure 3-2 Representative 3-D surface plots and 2-D profiles of experimental substrata used. Images collected from confocal laser scanning microscopy.

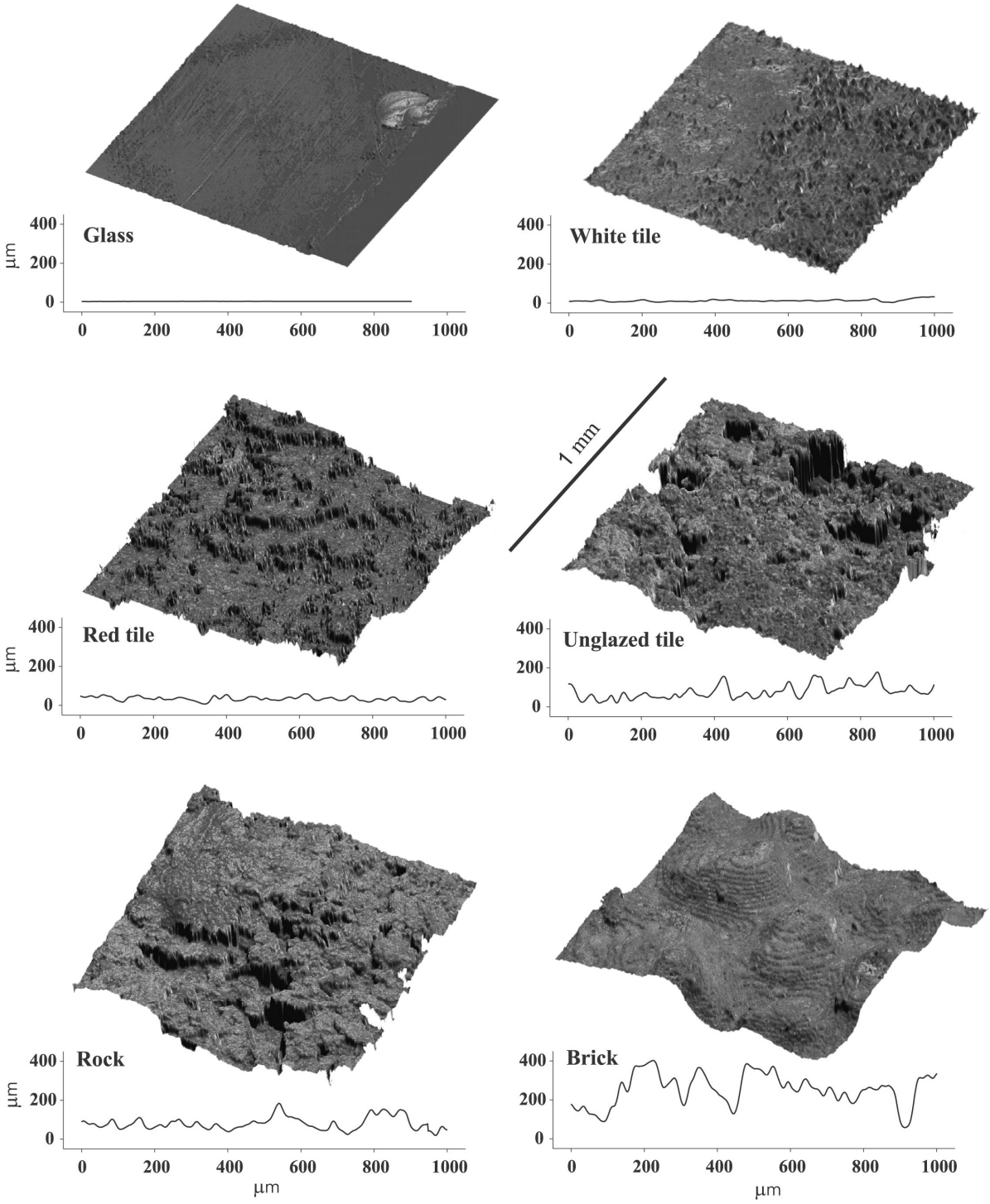

Figure 3-3 (a) Distribution of benthic algal chl a on tiles set out at 0~, 45~, and 90~ relative to stream bottom and divided into loosely attached, adnate, and total chl. (b) Benthic algal chl a values for substrata of varying surface roughness. Boxes represent the median, and 25th and 75th quartiles. Whiskers show values within 1.5 times the interquartile range. Boxes with the same letter indicate no significant difference, P < 0.05.

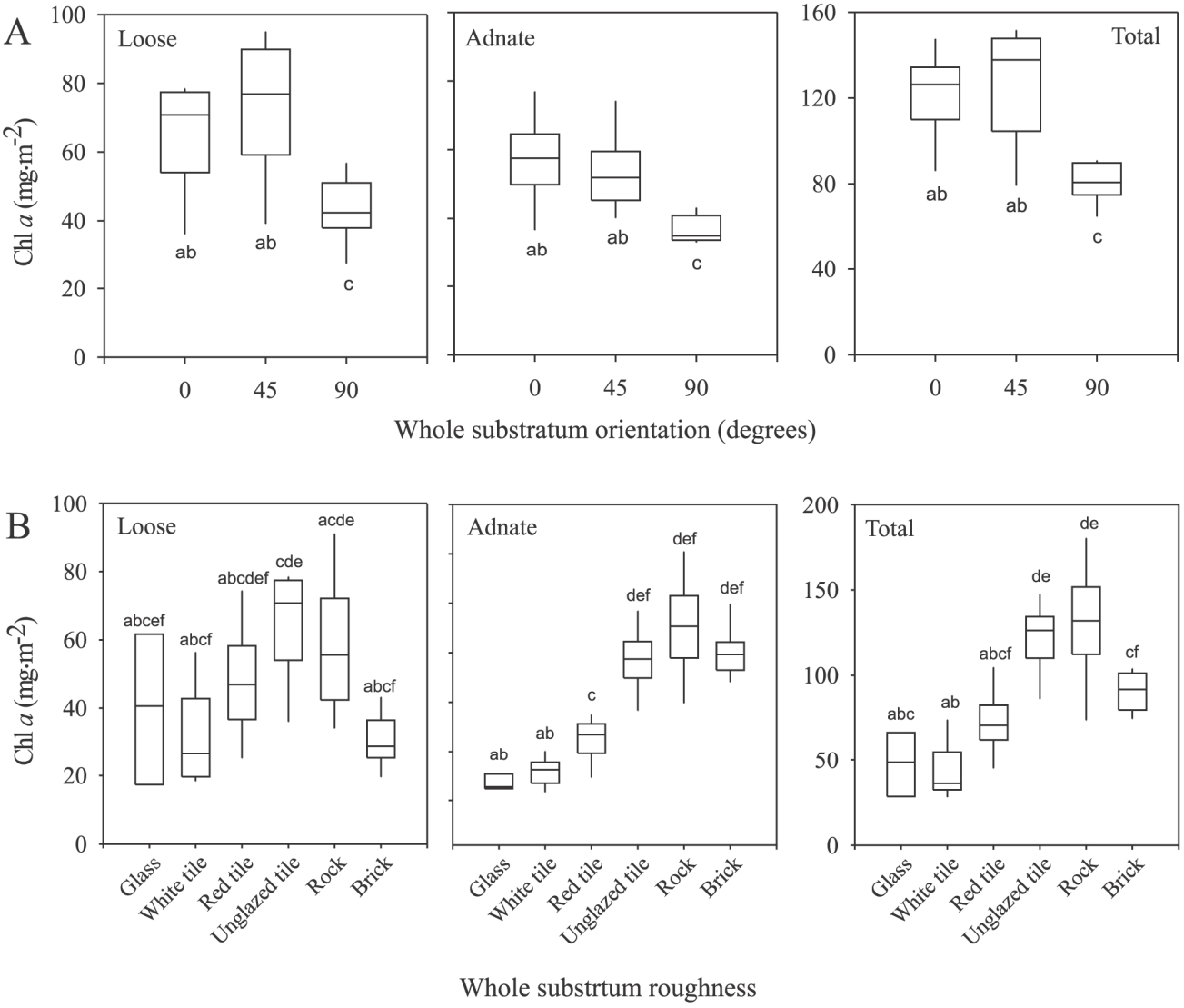

Figure 3-4 Chlorophyll a concentration versus mean microslope angle (i.e., angle of pit walls) for loose, adnate, and total benthic algae. Biomass increases with increased pit wall angle up to approximately 50~ and then decreases. Bars are 95% confidence intervals, and only the top interval is shown.

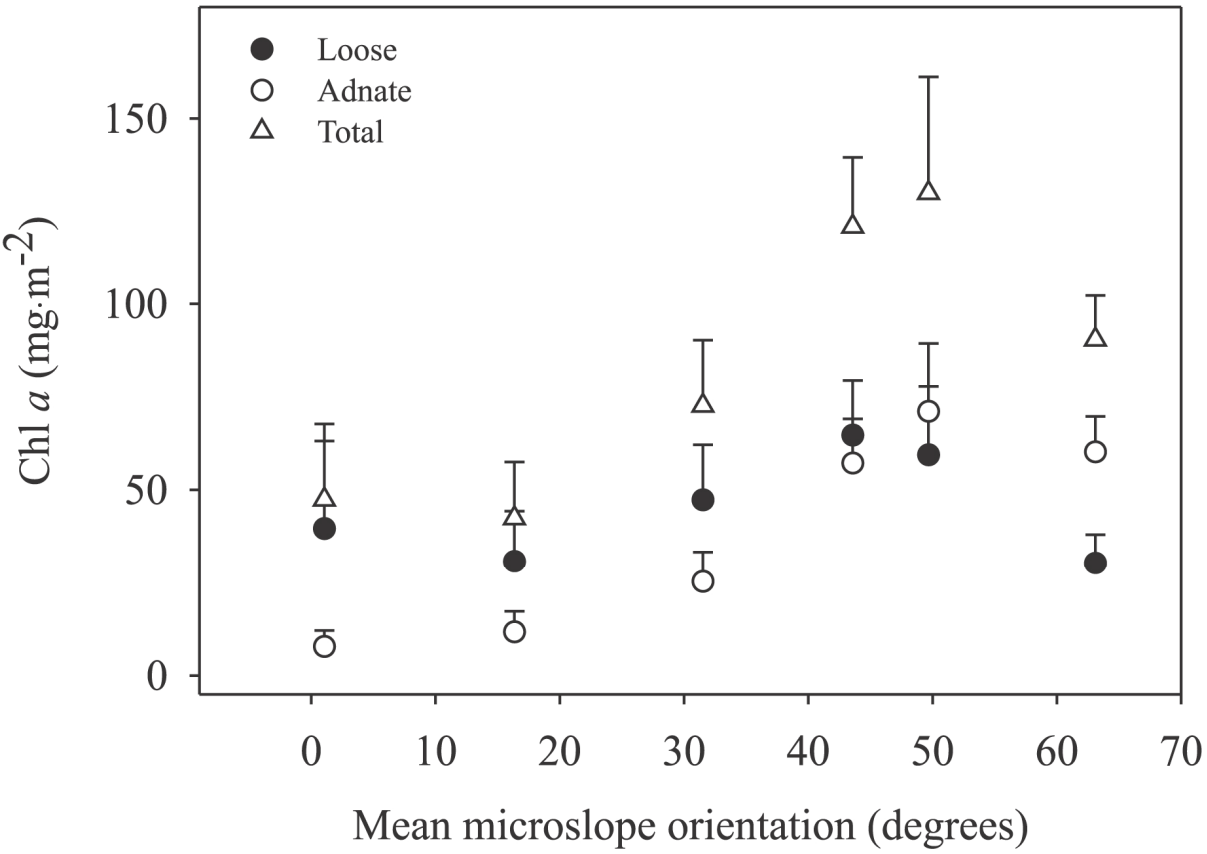

Figure 3-5 Chlorophyll a concentration versus mean roughness for loose, adnate, and total benthic algae. Biomass increases linearly with roughness until approximately 17 lm and then begins to decrease. A shift in dominance from loosely attached to adnate forms occurs around a roughness of 15–17 lm. Bars are 95% confidence intervals.

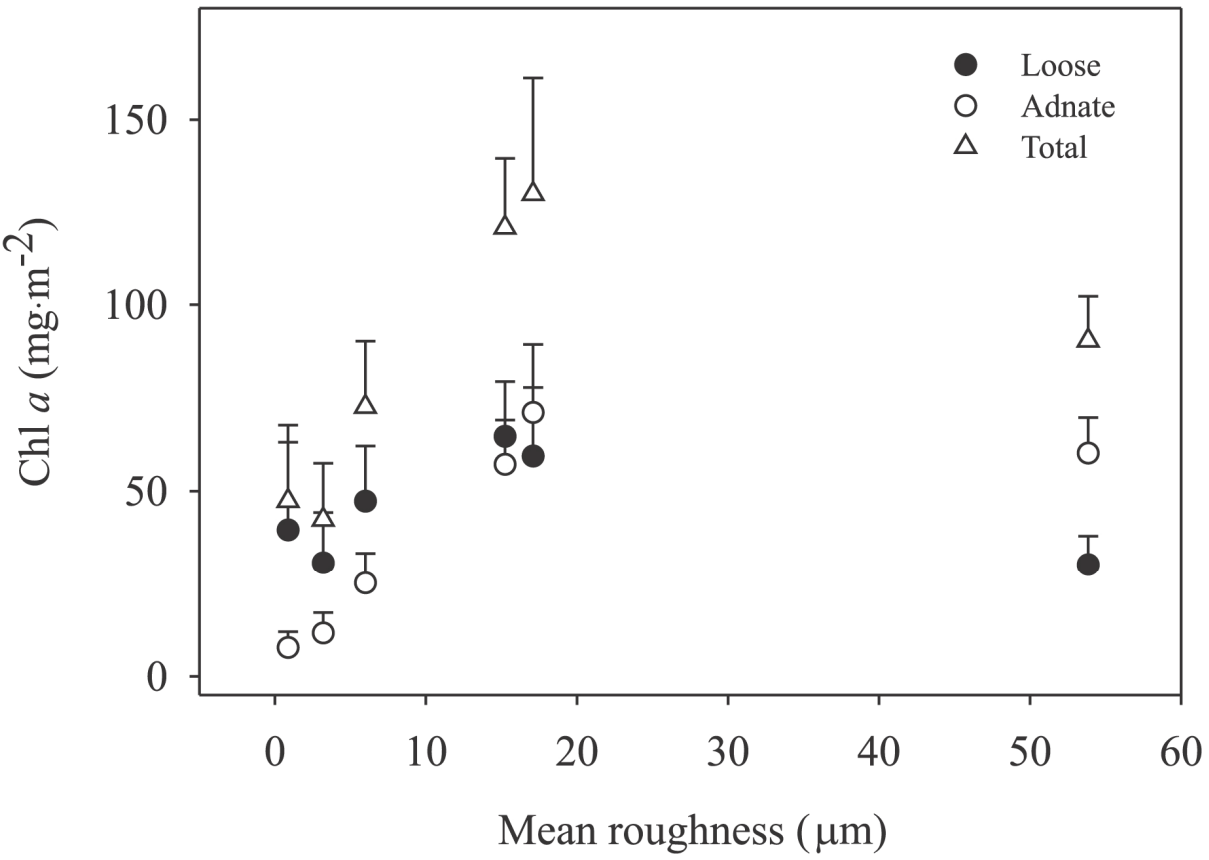

Figure 3-6 Comparison of the variation of roughness on a substratum (coefficient of variation, CV) with the mean algal biomass and biomass variability (CV) on each substratum type. Algal biomass increased with roughness heterogeneity across a surface, but algal biomass variability decreased with roughness heterogeneity.

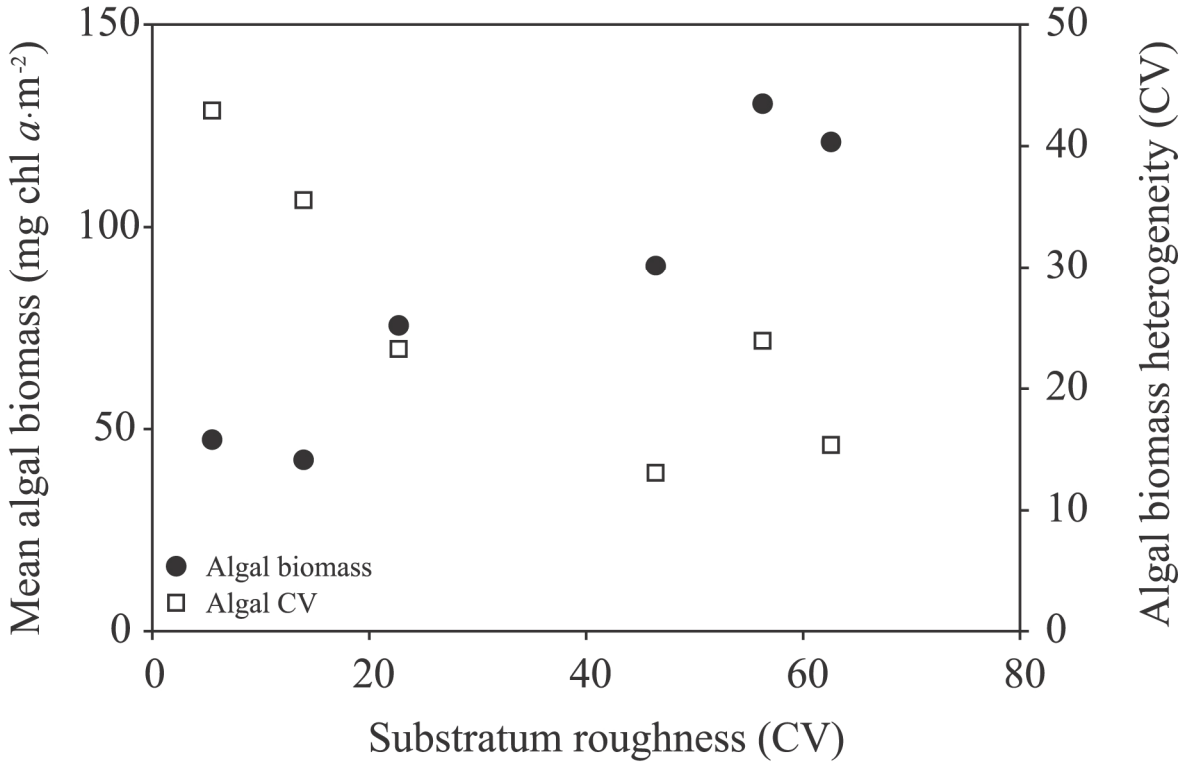

Figure 3-7 Chlorophyll a values for loose, adnate, and total benthic algae adjusted for increased surface area due to increased roughness. This equalizes the surface area and chl relationships among all substrata. Loose forms only differed significantly on the roughest surface, while adnate and total forms still showed a pattern similar to before adjustment. Bars are 95% confidence intervals.

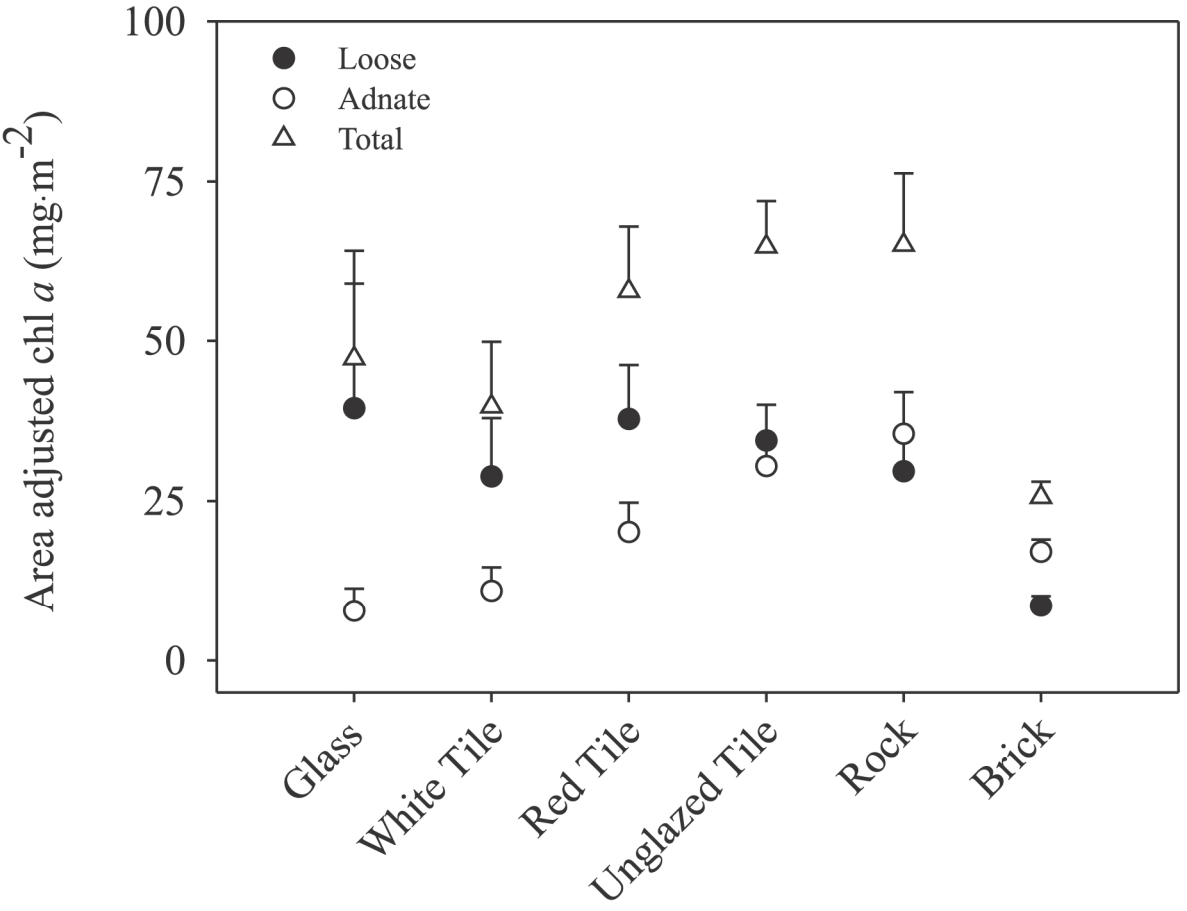

CHAPTER 4 - Subcellular localized chemical imaging of benthic algal nutritional content via HgCdTe array FT-IR[2]

Justin N. Murdock, Walter K. Dodds, and David L. Wetzel

[2] Reprinted with permission from "Subcellular localized chemical imaging of benthic algal nutritional content via HgCdTe array FT-IR" by Justin N. Murdock, Walter K. Dodds, and David L. Wetzel. Vibrational Spectroscopy, In Press.

ABSTRACT

Algae respond rapidly and uniquely to changes in nutrient availability by adjusting pigment, storage product, and organelle content and quality. Cellular and subcellular variability of the relative abundance of macromolecular pools (e.g. protein, lipid, carbohydrate, and phosphodiesters) within the benthic (bottom dwelling) alga *Cladophora glomerata* (a common nuisance species in fresh and saline waters) was revealed by FT-IR microspectroscopic imaging. Nutrient heterogeneity was compared at the filament, cellular, and subcellular level, and localized nutrient uptake kinetics were studied by detecting the gradual incorporation of isotopically labeled nitrogen (N) (as $K^{15}NO_3$) from surrounding water into cellular proteins. Nutritional content differed substantially among filament cells, with differences driven by protein and lipid abundance. Whole cell imaging showed high subcellular macromolecular variability in all cells, including adjacent cells on a filament that developed clonally. N uptake was also very heterogeneous, both within and among cells, and did not appear to coincide with subcellular protein distribution. Despite high intercellular variability, some patterns emerged. Cells acquired more ^{15}N the further they were away from the filament attachment point, and ^{15}N incorporation was more closely correlated with phosphodiester content than protein, lipid, or carbohydrate content. Benthic algae are subject to substantial environmental heterogeneity induced by microscale hydrodynamic factors and spatial variability in nutrient availability. Species specific responses to nutrient heterogeneity are central to understanding this key component of aquatic ecosystems. FT-IR microspectroscopy, modified for benthic algae, allows determination of algal physiological responses at scales not available using current techniques.

INTRODUCTION

Algae growing on the bottom of aquatic habitats (i.e. benthic algae) play a major role in ecosystem energy flow in all shallow lighted habitats such as streams, shallow lake bottoms, estuaries, wetlands, and coastal marine habitats. These algae take up inorganic nutrients from the water, metabolize them into organic form, and transfer the nutrients to the organisms that eat them. Benthic algae often respond to excessive nutrient input with extreme growth that may harm water quality and other aquatic organisms (Dodds and Welch 2000, Smith 2003). Current methods limit the distinctions of in situ algal stoichiometric responses to nutrient availability to a whole community scale because they depend upon quantitative analysis of macro-scale quantities (e.g. deciliters of water or milligram of tissue). Species have evolved unique growth responses to changing environmental nutrient availability by adjusting cellular content and quality of macromolecular pools devoted to pigments, storage products, and organelles. Understanding species-specific growth responses to changes in stream nutrient concentrations will assist in predicting how algal assemblages will change with increased human-induced nutrient loadings, as well as describing the basic ecological interactions among these organisms.

Algal nutritional analysis with Fourier transform infrared (FT-IR) microspectroscopy is a quickly expanding area and has been applied to the analysis of cultured single cell and colonial algae [Beardall et al. 2001, Stehfest et al. 2005, Hirchmugl et al 2006, Laing et al. 2006), and natural phytoplankton (algae suspended in the water column) communities in lake (Sigee et al. 2002, Dean and Sigee 2006, Dean et al. 2007) and marine (Giordano et al. 2001) environments. FT-IR algal investigations have focused on the cellular response of major organic functional groups, or macromolecular pools (e.g. proteins, lipids, carbohydrates, and phosphodiesters), to changing environmental nutrient concentrations. Measurable responses have been observed in

diatoms (Giordano et al. 2001, Stehfest et al. 2005), green algae (Sigee et al. 2002, Hirchmugl et al 2006, and cyanobacteria (Noguchi and Sugiura 2003, Dean and Sigee 2006). For example, nitrogen limitation in algae often causes decreases in protein, and increases in lipid and carbohydrate content (Giordano et al. 2001). Currently, most analyses have been done with individual spectra within spatial areas from approximately 10 to 30 μm^2, or line mapping. Since algal cell sizes can differ by an order of magnitude among species and cellular content is often distributed across a heterogeneous matrix throughout the cell, whole cell/colony imaging may provide a more accurate determination of whole cell/colony responses to micro- and macro-habitat environmental change.

Benthic algae and phytoplankton develop in different nutritional environments. Benthic algae grow in a three-dimensional matrix attached to a surface (e.g. rocks, sediment, aquatic plants, or other benthic algae) (Figure 4-1), and obtain nutrients from water passing over or through the mat, or mineralized from nearby algae. As algal mats develop, space separating individual algae decreases and inter- and intraspecific competition for nutrients increases. Enhanced competition and variable nutrient diffusion rates into mats create patchy microenvironments unique to benthic algal communities. This environmental variability can translate into nutritional variability within the community (Dodds 2003) and may extend to nutritional heterogeneity in individual algal filaments, colonies, or cells.

The goal of this study was to assess the applicability of FTIR microspectroscopic imaging to detect nutritional heterogeneity and nutrient uptake in benthic algae at the filament, cellular, and subcellular level. Adjustments to current phytoplankton sample preparation techniques were implemented to study the macromolecular pool distribution in the filamentous alga *Cladophora glomerata*. Nutrient uptake kinetics was studied by localizing the incorporation

of ^{15}Nitrogen (as $K^{15}NO_3$) into cellular proteins (Haris 1992, Noguchi and Sugiura 2003). *Cladophora* has proliferated in streams globally due to increased nutrient loading, and can often reach nuisance levels (Dodds and Gudder 1992). Excessive growth decreases streambed habitat, food resources, and water quality for other aquatic organisms, clogs municipal water intake pipes, and decreases stream recreational value (Dodds and Welch 2000). More information is needed on the physiological response of *Cladophora* to nutrient pollution to help mitigate excessive growth.

METHODS

Sample collection and processing

Rocks dominated by natural assemblages of the green filamentous alga *C. glomerata* were collected from a shallow prairie stream on the Konza Prairie Biological Station (KPBS) near Manhattan, KS, USA. KPBS is a 1637 ha pristine tallgrass prairie ecosystem containing low nutrient headwater streams that are minimally disturbed by human influences. In the laboratory, five rocks were placed into each of two 22 L recirculating chambers filled with low nitrogen stream water (~7.2 µmol total N, ~0.65 µmol nitrate, <0.28 µmol ammonium), and incubated for 4 days under constant light (~300 µmol quanta m^{-2} s^{-1} photosynthetically available radiation supplied by fluorescent lights). Chambers were spiked daily with either 0.32 µmol of $K^{14}NO_3$ or$K^{15}NO_3$, the amount of nitrogen taken up by a similar amount of benthic algae in a 24 h period (Murdock, unpublished data). Additionally, 0.012 µmol of KH_2PO_4 was added daily to prevent phosphorus limitation of algal growth.

Filaments were gently removed with forceps at the point of attachment from rocks and rinsed three times with deionized water (Sigee et al. 2002). Cells were examined under light

microscopy to determine if cell walls or cellular contents were physically changed due to possible ionic imbalance from rinsing (Dean and Sigee 2006). No visible changes were observed. To create areas of single cell layers required for analysis, filaments were placed on an IR reflective (Low-e) slide (Kevley Technology, Chesterfield, OH, USA) with a few drops of deionized water to float the filaments and allow even spreading of the filament branches. Excess water was slowly removed with a pipette and slides were dried in a desiccator for approximately 12 h. Slides were reexamined to check for physical changes in cellular content distribution due to drying. Some cells had expelled portions of their cellular content, but most appeared intact and minimally altered. Spectra were recorded from only unchanged cells.

Spectra and map acquisition

Samples were analyzed with a PerkinElmer Spotlight 300 FT-IR microspectrometer with a 16 element mercury– cadmium–telluride (MCT) pushbroom focal plane array producing a rectangular (x, y) image. The optical arrangement results in a projection of the detector elements that provide a minimum nominal pixel size of 6.2 μm x 6.2 μm. This optical arrangement was used to obtain reflection absorption spectra of whole algal cells. Additionally, individual spectra were obtained in single detector mode from the center of randomly selected cells along a filament using a nominal pixel size of 25 μm x 25 μm.

Spectra were collected from 4000 to 700 cm^{-1} with a spectral resolution of 4 cm^{-1}, and 64 scans co-added. Background spectra were obtained from a clean section of the IR reflective slide. A constant sample temperature of 21.8^{o}C was maintained during spectra collection. Image absorption spectra were baseline corrected using Spectrum V. 5.3.1 (PerkinElmer).

Macromolecular bands of interest were amides I and II (1655 cm^{-1} and 1545 cm^{-1}, respectively), lipid carbonyl (2927 cm^{-1}) and CH_2 (1729 cm^{-1}), carbohydrate (1025 cm^{-1}), and

phosphodiester P O (1240 cm^{-1}) as stated in Table 4-1. The enhanced CH_2 stretch vibrational band at 2927 cm^{-1} that accompanies the 1729 cm^{-1} carbonyl band was used to image lipid content because the larger peaks allowed for better area differentiation among spectra (Montechiaro et al. 2006). Peak areas of the 1729 cm^{-1} band in close proximity of the amide I band were less reliably determined in this application. Bands monitored in this study were identified in the previous algal and bacterial FTIR studies of Naumann (2001), Giordano et al. (2001), Sigee et al. (2002), and Heraud et al. (2005).

Spectra from the center of 15 individual cells were randomly collected along the length of each filament, and images of six complete *Cladophora* cells (~75 μm x 200 μm per cell, containing approximately 300 individual spectra per cell) were produced. Cell to cell distances along a filament were measured from brightfield photomicrographs of whole filaments using Image J digital image analysis software (Abrmoff and Magelhaes 2004). Cell distance was measured as the linear distance from the point of spectral collection along the filament and branches to the point the filament attached on the rock.

Data analysis

The absorption bands of protein, carbohydrate, lipid, and phosphodiester from individual spectra of cells along a filament were compared with (1) hierarchical cluster analysis using Ward's method and Pearson's correlation coefficient distances, and (2) principal component analysis (PCA) to explore intracellular nutritional variability (Naumann 2001, Choo-Smith et al. 2001). Baseline corrected peak areas were calculated from the band area at the wavenumber ranges stated previously for each macromolecular pool.

Rectangular (x, y) images of whole cells were used to explore subcellular nutritional variability. Principal component analyses were used to delineate areas of contrasting

macromolecular composition within whole cell images. PCA factor images were produced using data from the fingerprint region and CH_2 stretching vibrational region of each spectra within a cell at a pixel size of 6.2 μm x 6.2 μm. Factor scores were plotted to show spatial heterogeneity of nutritional content, and loading plots indicated which absorption bands were driving subcellular differences (Dean and Sigee 2006).

^{15}N uptake by cells was measured through a shift in the amide II peak. A change in the peak frequency provided rudimentary evidence of ^{15}N incorporation into cellular proteins. An initial estimate of ^{15}N incorporation was made by calculating the ratio of the resultant amide II peak height at 1535 cm^{-1} to the original ^{14}N amide II peak height at 1545 cm^{-1}. The wavenumber of the ^{14}N amide II peak (1545 cm^{-1}) was determined as the average amide II peak location from 20 *Cladophora* cells from the $K^{14}NO_3$ treatment. This method was used to create whole cell images of ^{15}N incorporation.

Peak modeling was used as an alternative quantitative approach to measure ^{15}N uptake. Fourier self-deconvolution was applied to individual spectra from the ^{15}N treatment to enhance the resolution of the separate ^{14}N and ^{15}N peaks in the amide II band. The ^{14}N and ^{15}N peaks were modeled using Gaussian and Lorentzian curve fitting with an iterative curve fitting process (Grams/AI Version 7.02, Thermo Scientific, Waltham, MA, USA) using a full width at half height (FWHH) of 10, and the area under each peak was determined. The ratio of the shifted peak area to the original peak area was used as the measure of ^{15}N incorporation. Linear regression analysis was used to compare nutrient content and cell location along the filament to the magnitude of ^{15}N uptake.

RESULTS

Nutrient variability

Differences among cells

Macromolecular pools were highly variable among spatially disparate *Cladophora* filaments (cm apart), as well as among cells within a single filament (mm apart) (Table 4-1). However, the variability of each nutrient pool was similar (CV ranged from 32 to 53%, Table 4-1). Cluster analyses based on macromolecule peak areas separated cells into three distinct groups, and into four groups based on peak area ratios. However, there was no apparent meaningful grouping variable such as distance apart on a filament or day filament was sampled. Principal component analysis also did not differentiate cells by nutritional content based on peak area or peak ratio. Despite a lack of spatial differentiation, some trends in *Cladophora* cellular content were evident.

There was a considerable difference in the co-occurrence of macromolecular pools among all *Cladophora* cells. The amide I (protein) and lipid bands had a strong positive correlation ($r = 0.91$, $n = 50$), while carbohydrate correlations with proteins and lipids were weaker, but still significant. Phosphodiester content had only a weak correlation with carbohydrates ($r = 0.34$, $n = 50$) (Table 4-2). A multivariate comparison of macromolecular pool composition among cells with PCA further supported the importance of protein and lipid in differentiating *Cladophora* cells. The first two factors accounted for 83.2% of the nutrient variation (factor 1, 59.8%). Factor 1 was characterized by the dominance of proteins and lipids, with factor 2 dominated by high carbohydrates and phosphodiesters (Figure 4-2A). A PCA of nutrient ratios among cells showed a close relationship of protein and lipid content remained

relatively constant, and intracellular variation appeared to be driven by changes in the proportions of carbohydrate and phosphodiester concentrations relative to lipid and protein (Figure 4-2B).

Subcellular differences

Subcellular imaging of entire *Cladophora* cells showed evidence of high nutritional variability within a cell. For example, Figure 4-3 illustrates that discrete measurements in a single cell can produce different spectra at the base, middle, and tip. When adjacent cells were imaged, distinct differences in individual macromolecular pool distribution were evident. Notice in Figure 4-4 that high phosphodiester content that occurred in one cell was absent in the other. Carbohydrate concentrations were high in the base and tip of the cells, but were more evenly distributed throughout the cell than the other components. Despite these differences some subcellular patterns were evident. Similar to intracellular patterns, the location of protein and lipid concentrations were coincident in both cells. Also, subcellular images showed that the overall concentration of nutritional pools was consistently greater at terminal ends of cells and at the nodes of adjoining cells.

Subcellular imaging of nutritional ratios revealed nutrient co-occurrence in *Cladophora* cells. In Figure 4-5, macromolecular peak ratio images show the cell perimeter is dominated by lipids, evidenced by the high lipid:carbohydrate and lipid:protein content. In contrast, the interior contains areas of high protein and phosphodiester concentration. These images confirm that nutrient ratios within single cells can be at least as spatially variable as individual macromolecular pools.

Principal component analysis further delineated the spatial distribution of the complex combinations of all macromolecular pools within a cell. Figure 4-6 shows PCA factor images

and spectra loadings of three separate cells (A, B, and C) for factors 2 (top image in each pair of images) and 3. Factor 1 was driven by physical differences within the cell and was not considered. All cells showed a defined perimeter that had a very different chemical makeup than the center. In cells (A) and (B) this perimeter was dominated by lipids and carbohydrates, while C's perimeter contained high carbohydrate but low lipid content. Distinct areas dominated by proteins are evident in all cells in factor 3 images.

Imaging adjacent cells (as done in Figures 4–6) shows that in natural benthic algal communities, cells of the same species that are only mm apart can vary substantially in their nutritional heterogeneity. The spatial resolution of this technique also allowed the distinction of different algal species physically touching one another, e.g. the discrete spectra of a diatom attached to a *Cladophora* cell was resolved in spectrum 9 of Figure 4-3.

Nitrogen uptake

Differences among cells

^{15}N incorporation in Cladophora cells was observed as a shift in the amide II peak from 1545 to 1535 cm^{-1}. There was an average peak shift of 7 cm^{-1} (to 1538 cm^{-1}) after 3 days, and 10 cm^{-1} (to 1535 cm^{-1}) after 4 days (Figure 4-7A). As the heavier ^{15}N isotope was incorporated into amine group proteins there was a reduction in the 1545 cm^{-1} peak and increase in the 1535 cm^{-1} peak. An intermediate peak appeared at 1541 cm^{-1} at the position of an original amide II shoulder; however it vanished upon spectral subtraction of the original ^{14}N spectra. Thus, this artifact was disregarded. A gradual progression of the amide II peak towards 1535 cm^{-1} was evidenced by a frequent peak doublet appearing in spectra from days 3 and 4 during the

incorporation of the ^{15}N isotope. Fourier self-deconvolution sharpened the ^{14}N and ^{15}N peaks in the amide II band (Figure 4-7B) and second derivative spectra clarified the existence of separate peaks (Figure 4-7C). Several spectra with single amide II peaks at 1535 cm^{-1} were observed after 4 days indicating that some proteins had become completely labeled with ^{15}N by this time. No change in the peak position was detectable in day 1 or 2 spectra.

Amide II ^{15}N:^{14}N peak height ratios provided a cursory indicator of the extent of ^{15}N uptake. However, curve modeling was chosen for quantification and resulted in mean ratios of 0.93 (S.D. 0.5) and 1.75 (S.D. 1.2) for days 3 and 4 individual spectra, respectively. Amide II ^{15}N:^{14}N peak height ratios were less subjective and less variable between cells, but showed weaker relationships with cell macromolecular pools. On day 4, ^{15}N uptake by a *Cladophora* filament exhibited an exponential relationship with distance from the point of attachment (Figure 4-8). Less than 3 mm from the rock, cells had a consistent 1:1 peak area ratio of ^{15}N to ^{14}N, but exhibited a 5-fold increase from 3 to 4 mm. Nutritional relationships with the modeled ^{15}N ratios were weak, with the strongest being a positive linear relationship with phosphodiester content (r^2 = 0.34, n = 29). The other constituents only showed a weak positive relationship with ^{15}N after day 4, e.g. lipid (r^2 = 0.21), and protein (amide I, r^2 = 0.26).

Subcellular differences

Whole cell images of ^{15}N content were produced to show where N was most readily incorporated within the cells, and representative images are displayed in Figure 4-9. Intensity values corresponds to the ratio of the ^{15}N (1535 cm^{-1}) to ^{14}N (1545 cm^{-1}) peak heights. Peak height ratios were used because modeling of the hundreds of individual spectra that make up each image was not feasible in this study. Although the cells in each image developed very close

together, they have taken up different amounts of ^{15}N, and incorporated it into different locations. When compared to the protein distribution of these cells (Figure 4-4), it is apparent that ^{15}N uptake did not necessarily coincide with areas of elevated protein concentration. Additionally, there was no coincidence of ^{15}N uptake with areas of high protein:lipid content at a subcellular level. Because whole cell images were taken from different filaments it was not possible to compare ^{15}N uptake and distance relationship at the subcellular level beyond two adjacent cells.

DISCUSSION

Cladophora filaments that developed in a natural stream had an extremely patchy nutrient distribution. Cells could not be differentiated by spatial distance or cell type based on nutritional content using a nominal pixel size of 25 μm x 25 μm (approximately one fourth to one third the area of the cell). Thus we were unable to determine if some filaments, or cells along a filament, were nutritionally 'healthier' than others. However, we were able to define which macromolecular pools (i.e. lipids and proteins) were highly correlated among *Cladophora* cells, and that lipid and protein content were also driving subcellular variability within this species.

Subcellular imaging of the macromolecular pool distribution provided insight into the lack of intracellular patterns seen from discrete spectra. The finding that genetically identical, adjacent cells had very different subcellular nutrient content and distribution suggests that consistent nutritional spatial patterns may not exist. It also emphasizes the highly plastic stoichiometric nature of this species. We found that spectra from single points in *Cladophora* cells can be very different at high spatial resolution (e.g. Figures 4-3 and 4-4). Thus taking spectra in the middle of the cell without considering cell wall content or areas of rapid growth

can potentially give results that do not accurately reflect the nutritional content of the entire cell. The appropriate nominal pixel size and spectral collection location will likely vary between inter- and intracellular investigations of different algal species.

One distinct pattern often seen in whole cell images was a higher concentration of total nutritional content at the ends of the cells. *Cladophora* filaments grow through apical (branching) and intercalary (cell lengthening) growth, and the dominant growth pathway is greatly dependent on environmental conditions (Whitton 1970). Thus, accumulation of macromolecular pools at the branch apical tips, and cellular nodes would correspond to keeping nutrients in portions of the cell with high-energy demand.

In *Cladophora*, proteins are mainly associated with chloroplasts and nuclei, lipids with cell and thykaloid membranes, carbohydrates with starch storage products and cellulose cell walls, and phosphorus with nuclei and polyphosphate storage products (Heraud et al. 2005). Cells are multi-nucleated with chloroplasts evenly distributed throughout the intercellular space. Contents can also shift depending on cell state and light availability (Whitton 1970). PCA factor images and nutrient ratio images of whole cell lipid, protein, and carbohydrate locations were consistent with these known nutrient distributions. Due to the relatively complex composition of algal cellular components, a somewhat heterogeneous distribution of macromolecular pools within *Cladophora* cells was expected. However, the high nutritional variability between adjacent cells, i.e. cells that were created by cloning, was not anticipated a priori.

A temporal progression of ^{15}N incorporation into cellular proteins was evidenced by a doublet in the amide II peak region. This suggests that some proteins had incorporated ^{15}N and some had not. As a greater proportion of the proteins became labeled, the lower frequency peak got taller while the higher frequency peak decreased, causing an overall shift in the amide II peak

as more ^{15}N was incorporated into cellular proteins (Kimura et al. 2003). The amide II shift was similar to that observed by Kimura et al. (2003) in cyanobacterial cells fully labeled with ^{15}N. This trend was more pronounced from the deconvolved spectra where a progression through three frequencies became evident.

Calculations of peak areas through modeling provided ^{15}N ratios that better coincided with cellular nutrient content and N uptake than the preliminary direct measurements of peak heights of the raw spectra. The use of this method to obtain ^{15}N to ^{14}N ratios shows promise. Since execution of this method relies on the subjective selection of curve fitting parameters, and the vibrational contributions to the amide II band have not been as well studied as the amide I band, more data sets are needed to refine selection of parameter values for modeling the amide II band. Further investigation of N uptake from different sources (i.e. ammonium and dissolved organic N) is also warranted.

Whole cell imaging provided individual cell physiological responses by localizing subcellular N incorporation. Our observation that N uptake did not correlate with regions where proteins were most concentrated suggests that other cell constituents, such as amino acids (Veuger et al. 2007), are initially taking up N throughout the cell. Localizing N uptake can provide insight into where nutrient microenvironmental hotspots are occurring and how cells close to this region respond compared to cells in less nutrient replete areas of the mat.

External nutrient availability regulates internal algal nutrient content (Dodds 2002), yet it is difficult to analytically detect differences in dissolved nutrient concentration in the water at scales relevant to individual cells. The high nutrient variability within adjacent cells suggests the existence of sub-millimeter and possibly sub-micrometer nutrient microenvironments within benthic algal mats. This finding supports previous studies that proposed the existence of

microscale nutrient gradients due to microscale differences in water velocity (Dodds et al. 1999), substratum topography (Murdock and Dodds 2007), and light availability (Dodds and Biggs 2002) within benthic algal mats. Whole cell, spatially resolved imaging of nutritional content has potential to help predict nutrient availability within different portions of a benthic algal mats given different environmental conditions.

Previous work on phytoplankton using individual point spectra has illustrated very good differentiation among different species and among single species exposed to nutrient replete or depleted environments (Giordano et al. 2001, Dean and Sigee 2006, Dean et al. 2007). However, since phytoplankton are suspended in the water column, regardless of if they are cultured or taken from natural communities, they are exposed to
more homogeneous ambient nutritional conditions than are algae in benthic mats. Thus studying benthic algal communities requires a modified approach in both sample preparation and cellular spectral measurement to best reveal response patterns. Imaging the subcellular distribution of single cell and filamentous phytoplankton will shed light on the influence of nutrient availability in benthic mats on intracellular nutrient heterogeneity.

Current FT-IR microspectroscopy allows a relatively fast image acquisition time for entire cells (less than 1 h per 75 μm x 200 μm cell at relatively high spatial and spectral resolution), which is needed to accurately characterize larger algal cells grown in heterogeneous environments. This method is still limited to algal species that do not change physical cell shape when dehydrated. For example, whereas *Cladophora* appeared to maintain even distribution of cell contents upon drying, we observed two other species of green filamentous algae, *Ulothrix spp*. and *Spirogyra spp*. that did not. Methods have been developed to analyze live, hydrated phytoplankton cells (Heraud et al. 2005). Development of similar methodology for

benthic algae will enable more accurate subcellular measurements and whole community analysis.

FT-IR microspectroscopy has great potential in helping to understand benthic microbial ecology. Determination of individual cell and subcellular stoichiometric ratios can partition the contribution of certain species/cells, to the removal of nutrients from the surrounding water, and determine if all cells in a filament or colony have a similar response. Most lakes, streams, and wetlands have a substantial benthic algal component, and attached algae are also important in biofouling in lighted aquatic environments. A stronger understanding of environmental conditions experienced by individual cells of attached algae may ultimately offer insights into the ecology and management of these organisms.

Table 4-1 Point spectra (intercellular) summary statistics for macromolecular peak areas and peak ratios (n = 50 cells).

	Wavenumber (cm-1)	Assignment	Minimum	Maximum	Mean	CV
Peak areas						
Lipid (as straight chain CH_2)	2927	C-H stretch of CH_2 (asymetric)	8.33	38.4	22.0	0.37
Protien (Amide I)	1655	C=O stretch of amide I	5.72	33.0	18.5	0.36
Protein (Amide II)	1545	N-H bend and C-N stretch of amide II	0.24	13.1	6.12	0.53
Carbohydrate	1025	C-O-C stretch of pollysaccharides	7.85	93.8	55.3	0.39
Phosphodiester	1240	P=O stretch (symmetric) of polyphosphate storage products, phosphoralated protiens, DNA, RNA	3.06	15.7	8.15	0.32
Peak ratios						
Amide I / Lipid			0.51	1.16	0.85	0.16
Amide I / Carbohydrate			0.12	1.32	0.41	0.65
Amide I / Phosphodiester			0.95	7.03	2.47	0.50
Lipid / Carbohydrate			0.15	2.10	0.49	0.70
Lipid / Phosphodiester			1.07	9.21	2.97	0.52
Carbohydrate / Phosphodiester			1.92	19.6	7.18	0.49

Table 4-2 Point spectra (intercellular) macromolecular peak area correlation coefficients.

	Lipid	Protien (Amide I)	Protein (Amide II)	Carbohydrate	Phosphodiester
Lipid	-	**0.906** ***<0.001***	**0.767** ***<0.001***	**0.475** ***0.0004***	0.232 *0.1020*
Protien (Amide I)		-	**0.887** ***<0.001***	**0.419** ***0.0022***	0.241 *0.0889*
Protein (Amide II)			-	0.198 *0.1627*	-0.003 *0.9837*
Carbohydrate				-	**0.340** ***0.0147***
Phosphodiester					-

Pearson Correlation coefficients (n=50) (2-tailed significance)
P-values are in italics below the correlation coefficient. Bold values significant at p=0.05.

Figure 4-1 Top panel) The benthic alga *Cladophora glomerata* growing in a stream (the small specks in the filaments are snails that are approximately 5 mm long). Bottom panel) Photomicrograph of filaments. Scale bar in all photomicrographs is 50 µm. In the electronic version, cell walls are stained blue with the fluorochrome Calcofluor, and the red within the cell is chlorophyll autoflourescence. Note the branching pattern of filaments.

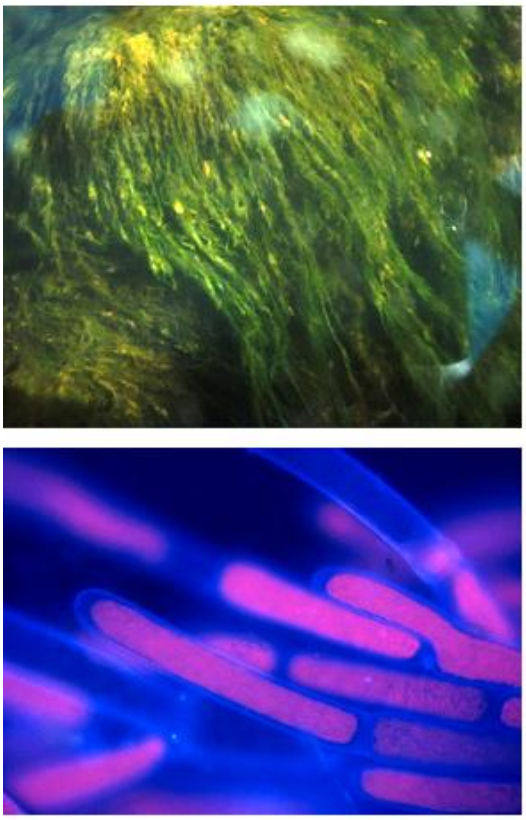

Figure 4-2 PCA biplots of the factors 1 and 2 of A) macromolecular pool peak areas, and B) peak area ratios in individual *Cladophora* cells (point measurements, n = 50). The first 2 factors were driven by lipid and protein content and explain 83% of the macromolecular pool variability and 81% of the pool ratios among cells.

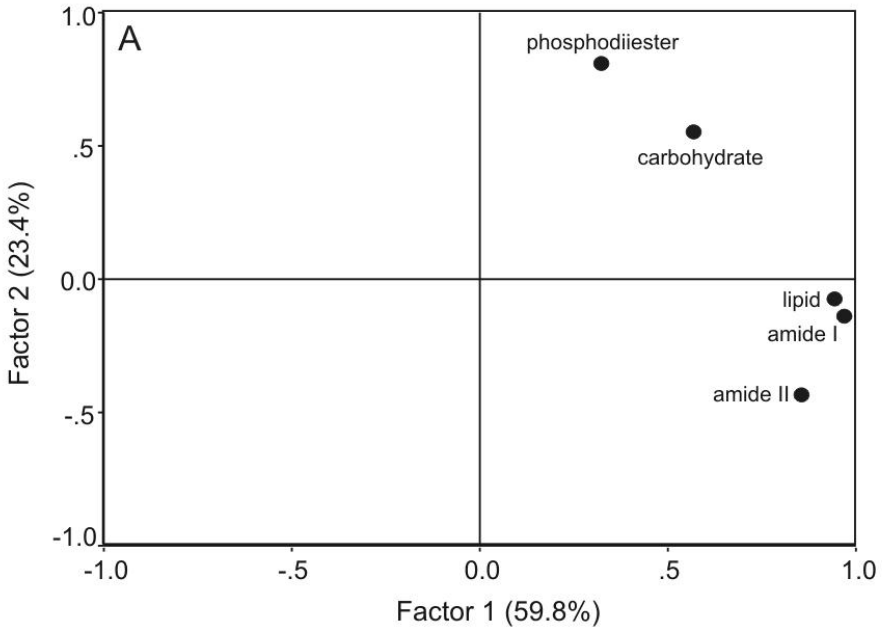

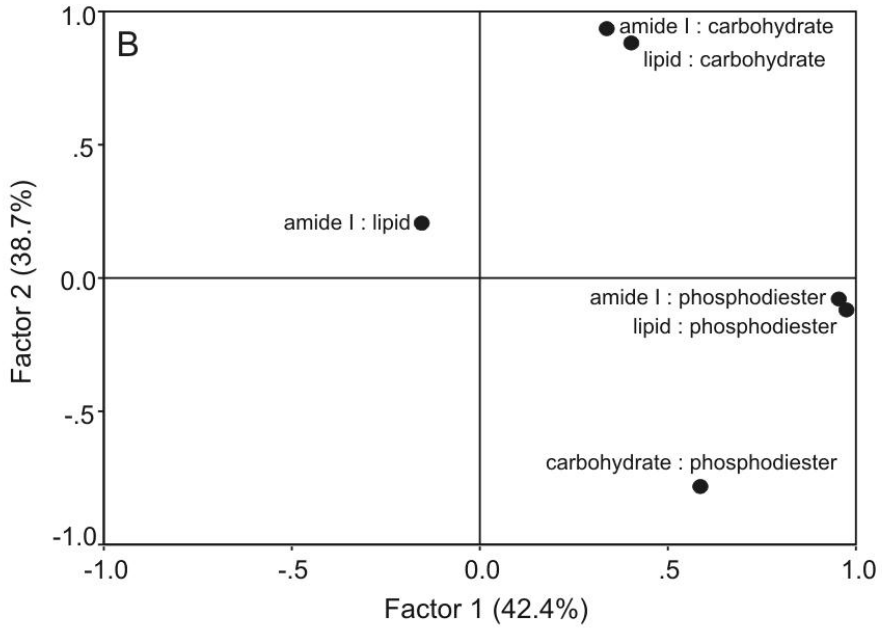

Figure 4-3 Rectangular x, y Grahm-Schmidt function (total absorbance intensity) image of two *Cladophora* cells. Three individual spectra from three areas (9 total) show the high variability in macromolecular pools that occur within and between two adjacent cells. Spectra 9 is of a diatom growing attached to the side of the *Cladophora* cell and is visibly distinct, containing a much higher lipid: protein ratio than the larger green alga and a distinct silica band at 1080 cm^{-1}. In the electronic version, red areas in spectral images enote areas of higher absorbance, and purple areas indicate low absorbance.

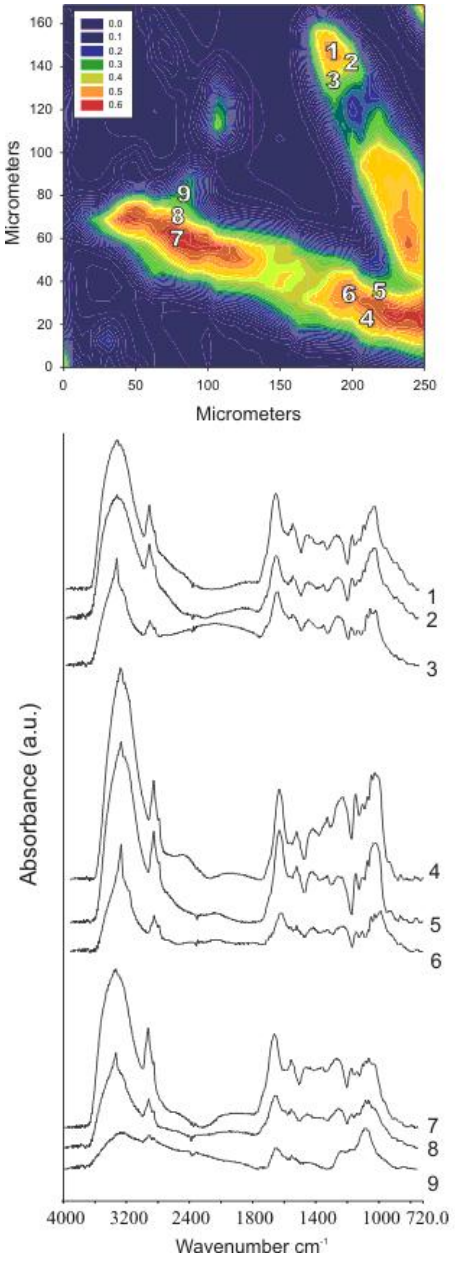

Figure 4-4 X, y images of the subcellular distribution of individual macromolecular pools of A) protein ~1645 cm^{-1}, B) carbohydrate ~1025 cm^{-1}, C) lipid ~2927 cm^{-1}, and D) phosphodiesters ~1240 cm^{-1} within the two *Cladophora* cells from Figure 4-2 at 6.2 µm x 6.2 µm nominal pixel size. The scale box in panel A is absorbance intensity and frame in the photomicrograph of the two cells indicated the area imaged. Note the locus at protein concentration is coincident with that of the lipid, but that the carbohydrates are more widely distributed throughout the cells.

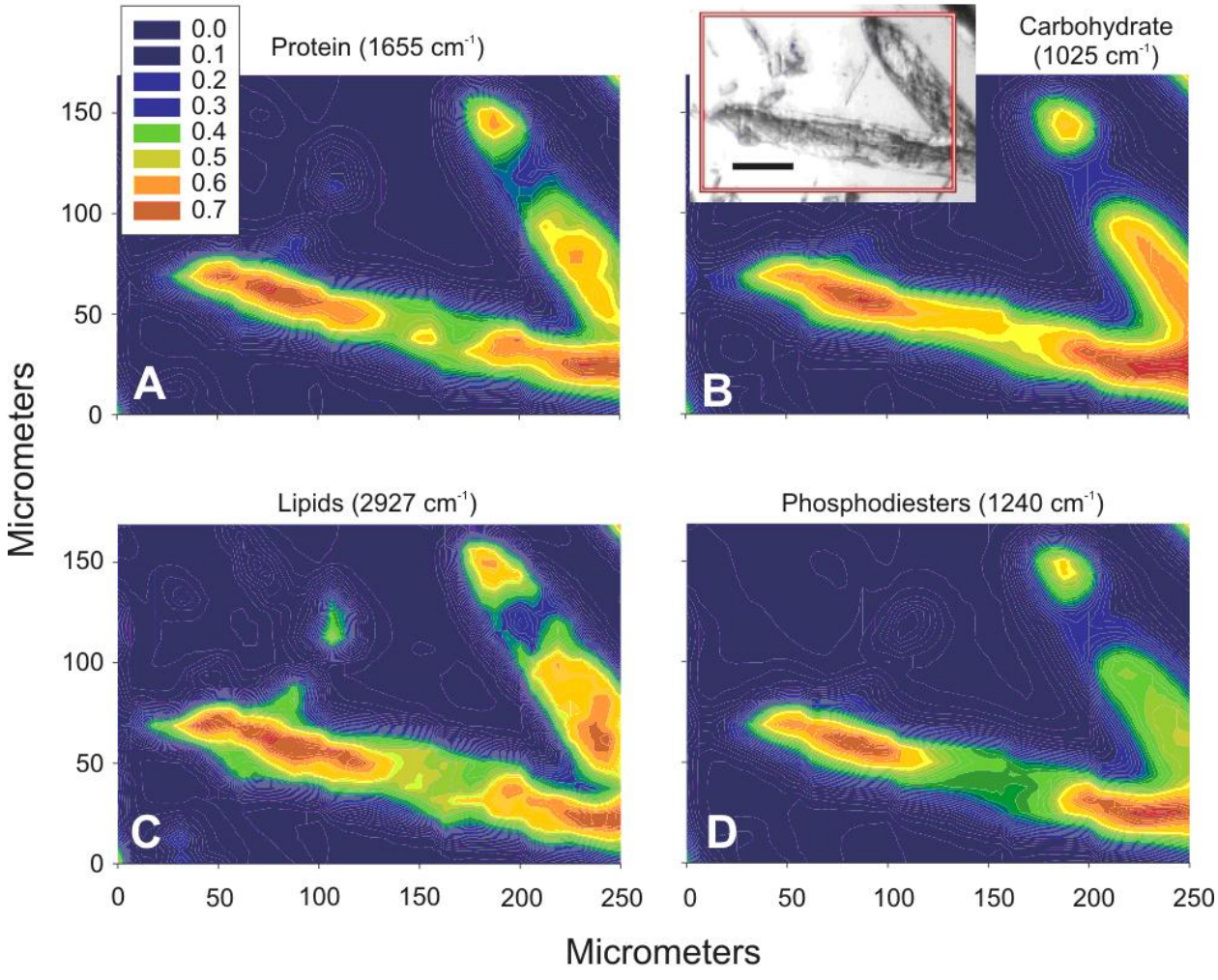

Figure 4-5 Example of macromolecular ratio images of two adjacent Cladophora cells. The upper cell is a thallus cell and the lower cell a newer branch tip. Scale boxes are absorbance intensity and the red box in the photomicrograph of the two cells indicates the area imaged. Note the high lipid content near the cell walls, and the protein hotspot in the tip cell. Carbohydrates appear slightly higher in the thallus cell.

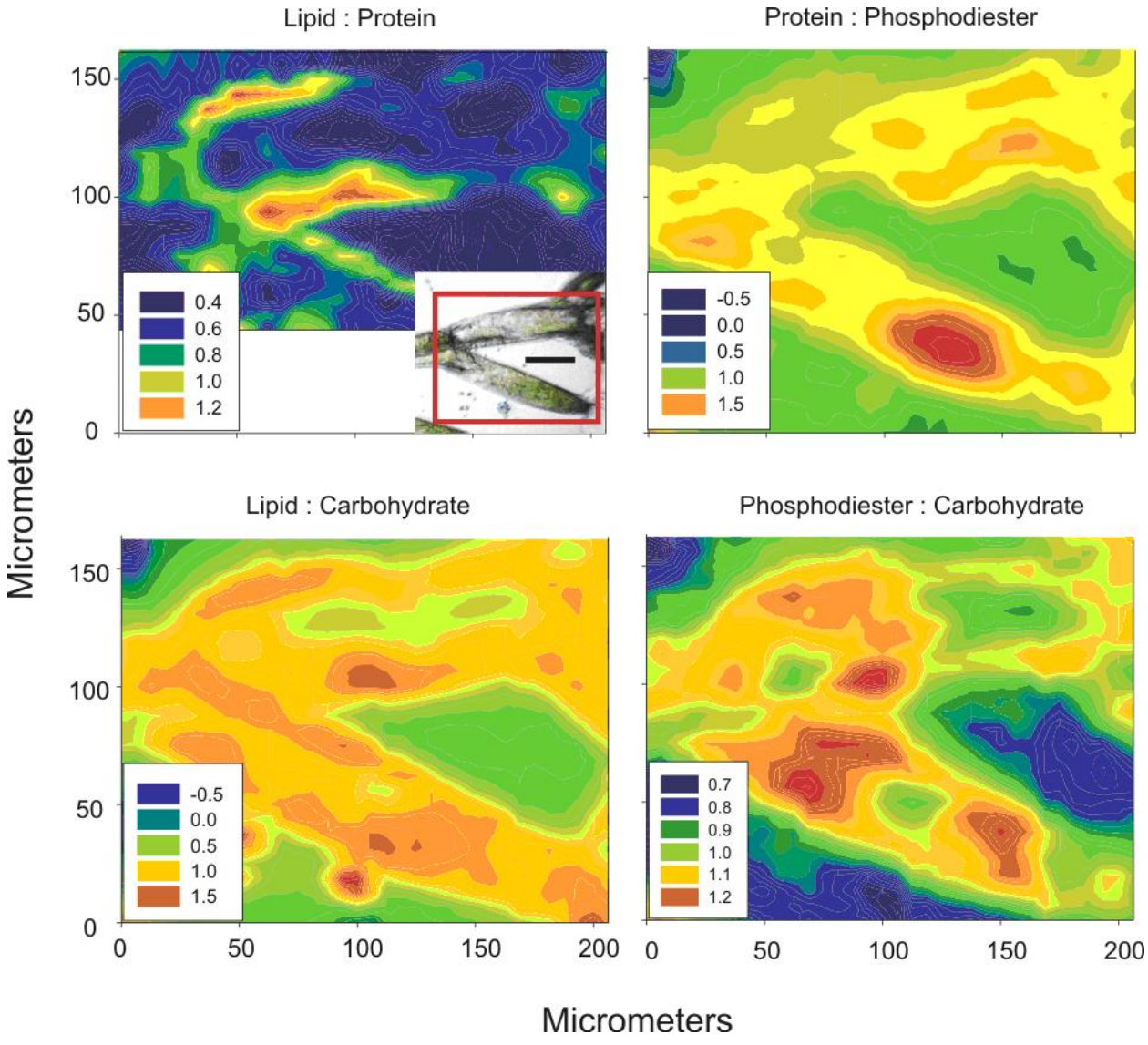

Figure 4-6 PCA factor images of 3 *Cladophora* cells using the spectrum range 3000-2900 cm^{-1} and 1750-900 cm^{-1} and corresponding loading plots for factors 2 and 3. In each pair of images, factor 2 is on top. Scale bars are 100µm.

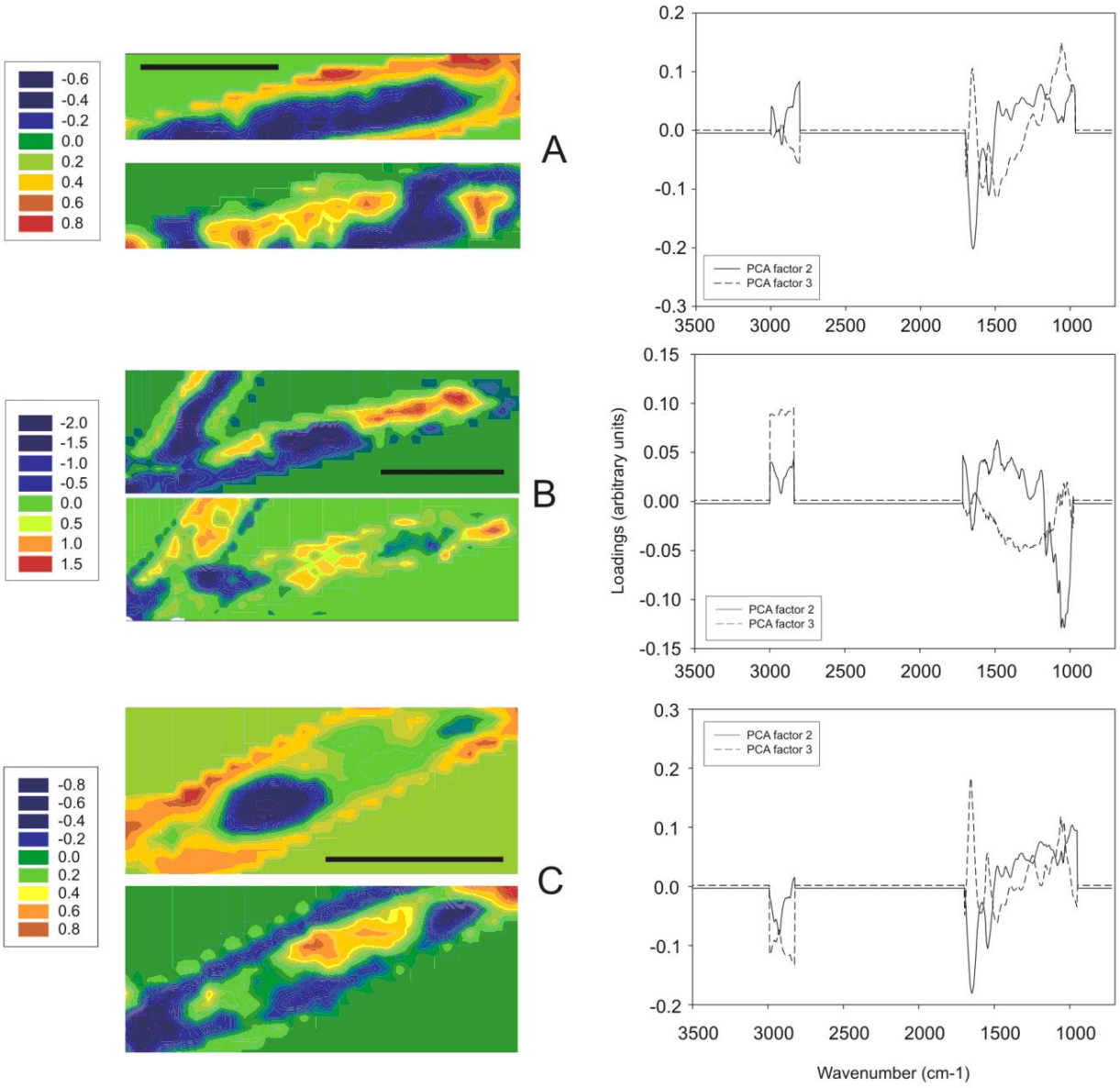

Figure 4-7 A) Average of the amide II peak absorbance from cells incubated in ^{14}N and after 3 and 4 days in ^{15}N. The peak shifted showed a progression of protein labeling over time. B) Raw and Fourier self-deconvolved spectra typical of ^{14}N, day 3 ^{15}N, and day 4 ^{15}N enhancing the change in height of the 1545 and 1535 cm^{-1} peaks with increased ^{15}N incorporation. C) The second derivatives of spectra in panel A. Note the change in the 1545 cm^{-1} :1535 cm^{-1} peak heights between the ^{14}N and day 4 ^{15}N spectra.

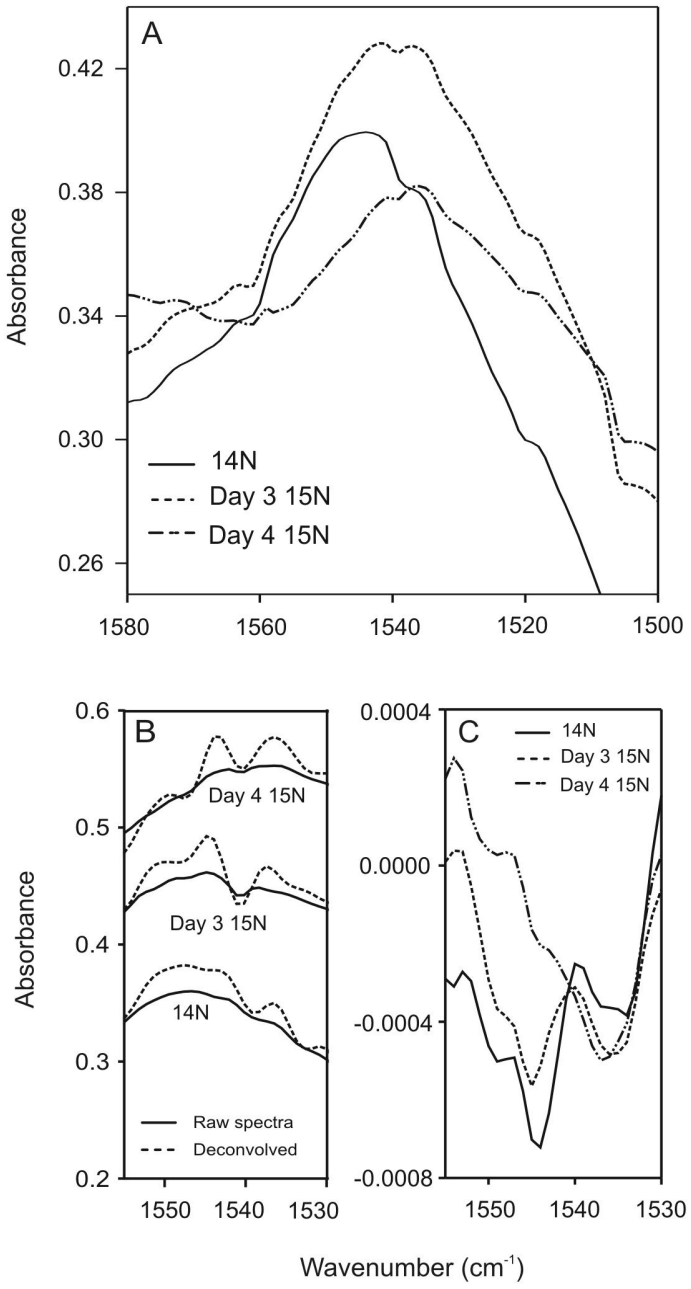

Figure 4-8 Relationship between the location of a cell on a filament (in relation to the filament attachment point) and the amount of ^{15}N incorporated into the cell after 4 days of incubation in $K^{15}NO_3$. ^{15}N uptake was substantially higher > 3 mm from the filament attachment point.

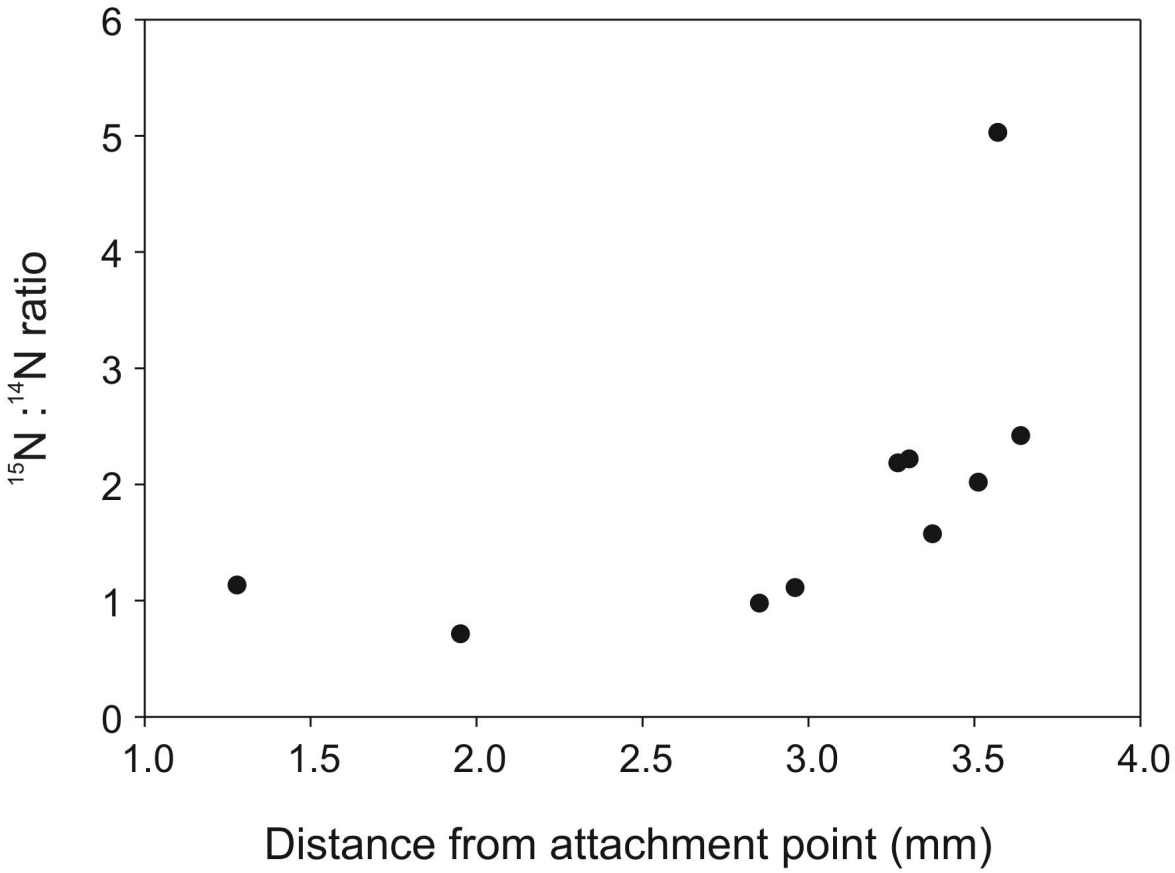

Figure 4-9 Two subcellular x, y images of localized ^{15}N incorporation. Red squares in each photomicrograph denote the area imaged. Scale boxes indicate the ^{15}N / ^{14}N peak height ratio in cellular proteins and red indicates areas of higher ^{15}N incorporation.

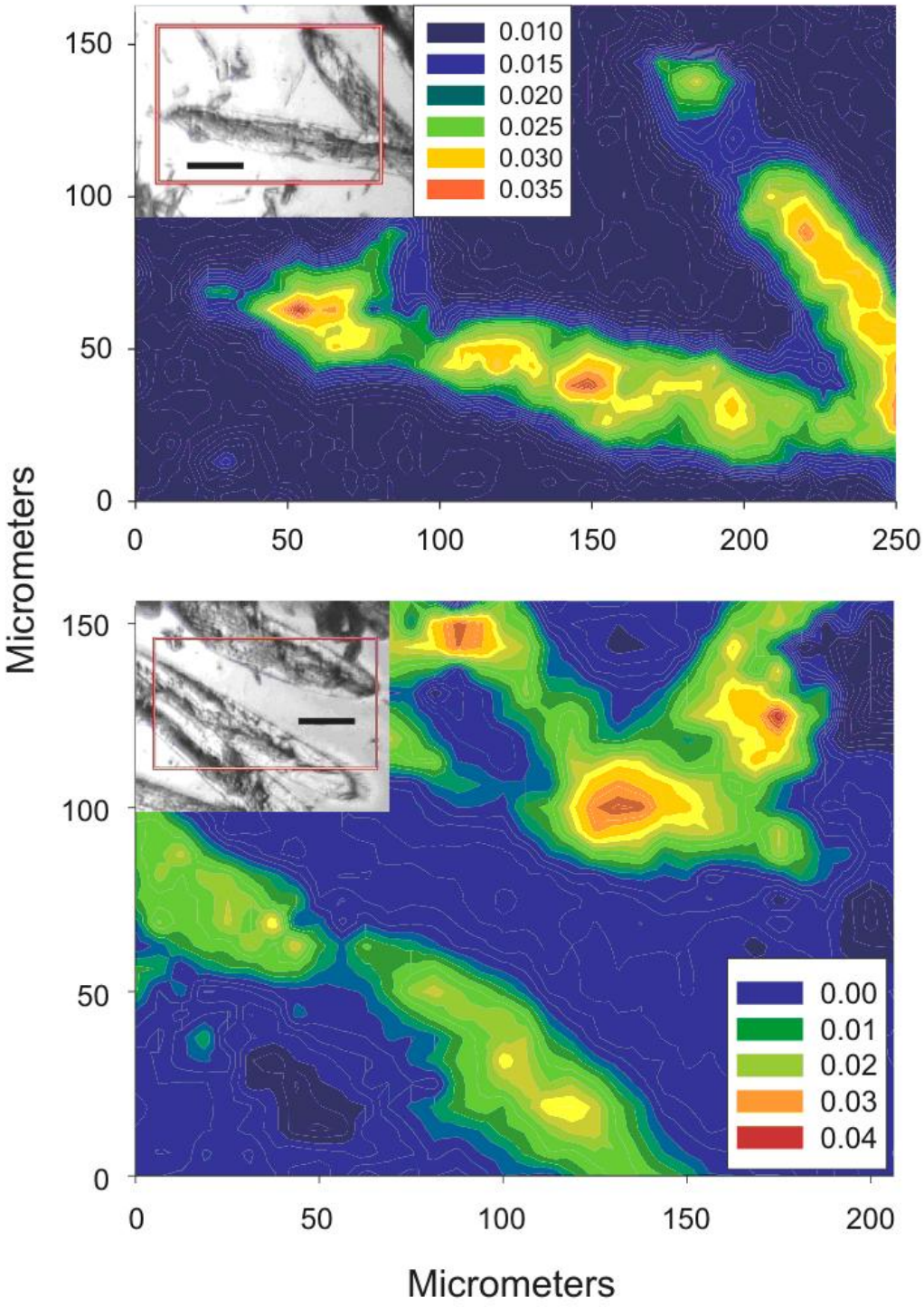

SUMMARY AND CONCLUSIONS

Stream ecosystems in the Great Plains are changing due to anthropogenic modifications of discharge, nutrient availability, biodiversity, and sedimentation rates. It is not entirely clear how each of these changes by themselves will alter natural recovery trajectories, let alone how they will interact to alter stream communities. Up to this point, the focus on nutrient/producer/consumer relationships in aquatic systems has been during steady state conditions. This dissertation examined the chemical, biological, and physical factors, and possible interactions, that regulate stream succession after a disturbance with the goal to increase the ability to predict how community structure and ecosystem function in these non-equilibrium systems will respond to future alterations.

The first chapter explored the importance of large consumers on steam structural and functional recovery after a nine month drought, as larger consumers may be more susceptible to hydrologic alterations and decreased stream connectivity than smaller macroinvertebrate consumers (Matthews and Marsh-Matthews 2003, Dodds et al 2004). Cages with sides open to large consumers (fish and crayfish) or closed off to large consumers were put into pools in an intermittent prairie stream, and the structural and functional recovery within each side of the cage was monitored for 9 weeks after rewetting. Large consumers acted mostly as grazers, removing long algal filaments that had recovered quickly upon rewetting. Consumers decreased algal biomass, algal filament length, gross primary productivity, and nitrogen uptake potential. They also slowed the recovery of macroinvertebrates (non-crayfish) by two weeks, presumably through bioturbation related mechanisms rather than consumption. The strong consumer effect was temporary and quickly decreased after week five when filaments in the ungrazed areas

senesced, leaving algal and invertebrate assemblages similar to the grazed areas. The effects of grazing fish alone were isolated in large mesocosms and were found to be weaker than whole consumer assemblage effects in the stream, suggesting limited functional redundancy in consumers during recovery. Large consumer impacts did not drastically alter the recovery trajectory endpoint, as consumers mainly altered the proportions of algal and macroinvertebrate species present, rather than excluding any one species from colonizing. Benthic communities eventually became similar with or without large consumers after five to six weeks.

The second chapter investigated the relationships between grazing fish density and nutrient availability, on benthic algae development after a flood. Large mesocosms were used to create a factorial design of nutrient and fish gradients to study individual factors and their interactive effects. Nutrients were a much stronger driver of algal recovery than grazers, and were more closely correlated with functional variables such as gross primary productivity and nutrient retention than structural variables. Grazer effects (while weak) had an impact on all algal structural variables measured. However, the strength of both factors changed during recovery as grazer influence got weaker and nutrient influence got stronger. The only nutrient by grazer interaction found was in riffle algal biomass where grazers had no net reduction of algae at low nutrients, but significantly reduced algae at high nutrients. No stimulation of algal growth by grazers was found. Relationships from this experiment were used to construct a simulation model which found that nutrient loadings in ambient treatments were too high for nutrient remineralization by grazers to increase algal growth.

The third chapter looked at the relationships among the physical properties of the substrata and benthic algal accumulation. Surface orientation and roughness may alter the amount of light and nutrients available to algae (Vogel 1994), and can provided a refuge from

grazers and floods (Bergey and Weaver 2004, Bergey 2005). Tiles of varying orientation, and substrata with varying roughness were placed in a stream for three weeks. The microtopography characteristics of the substrata were measured with confocal laser scanning microscopy and related to algal accumulation. Algal growth decreased on surfaces that were greater than 45 degrees relative to the stream bottom. Also, rougher surfaces collected more algae up to an average roughness of 17 μm (pit depth), and then decreased on rougher surfaces. Smoother surfaces collected more loosely attached algae forms such as filaments, and rougher surface collected smaller, adnately attached forms such as single cell diatoms.

The mechanisms for the algal and substrata relationships from chapter three were unclear, but could not be further investigated with current methods. This required detecting the physiological responses of individual species and cells to microscale spatial changes in algal assemblages. Chapter four describes the development of a new method using Fourier-Transform infrared microspectroscopy to measure nutrient content and uptake in single benthic algal cells. Results from this method proved very promising for future algal research. In the test alga, the green filament *Cladophora glomerata,* no strong spatial patterns of nutrient content were found among filaments, but cell differences were found to be driven by changes in protein and lipid content. Nutrient concentrations along a filament were also not significantly different, but there was a 3-fold increase in nitrogen uptake in cells that were likely positioned outside the boundary layer of turbulent and laminar flow (i.e. the molecular diffusion layer) that develops in algal mats.

Combining results from all experiments found that abiotic controls of algae were stronger than consumer controls during recovery. This is opposite of the majority of previous findings that occur during steady state conditions (Steinman 1996, Gruner et al. 2008). Nutrients had a

stronger influence on stream function over structure, while consumers had a stronger impact on structural development. Consumers had a stronger effect on stream function after drought than after the flood, which was caused indirectly by removing algal biomass.

The strength of both consumer and nutrient influence changed during succession. Consumers had a stronger effect early in recovery and nutrients were stronger later in recovery. The reduction in consumer influence on algae did not appear to be due to changes in consumer dynamics, but by changes in algal growth. After drought, ungrazed filaments senesced from apparent nutrient limitation, and after flood, algae underwent rapid growth which quickly exceeded consumption rates. Results from both mesocosms experiments showed weak grazer effects, and when only grazing fish were in the stream after drought, they could only prevent additional algal accumulation. It is likely that after a disturbance, more than one functional grazing group may be needed to significantly reduce biomass.

Interactions between nutrient and consumers were rare during recovery as algae were not nutrient limited in ambient concentrations (~150 $\mu g\ L^{-1}$ total nitrogen, 30 $\mu g\ L^{-1}$ total phosphorus) during flood recovery so additional nutrients remineralized by grazers went unused. It is likely that increasing nutrients will act to further suppress grazer and nutrient interactions, even during steady state conditions. Increasing sedimentation of stream channels should act to increase grazer effects as smoother surfaces increase loosely attached and more grazer accessible algae. This combined with decreased substrata heterogeneity will likely lead to a further decrease in overall algal biomass, further reduce stream nutrient retention. The work in this dissertation has shown that complex, temporally variable abiotic and biotic interactions exist in post-disturbance environments, and that factors that regulate non-equilibrium situations can be different than during steady state conditions.

LITERATURE CITED

Abramoff M. D., P. J. Magelhaes, and S. J. Ram. 2004. Image Processing with Image J. Biophotonics International **11**: 36-42.

Akaike, H. 1973. Information theory and an extension of the maximum-likelihood principle. In Petrov, B. N., F. Csaki [Eds.]. Second International Symposium on Information Theory. Akademiai Kiado: Budapest, Hungary.

Aloi J. E. 1990. A critical review of recent freshwater benthic algae field methods. Canadian Journal of Fisheries and Aquatic Sciences **47**: 656-70.

American Public Health Association (APHA). 1998. Standard methods for the examination of water and wastewater. American Public Health Association, Washington, D.C.

Barbiero R. P. 2000. A multi-lake comparison of epilithic diatom communities on natural and artificial substrates. Hydrobiologia **438**:157-170.

Baynes T. W. 1999. Factors structuring a subtidal encrusting community in the southern Gulf of California. Bulletin of Marine Science **64**:419-450.

Beardall, J., T. Berman, P. Heraud, M.O. Kadiri, B.R. Light, G. Patterson, S. Roberts, B. Sulzberger, E. Sahan, U. Uehlinger, and B. Wood. 2001. Aquatic Sciences. **63**: 107.

Bengtson J.R., M. Evans-White, and K.B. Gido. In press. Effects of grazing minnows (*Phoxinus erythrogaster*) and crayfish (*Orconectes nais* and *O. neglectus*) on stream ecosystem structure and function. Journal of the North American Benthological Society.

Benke A. C., A. D. Huryn, L. A. Smock, and J. B. Wallace. 1999. Length-mass relationships for freshwater macroinvertebrates in North America with particular reference to the Southeastern United States. Journal of the North American Benthological Society **18**:308-343.

Benzie J. A. H. 1989. The Distribution and Habitat Preference of Ostracods (Crustacea, Ostracoda) in a Coastal Sand-Dune Lake, Loch of Strathbeg, Northeast Scotland. Freshwater Biology **22**:309-321.

Bergey, E. A. 1999. Crevices as refugia for stream diatoms: Effect of crevice size on abraded substrates. Limnology and Oceanography. **44**:1522-9.

Bergey E. A., and J. E. Weaver. 2004. The influence of crevice size on the protection of epilithic algae from grazers. Freshwater Biology **49**:1014-1025.

Bergey E. A. 2005. How protective are refuges? Quantifying algal protection in rock crevices. Freshwater Biology **50**:1163-1177.

Bergey E. A. 2006. Measuring the surface roughness of stream stones. Hydrobiologia **563**: 247-252.

Bertrand, K. N., K. B. Gido, and C. S. Guy. 2006. An evaluation of single-pass versus multiple-pass backpack electrofishing to estimate trends in species abundance and richness in prairie streams. Transactions of the Kansas Academy of Science **109**:131-138.

Bertrand K. N. 2007. Fishes and floods: stream ecosystem drivers in the Great Plains. Ph.D. Dissertation. Kansas State University.

Bertrand K. N., and K. B. Gido. 2007. Effects of the herbivorous minnow, southern redbelly dace (Phoxinus erythrogaster), on stream productivity and ecosystem structure. Oecologia **151**:69-81.

Biggs B. J. F., and H. A. Thomsen. 1995. Disturbance of Stream Periphyton by Perturbations in Shear-Stress - Time to Structural Failure and Differences in Community Resistance. Journal of Phycology **31**:233-241.

Biggs, B.J.F. 1996. Patterns in benthic algae in streams. Pages 31-56 in R.J. Stevenson, M.L. Bothwell, and R.L. Lowe. [Eds.] Algal Ecology. Academic Press, Elsevier Inc, Burlington, Massachusetts.

Biggs B. J. F., D. G. Goring, and V. I. Nikora. 1998. Subsidy and stress responses of stream periphyton to gradients in water velocity as a function of community growth form. Journal of Phycology **34**:598-607.

Biggs B. J. F., R. J. Stevenson, and R. L. Lowe. 1998. A habitat matrix conceptual model for stream periphyton. Archiv Fur Hydrobiologie **143**:21-56.

Biggs B. J. F., V. I. Nikora, and T. H. Snelder. 2005. Linking scales of flow variability to lotic ecosystem structure and function. River Research and Applications **21**:283-298.

Bott T. L., J. T. Brock, A. Battrup, P. Chambers, W.K. Dodds, K. Himbeault, J.R. Lawrence, D. Planas, E. Snyder, and G.M. Wolfaardt. 1997. An evaluation of techniques for measuring benthic algae metabolism in chambers. Canadian Journal of Fisheries and Aquatic Sciences **54**: 715-25.

Boulton A. J. 2003. Parallels and contrasts in the effects of drought on stream macroinvertebrate assemblages. Freshwater Biology **48**:1173-1185.

Burkholder J. A. 1996. Interactions of benthic algae with their substrata. In Stevenson, R. J., Bothwell, M. L., & Lowe, R. L. [Eds.], Algal Ecology: Freshwater Benthic Ecosystem. Academic Press, pp. 321-40.

Burnham, K. P., and D. R. Anderson. 1998. Model selection and inference: a practical information-theoretic approach. Springer-Verlag, New York.

Cardinale B. J., M. A. Palmer, A. R. Ives, and S. S. Brooks. 2005. Diversity-productivity relationships in streams vary as a function of the natural disturbance regime. Ecology **86**:716-726.

Cattaneo A., and G. Roberge. 1991. Efficiency of a Brush Sampler to Measure Periphyton in Streams and Lakes. Canadian Journal of Fisheries and Aquatic Sciences **48**:1877-1881.

Cattaneo A., and M.C. Amireault. 1992. How artificial are artificial substrata for benthic algae? Journal of North American Benthological Society **11**: 244-56.

Cattaneo A., and B. Mousseau. 1995. Empirical-Analysis of the Removal Rate of Periphyton by Grazers. Oecologia **103**:249-254.

Cattaneo A., T. Kerimian, M. Roberge, and J. Marty. 1997. Benthic algae distribution and abundance on substrata of different size along a gradient of stream trophy. Hydrobiologia **354**:101-110.

Chinga, G., Ø. Gregersen, and B. Dougherty. 2003. Paper surface characterization by laser profilometry and image analysis. Journal of Microscopy and Analysis **84**: 5-7.

Choo-Smith L. P., K. Maquelin, T. van Vreeswijk, H. A. Bruining, G. J. Puppels, N. A. G. Thi, C. Kirschner, D. Naumann, D. Ami, A. M. Villa, F. Orsini, S. M. Doglia, H. Lamfarraj, G. D. Sockalingum, M. Manfait, P. Allouch, and H. P. Endtz. 2001. Investigating microbial (micro)colony heterogeneity by vibrational spectroscopy. Applied and Environmental Microbiology **67**:1461-1469.

Clifford H. F., R. J. Casey, and K. A. Saffran. 1992. Short-Term Colonization of Rough and Smooth Tiles by Benthic Macroinvertebrates and Algae (Chlorophyll-A) in 2 Streams. Journal of the North American Benthological Society **11**:304-315.

Comte K., S. Fayolle, and M. Roux. 2005. Quantitative and qualitative variability of epiphytic algae on one Apiaceae (Apium nodiflorum L.) in a karstic river (Southeast of France). Hydrobiologia **543**:37-53.

Connell J. H. 1978. Diversity in tropical rain forests and coral reefs. Science **199**:1302-1310.

Connelly, S., C. M. Pringle, R. J. Bixby, R. Brenes, M. R. Whiles, K. R. Lips, S. Kilham, and A.D. Huryn. *In press*. Changes in stream primary producer communities resulting from loss of tadpoles: can small-scale experiments predict the effects of large-scale catastrophic amphibian declines? Ecosystems.

Consalvey M., D. M. Paterson, and G. J. C. Underwood. 2004. The ups and downs of life in a benthic biofilm: Migration of benthic diatoms. Diatom Research **19**:181-202.

Dade, W.B., A.J. Hogg, and B.P. Boudreau. 2001. Physics of flow above the sediment water interface. In Boudreau, B.P. & Jørgenson, B.B. [Eds.] The Benthic Boundary Layer. Oxford University Press, pp. 4-43.

de Fraiture C., M. Giordano, and Y.S. Liao. 2008. Biofuels and implications for agricultural water use: blue impacts of green energy. Water Policy **10**: 67-81.

Dean A. P., and D. C. Sigee. 2006. Molecular heterogeneity in Aphanizomenon flos-aquae and Anabaena flos-aquae (Cyanophyta): a synchrotron-based Fourier-transform infrared study of lake micropopulations. European Journal of Phycology **41**:201-212.

Dean A. P., M. C. Martin, and D. C. Sigee. 2007. Resolution of codominant phytoplankton species in a eutrophic lake using synchrotron-based Fourier transform infrared spectroscopy. Phycologia **46**:151-159.

DeAngelis, D.L. 1992. Dynamics of nutrient cycling and food webs. Chapman & Hill, London.

DeNicola D. M., K. D. Hoagland, and S. C. Roemer. 1992. Influences of Canopy Cover on Spectral Irradiance and Periphyton Assemblages in a Prairie Stream. Journal of the North American Benthological Society **11**:391-404.

DeNicola, D. M., and C.D. McIntire. 1990. Effects of substrate relief on the distribution of periphyton in laboratory streams 1. Hydrology. Journal of Phycology **26**:624-33.

Dodds, W. K. 1991. Micro-environmental characteristics of filamentous algal communities in flowing freshwaters. Freshwater Biology **25**:199-209.

Dodds W. K., and D. A. Gudder. 1992. The Ecology of Cladophora. Journal of Phycology **28**: 415-427.

Dodds W. K., R. E. Hutson, A. C. Eichem, M. A. Evans, D. A. Gudder, K. M. Fritz, and L. Gray. 1996. The relationship of floods, drying, how and light to primary production and producer biomass in a prairie stream. Hydrobiologia **333**:151-159.

Dodds W. K., J. Brock. 1998. A portable flow chamber for in situ determination of benthic metabolism. Freshwater Biology **39**:49-59.

Dodds W. K., and E. B. Welch. 2000. Establishing nutrient criteria in streams. Journal of the North American Benthological Society **19**:186-196.

Dodds W.K. 2002. Freshwater Ecology: Concepts and Environmental Applications. Academic Press, San Diego, CA. 569 pp.

Dodds, W.K. & Biggs, B.J.F. 2002. Water velocity attenuation by stream benthic algae in relation to growth form and architecture. J.N. Amer. Benthol. Soc. **21**:2-15.

Dodds W. K., A. J. Lopez, W. B. Bowden, S. Gregory, N. B. Grimm, S. K. Hamilton, A. E. Hershey, E. Marti, W. H. McDowell, J. L. Meyer, D. Morrall, P. J. Mulholland, B. J. Peterson, J. L. Tank, H. M. Valett, J. R. Webster, and W. Wollheim. 2002. N uptake as a

function of concentration in streams. Journal of the North American Benthological Society **21**:206-220.

Dodds W. K., V. H. Smith, and K. Lohman. 2002. Nitrogen and phosphorus relationships to benthic algal biomass in temperate streams. Canadian Journal of Fisheries and Aquatic Sciences **59**:865-874.

Dodds W. K. 2003. The role of periphyton in phosphorus retention in shallow freshwater aquatic systems. Journal of Phycology **39**:840-849.

Dodds W. K., K. Gido, M. R. Whiles, K. M. Fritz, and W. J. Matthews. 2004. Life on the edge: The ecology of great plains prairie streams. Bioscience **54**:205-216.

Dodds, W. K. and M. R. Whiles. 2004. Factors related to quality and quantity of suspended particles in rivers: general continent-scale patterns in the United States . Environmental Management. **33:**355-367.

Downes B. J., P. S. Lake, E. S. G. Schreiber, and A. Glaister. 1998. Habitat structure and regulation of local species diversity in a stony, upland stream. Ecological Monographs **68**:237-257.

Dudley T. L., and C. M. Dantonio. 1991. The Effects of Substrate Texture, Grazing, and Disturbance on Macroalgal Establishment in Streams. Ecology **72**:297-309.

Easterling, D. R., G. A. Meehl, C. Parmesan, S. A. Changnon, T. R. Karl, and L. O. Mearns. 2000. Climate extremes: observations, modeling, and impacts. Science **289**:2068-2074

Elmquist T, C. Folke, M. Nystrom, G. Peterson, J. Bengtsson, B. Walker, and J. Norberg. 2003. Response diversity, ecosystem change, and resilience. Frontiers in Ecology and the Environment **1**:488–494.

Evans J.H.1959. The survival of freshwater algae during dry periods: Part II. Drying experiments: Part III. Stratification of algae in pond margin litter and mud. Journal of Ecology. **47**:55-81.

Evans-White M., W. K. Dodds, L. J. Gray, and K. M. Fritz. 2001. A comparison of the trophic ecology of the crayfishes (Orconectes nais (Faxon) and Orconectes neglectus (Faxon)) and the central stoneroller minnow (Campostoma anomalum (Rafinesque)): omnivory in a tallgrass prairie stream. Hydrobiologia **462**:131-144.

Feminella J. W., and C. P. Hawkins. 1995. Interactions between stream herbivores and periphyton: A quantitative analysis of past experiments. Journal of the North American Benthological Society **14**:465-509.

Flecker A. S. 1992. Fish Predation and the Evolution of Invertebrate Drift Periodicity - Evidence from Neotropical Streams. Ecology **73**:438-448.

Flecker A. S., B.W. Taylor, E.S. Bernhardt, J.M. Hood, W.K. Coenwell, S.R. Cassatt, M.J. Vanni, and N.S.Altman. 2002. Interactions between herbivorous fishes and limiting nutrients in a tropical stream ecosystem. Ecology **83**:1831-1844.

Fowler R. T. 2004. The recovery of benthic invertebrate communities following dewatering in two braided rivers. Hydrobiologia **523**:17-28.

Franssen N. R., K. B. Gido, C. S. Guy, J. A. Tripe, S. J. Shrank, T. R. Strakosh, K. N. Bertrand, C. M. Franssen, K. L. Pitts, and C. P. Paukert. 2006. Effects of floods on fish assemblages in an intermittent prairie stream. Freshwater Biology **51**:2072-2086.

Fritz K. M., and W. K. Dodds. 2004. Resistance and resilience of macroinvertebrate assemblages to drying and flood in a tallgrass prairie stream system. Hydrobiologia **527**:99-112.

Gelwick F. P., and W. J. Matthews. 1992. Effects of an Algivorous Minnow on Temperature Stream Ecosystem Properties. Ecology **73**:1630-1645.

Gido K. B. 2002. Interspecific comparisons and the potential importance of nutrient excretion by benthic fishes in a large reservoir. Transactions of the American Fisheries Society **131**:260-270.

Giordano M., M. Kansiz, P. Heraud, J. Beardall, B. Wood, and D. McNaughton. 2001. Fourier transform infrared spectroscopy as a novel tool to investigate changes in intracellular macromolecular pools in the marine microalga Chaetoceros muellerii (Bacillariophyceae). Journal of Phycology **37**:271-279.

Glasby T. M., and S. D. Connell. 2001. Orientation and position of substrata have large effects on epibiotic assemblages. Marine Ecology-Progress Series **214**:127-135.

Gray, L.J., and W.K. Dodds. 1998. Structure and dynamics of aquatic communities. In Knapp A. K., Briggs, J. M., Harnett, D. C. & Collins S. L. [Eds.] Grassland Dynamics. Oxford University Press, pp 177-92.

Gray, L.J., G.L.Macpherson, J.K. Koelliker, and W.K. Dodds. 1998. Hydrology and aquatic chemistry. In Knapp A. K., Briggs, J. M., Harnett, D. C. & Collins S. L. [Eds.] Grassland Dynamics. Oxford University Press, p 159-76.

Gresens S. E., and R. L. Lowe. 1994. Periphyton Patch Preference in Grazing Chironomid Larvae. Journal of the North American Benthological Society **13**:89-99.

Griffith M. B., B. H. Hill, A. Herlihy, and P. R. Kaufmann. 2002. Multivariate analysis of periphyton assemblages in relation to environmental gradients in Colorado Rocky Mountain streams. Journal of Phycology **38**:83-95.

Groisman P. Y., T. R. Karl, D. R. Easterling, R. W. Knight, P. F. Jamason, K. J. Hennessy, R. Suppiah, C. M. Page, J. Wibig, K. Fortuniak, V. N. Razuvaev, A. Douglas, E. Forland, and P. M. Zhai. 1999. Changes in the probability of heavy precipitation: Important indicators of climatic change. Climatic Change **42**:243-283.

Gruner, DS, Smith, JE, Seabloom, EW, Sandin, SA, Ngai, JT, Hillebrand, H, Harpole, WS, Elser, JJ, Cleland, EE, Bracken, MES, Borer, ET, Bolker, BM. 2008. A cross-system synthesis of consumer and nutrient resource control on producer biomass. Ecology letters **11**: 740-755.

Hall, R.O., B.J. Koch, M.C. Marshall, B.W. Taylor, and L.M. Tronstad. 2007. How body size mediates the role of animals in nutrient cycling in aquatic ecosystems. In A Hildrew, D. Raffaelli, and R. Edmods-Brown [Eds.] Body Size: The structure and function of aquatic ecosystems. Cambridge University Press.

Hargrave, C.W., R. Ramirez, M. Brooks, M.A. Eggleton, K. Sutherland, R. Deaton and H. Galbraith. 2006. Indirect food web interactions increase growth of an algivorous stream fish. Freshwater Biology **51**:1901-1910.

Haris P. I., G. T. Robillard, A. A. Vandijk, and D. Chapman. 1992. Potential of C-13 and N-15 Labeling for Studying Protein-Protein Interactions using Fourier-Transform Infrared-Spectroscopy. Biochemistry **31**:6279-6284.

Harrod, J. J., and R.E. Hall. 1962. A method for determining the surface area of various aquatic plants. Hydrobiologia **20**:173-8.

Hart, D. D., and C.M. Finelli. 1999. Physical-biological coupling in streams: The pervasive effects of flow on benthic organisms. Annual Review of Ecological Systems **30**:363-95.

Hawes I., C. Howardwilliams, and W. F. Vincent. 1992. Desiccation and Recovery of Antarctic Cyanobacterial Mats. Polar Biology **12**:587-594.

Heraud P., B. R. Wood, M. J. Tobin, J. Beardall, and D. McNaughton. 2005. Mapping of nutrient-induced biochemical changes in living algal cells using synchrotron infrared microspectroscopy. FEMS Microbiology Letters **249**:219-225.

Hill, W. R., M.G. Ryon, and E.M. Schilling. 1995. Light limitation in a stream ecosystem – responses by primary producers and consumers. Ecology **76**:1297-309.

Hillebrand H., and B. J. Cardinale. 2004. Consumer effects decline with prey diversity. Ecology Letters **7**:192-201.

Hirschmugl C. J., Z. E. Bayarri, M. Bunta, J. B. Holt, and M. Giordano. 2006. Analysis of the nutritional status of algae by Fourier transform infrared chemical imaging. Infrared Physics & Technology **49**:57-63.

Hutchinson N., S. Nagarkarl, J. C. Aitchison, and G. A. Williams. 2006. Microspatial variation in marine biofilm abundance on intertidal rock surfaces. Aquatic Microbial Ecology **42**:187-197.

Huston, M.A. 1979. A general hypothesis of species diversity. American Naturalist **113**:81-101.

Jassby A. D., T. Platt. 1976. Mathematical Formulation of Relationship between Photosynthesis and Light for Phytoplankton. Limnology and Oceanography **21**:540-547.

Johnson L. E. 1994. Enhanced Settlement on Microtopographical High Points by the Intertidal Red Alga Halosaccion Glandiforme. Limnology and Oceanography **39**:1893-1902.

Jones J. G. 1974. Method for Observation and Enumeration of Epilithic Algae Directly on Surface of Stones. Oecologia **16**:1-8.

Jørgenson, B. B. 2001. Life in the diffusive boundary layer. In Boudreau, B. P. & Jørgenson, B. B. [Eds.] The Benthic Boundary Layer. Oxford University Press, pp. 348-73.

Kaufman, G. A. and R. J. Beyers 1972. Relationships of weight, length and body composition in the Medaka, Oryzias latipes American Midland Naturalist **88**:239-245.

Kelly D. J., M. L. Bothwell, and D. W. Schindler. 2003. Effects of solar ultraviolet radiation on stream benthic communities: An intersite comparison. Ecology **84**:2724-2740.

Kimura Y., N. Mizusawa, A. Ishii, T. Yamanari, and T. A. Ono. 2003. Changes of low-frequency vibrational modes induced by universal N-15- and C-15-isotope labeling in S-2. Biochemistry **42**:13170-13177.

Knott N. A., A. J. Underwood, M. G. Chapman, and T. M. Glasby. 2004. Epibiota on vertical and on horizontal surfaces on natural reefs and on artificial structures. Journal of the Marine Biological Association of the United Kingdom **84**:1117-1130.

Kralj K., A. Plenkovic-Moraj, M. Gligora, B. Primc-Habdija, and L. Sipos. 2006. Structure of periphytic community on artificial substrata: influence of depth, slide orientation and colonization time in karstic Lake Visovacko, Croatia. Hydrobiologia **560**: 249-258.

Kuhl M., R. N. Glud, H. Ploug, and N. B. Ramsing. 1996. Microenvironmental control of photosynthesis and photosynthesis-coupled respiration in an epilithic cyanobacterial biofilm. Journal of Phycology **32**:799-812.

Lake P. S. 2000. Disturbance, patchiness, and diversity in streams. Journal of the North American Benthological Society **19**:573-592.

Lake P. S. 2003. Ecological effects of perturbation by drought in flowing waters. Freshwater Biology **48**:1161-1172.

Lamberti, G.A., S.V. Gregory, L.R. Ashenas, A.D. Steinman, and C.D. McIntire. 1989. Productive capacity of periphyton as a determinant of plant-herbivore interactions in streams. Ecology **70**:1840-1856.

Larson, C. & Passy, S.I. 2005. Spectral fingerprinting of algal communities: A novel approach to biofilm analysis and biomonitoring. Journal of Phycology **41**:439–46.

Lawrence J. R., B. Scharf, G. Packroff, and T. R. Neu. 2002. Microscale evaluation of the effects of grazing by invertebrates with contrasting feeding modes on river biofilm architecture and composition. Microbial Ecology **44**:199-207.

Lawrence J. R., M. R. Chenier, R. Roy, D. Beaumier, N. Fortin, G. D. W. Swerhone, T. R. Neu, and C. W. Greer. 2004. Microscale and molecular assessment of impacts of nickel, nutrients, and oxygen level on structure and function of river biofilm communities. Applied and Environmental Microbiology **70**:4326-4339.

Ledger M. E., A. G. Hildrew. 2001. Recolonization by the benthos of an acid stream following a drought. Archiv Fur Hydrobiologie **152**:1-17.

Leis A. P., S. Schlicher, H. Franke, and M. Strathmann. 2005. Optically transparent porous medium for nondestructive studies of microbial biofilm architecture and transport dynamics. Applied and Environmental Microbiology **71**:4801-4808.

Liang Y., J. Beardall, and P. Heraud. 2006. Changes in growth, chlorophyll fluorescence and fatty acid composition with culture age in batch cultures of Phaeodactylum tricornutum and Chaetoceros muelleri (Bacillariophyceae). Botanica Marina **49**:165-173.

Liess A., H. Hillebrand. 2004. Invited review: Direct and indirect effects in herbivore periphyton interactions. Archiv Fur Hydrobiologie **159**:433-453.

Lubcheno J. 1983. Littorina and Fucus: Effects of herbivores, substratum heterogeneity, and plant escapes during succession. Ecology **64**:1116-1123.

Lytle D. A., and N. L. Poff. 2004. Adaptation to natural flow regimes. Trends in Ecology & Evolution **19**:94-100.

Magoulick D. D., and R. M. Kobza. 2003. The role of refugia for fishes during drought: a review and synthesis. Freshwater Biology **48**:1186-1198.

Matthews, W. J., M.E. Power, and A.J. Stewart. 1986. Depth distribution of Campostoma grazing scars in an Ozark stream. Environmental Biology of Fishes. **17**:291-7.

Matthews W. J., and E. Marsh-Matthews. 2003. Effects of drought on fish across axes of space, time and ecological complexity. Freshwater Biology **48**:1232-1253.

Matthews W. J., K. B. Gido, G. P. Garrett, F. P. Gelwick, J. G. Stewart, and J. Schaefer. 2006. Modular experimental riffle-pool stream system. Transactions of the American Fisheries Society **135**:1559-1566.

McCormick P. V., R. J. Stevenson. 1991. Grazer Control of Nutrient Availability in the Periphyton. Oecologia **86**:287-291.

McCormick P. V., R. J. Stevenson. 1991. Mechanisms of Benthic Algal Succession in Lotic Environments. Ecology **72**:1835-1848.

McIntosh A. R., C. R. Townsend. 1996. Interactions between fish, grazing invertebrates and algae in a New Zealand stream: A trophic cascade mediated by fish induced changes to grazer behaviour? Oecologia **108**:174-181.

McIntyre P. B., L. E. Jones, A. S. Flecker, and M. J. Vanni. 2007. Fish extinctions alter nutrient recycling in tropical freshwaters. Proceedings of the National Academy of Sciences of the United States of America **104**:4461-4466.

Meier, P.G., D. O'Conner and D. Dilks. 1983. Artificial substrata for reducing periphytic variability on replicated samples. In R.G. Wetzel [Ed.] Benthic algae of Freshwater Ecosystems. Dr. W. Junk Publishers, pp. 283-6.

Merrit, R. W., K. W. Cummins, and M. B. Berg. 2007. An introduction to the aquatic of North America. 4th Edition. Kendall/Hunt Publishing.

Meyer J. L., E. T. Schultz, and G. S. Helfman. 1983. Fish Schools - an Asset to Corals. Science **220**:1047-1049.

Miller A. M., and S. W. Golladay. 1996. Effects of spates and drying on macroinvertebrate assemblages of an intermittent and a perennial prairie stream. Journal of the North American Benthological Society **15**:670-689.

Milliken, G. A., and D. E. Johnson. 2002. Analysis of messy data, Volume III: Analysis of covariance. Chapman & Hall, London, UK.

Mulholland, P. J., A. D. Steinman, A. V. Palumbo, J. W. Elwood, and D. B. Kirschtel. 1991. Role of nutrient cycling and herbivory in regulating periphyton communities in laboratory streams. Ecology **72**:966-982.

Mulholland, P.J., C. S. Fellows, J. L. Tank, N. B. Grimm, J. R. Webster, S. K. Hamilton, E. Martí, L. Ashkenas, W. B. Bowden, W. K. Dodds, W. H. McDowell, M. J. Paull, and B. J. Peterson 2001. Inter-biome comparison of factors controlling stream metabolism. Freshwater Biology **46**: 1503-1517.

Murdock, J.N., D.R. Roelke, and F.P. Gelwick. 2004. Interactions between flow, periphyton, and nutrients in a heavily impacted urban stream: implications for stream restoration effectiveness. Ecological Engineering **22**:197-207.

Murdock J. N., and W. K. Dodds. 2007. Linking benthic algal biomass to stream substratum topography. Journal of Phycology **43**:449-460.

Naumann, D. 2001. FT-infrared and FT-Raman spectroscopy in biomedical research, p. 323-377. In H.-U. Gremlich and B. Yan (ed.), Infrared and Raman spectroscopy of biological materials. Marcel Dekker, New York, N.Y.

National Research Council. 2008. Water implications of biofuels production in the United States. National Academies Press. Washington, DC.

Noguchi T., and M. Sugiura. 2003. Analysis of flash-induced FTIR difference spectra of the S-state cycle in the photosynthetic water-oxidizing complex by uniform N-15 and C-13 isotope labeling. Biochemistry **42**:6035-6042.

O'Brien J. M., W. K. Dodds, K. C. Wilson, J. N. Murdock, and J. Eichmiller. 2007. The saturation of N cycling in Central Plains streams: N-15 experiments across a broad gradient of nitrate concentrations. Biogeochemistry **84**:31-49.

O'Brien J. M., and W. K. Dodds. 2008. Ammonium uptake and mineralization in prairie streams: chamber incubation and short-term nutrient addition experiments. Freshwater Biology **53**:102-112.

Owens, M. 1974. Measurements on non-isolated natural communities in running waters. Pages 111-119 in Vollenweider, R. A. [Ed.]. A manual on methods for measuring primary production in aquatic environments. Blackwell Scientific, Oxford.

Parkhill K. L., J. S. Gulliver. 1999. Modeling the effect of light on whole-stream respiration. Ecological Modelling **117**:333-342.

Peterson C. G. 1996. Mechanisms of lotic microalgal colonization following space-clearing disturbances acting at different spatial scales. Oikos **77**:417-435.

Peterson C. G., and A. J. Boulton. 1999. Stream permanence influences microalgal food availability to grazing tadpoles in arid-zone springs. Oecologia **118**:340-352.

Poff N. L., and J. V. Ward. 1989. Implications of Streamflow Variability and Predictability for Lotic Community Structure - a Regional-Analysis of Streamflow Patterns. Canadian Journal of Fisheries and Aquatic Sciences **46**:1805-1818.

Poff N. L., and K. Nelson Baker. 1997. Habitat heterogeneity and algal-grazer interactions in streams: Explorations with a spatially explicit model. Journal of the North American Benthological Society **16**:263-276.

Power M. E., and W. J. Matthews. 1983. Algae-Grazing Minnows (Campostoma-Anomalum), Piscivorous Bass (Micropterus Spp), and the Distribution of Attached Algae in a Small Prairie-Margin Stream. Oecologia **60**:328-332.

Power M. E., A. J. Stewart, and W. J. Matthews. 1988. Grazer Control of Algae in an Ozark Mountain Stream - Effects of Short-Term Exclusion. Ecology **69**:1894-1898.

Power M. E., R. J. Stout, C. E. Cushing, P. P. Harper, F. R. Hauer, W. J. Matthews, P. B. Moyle, B. Statzner, and I. R. W. Debadgen. 1988. Biotic and Abiotic Controls in River and Stream Communities. Journal of the North American Benthological Society **7**:456-479.

Power M. E. 1990. Effects of fish in river food webs. Science **250**:811-814.

Power M. E., M.S. Parker, and W.E. Dietrich. 2008. Seasonal reassembly of a river food web: Floods, droughts, and impacts of fish, Ecological Monographs **78**:263-282.

Pringle C. M., and T. Hamazaki. 1997. Effects of fishes on algal response to storms in a tropical stream. Ecology **78**:2432-2442.

Quinn J. M., C. W. Hickey, and W. Linklater. 1996. Hydraulic influences on periphyton and benthic macroinvertebrates: Simulating the effects of upstream bed roughness. Freshwater Biology **35**:301-309.

Rabeni C. F. 1996. Prairie legacies-fish and aquatic resources. Pages 111–124. in F. Samson and F. Knopf. [Eds.] Prairie Conservation. Island Press, Washington DC.

Resh, V. H., A. V. Brown, A. P. Covich, M. E. Gurtz, H. W. Li, G. W. Minshall, S. R. Reice, A. L. Sheldon, J. B. Wallace, and R. C. Wissmar. 1988. The role of disturbance in stream ecology. Journal of the North American Benthological Society **7**:433-455.

Roberts S., S. Sabater, and J. Beardall. 2004. Benthic microalgal colonization in streams of differing riparian cover and light availability. Journal of Phycology **40**:1004-1012.

Robson B. J., and L. A. Barmuta. 1998. The effect of two scales of habitat architecture on benthic grazing in a river. Freshwater Biology **39**:207-220.

Robson B. J., and T. G. Matthews. 2004. Drought refuges affect algal recolonization in intermittent streams. River Research and Applications **20**:753-763.

Roll S. K., S. Diehl, and S. D. Cooper. 2005. Effects of grazer immigration and nutrient enrichment on an open algae-grazer system. Oikos **108**:386-400.

Romani A. M., and S. Sabater. 1997. Metabolism recovery of a stromatolitic biofilm after drought in a Mediterranean stream. Archiv Fur Hydrobiologie **140**:261-271.

Royall, R.M. 1997. Statistical evidence: a likelihood paradigm. Chapman and Hall, New York.

Sabater S., H. Guasch, A. Romani, and I. Munoz. 2002. The effect of biological factors on the efficiency of river biofilms in improving water quality. Hydrobiologia **469**:149-156.

Sanson G. D., R. Stolk, and B. J. Downes. 1995. A New Method for Characterizing Surface-Roughness and Available Space in Biological-Systems. Functional Ecology **9**:127-135.

Sartory D. P., and J. U. Grobbelaar. 1984. Extraction of Chlorophyll-a from Fresh-Water Phytoplankton for Spectrophotometric Analysis. Hydrobiologia **114**:177-187.

Scardino A. J., E. Harvey, and R. De Nys. 2006. Testing attachment point theory: diatom attachment on microtextured polyimide biomimics. Biofouling **22**:55-60.

Schaefer J. 2001. Riffles as barriers to interpool movement by three cyprinids (*Notropis boops*, *Campostoma anomalum* and *Cyprinella venusta*). Freshwater Biology **46**:379–388.

Schindler D.E. 2007. Fish extinctions and ecosystem functioning in tropical ecosystems. Proceedings of the National Academy of Sciences of the United States of America **104**:5707-5708.

Sekar R., V. P. Venugopalan, K. K. Satpathy, K. V. K. Nair, and V. N. R. Rao. 2004. Laboratory studies on adhesion of microalgae to hard substrates. Hydrobiologia **512**:109-116.

Sigee D. C., A. Dean, E. Levado, and M. J. Tobin. 2002. Fourier-transform infrared spectroscopy of Pediastrum duplex: characterization of a micro-population isolated from a eutrophic lake. European Journal of Phycology **37**:19-26.

Smith V. H. 2003. Eutrophication of freshwater and coastal marine ecosystems - A global problem. Environmental Science and Pollution Research **10**:126-139.

Somsueb S., M. Ohno, and H. Kimura. 2001. Development of seaweed communities on suspended substrata with three slope angles. Journal of Applied Phycology **13**:109-115.

Stanley E. H., S. G. Fisher, and J. B. Jones. 2004. Effects of water loss on primary production: A landscape-scale model. Aquatic Sciences **66**:130-138.

Stasiak R. H. 2007. Southern Redbelly Dace (*Phoxinus erythrogaster*): a technical conservation assessment. USDA Forest Service, Rocky Mountain Region.

Stehfest K., J. Toepel, and C. Wilhelm. 2005. The application of micro-FTIR spectroscopy to analyze nutrient stress-related changes in biomass composition of phytoplankton algae. Plant Physiology and Biochemistry **43**:717-726.

Steinman A. D., and C. D. Mcintire. 1990. Recovery of Lotic Periphyton Communities After Disturbance. Environmental management **14**:589-604.

Steinman, A. D. 1992. Does an increase in irradiance influence benthic algae in a heavily-grazed woodland stream. Oecologia. **91**:163-70.

Steinman A. D., P. J. Mulholland, and W. R. Hill. 1992. Functional-Responses Associated with Growth Form in Stream Algae. Journal of the North American Benthological Society **11**:229-243.

Steinman, A. D. 1996. Effects of grazers on freshwater benthic algae. In Algal ecology: Freshwater benthic ecosystems. R. J. Stevenson, M. L. Bothwell, and R. L. Lowe [Eds.]. pp 341-373. Academic Press, San Diego.

Stevenson, R.J. 1996. An introduction to algal ecology in freshwater benthic habitats. In Algal Ecology: Freshwater benthic ecosystems. R.J. Stevenson, M.L. Bothwell, and R.L. Lowe. [Eds.]. pp. 3-30. Academic Press, San Diego.

Stevenson R. J. 1997. Scale-dependent determinants and consequences of benthic algal heterogeneity. Journal of the North American Benthological Society **16**:248-262.

Taniguchi H., and M. Tokeshi. 2004. Effects of habitat complexity on benthic assemblages in a variable environment. Freshwater Biology **49**:1164-1178.

Tank, J.L., and W. K. Dodds 2003. Nutrient limitation of epilithic and epixylic biofilms in 10 North American streams. Freshwater Biology **48**: 1031-1049.

Tank, J.L., M.J. Bernot, and E.J. Rosi-Marshall. 2006. Nitrogen limitation and uptake. In Methods in stream ecology, F.R. Hauer and G.A. Lamberti [Eds]. pp. 213-238. Academic Press. San Diego.

Taylor B. W., A. S. Flecker, and R. O. Hall. 2006. Loss of a harvested fish species disrupts carbon flow in a diverse tropical river. Science **313**:833-836.

Thomas S., E. E. Gaiser, and F. A. Tobias. 2006. Effects of shading on calcareous benthic periphyton in a short-hydroperiod oligotrophic wetland (Everglades, FL, USA). Hydrobiologia **569**:209-221.

Underwood G. J. C., R. G. Perkins, M. C. Consalvey, A. R. M. Hanlon, K. Oxborough, N. R. Baker, and D. M. Paterson. 2005. Patterns in microphytobenthic primary productivity: Species-specific variation in migratory rhythms and photosynthetic efficiency in mixed-species biofilms. Limnology and Oceanography **50**:755-767.

Vandermeulen H., and R. E. DeWreede. 1982. The influence of orientation of an artificial substrtae (transite) on settlement of marine organisms. Ophelia **21**:41-48.

Vanni, M. J. 2002. Nutrient cycling by animals in freshwater ecosystems. Annual Reviews in Ecology and Systematics **33**:341-370.

Vannote R. L., G. W. Minshall, K. W. Cummins, J. R. Sedell, and C. E. Cushing. 1980. River Continuum Concept. Canadian Journal of Fisheries and Aquatic Sciences **37**:130-137.

Vaughn C. C., F. P. Gelwick, and W. J. Matthews. 1993. Effects of Algivorous Minnows on Production of Grazing Stream Invertebrates. Oikos **66**:119-128.

Vogel, S. 1994. Life in moving fluids, 2nd ed. Princeton University Press.

Warren, M.L. Jr and M. G. Pardew. 1998. Road crossings as barriers to small-stream fish movement. Transactions of the American Fisheries Society **127**:637–644.

Watermann F., H. Hillebrand, G. Gerdes, W. E. Krumbein, and U. Sommer. 1999. Competition between benthic cyanobacteria and diatoms as influenced by different grain sizes and temperatures. Marine Ecology-Progress Series **187**:77-87.

Welschmeyer, N. A. 1995. Fluorometric analysis of chlorophyll a in the presence of chlorophyll b and pheopigments. Limnology and Oceanography **39**:1985–92.

Wetzel, R.G. 2001. Limnology, 3rd ed. Academic Press.

Whiles, M. R., K. R. Lips, C. M. Pringle, S. S. Kilham, R. Brenes, S. Connelly, J. C. Colon Gaud, M. Hunte-Brown, A. D. Huryn, C. Montgomery, S. Peterson. 2006. The consequences of amphibian population declines to the structure and function of Neotropical stream ecosystems. Frontiers in Ecology and the Environment **4**: 27-34.

Whitton B. A. 1970. Biology of Cladophora in Freshwaters. Water research **4**:457-476.

Wilson K. C. 2005. Hyporheic oxygen flux and substratum spatial heterogeneity: effects on whole-stream dynamics. Master Thesis. Kansas State University.

Winemiller K. O., J. V. Montoya, D. L. Roelke, C. A. Layman, and J. B. Cotner. 2006. Seasonally varying impact of detritivorous fishes on the benthic ecology of a tropical floodplain river. Journal of the North American Benthological Society **25**:250-262.

Worm B., H. K. Lotze, H. Hillebrand, and U. Sommer. 2002. Consumer versus resource control of species diversity and ecosystem functioning. Nature **417**:848-851.

Zimmer K. D., B. R. Herwig, and L. M. Laurich. 2006. Nutrient excretion by fish in wetland ecosystems and its potential to support algal production. Limnology and Oceanography **51**:197-207.

Appendix A - Supplemental material to Chapter 1

Table A-0-1. Macroinvertebrate mean biomass (mg dry mass m^{-2}) and standard deviations (SD) for the Kings Creek drought experiment.

		Week 3				Week 5				Week 9			
		Ungrazed		Grazed		Ungrazed		Grazed		Ungrazed		Grazed	
Taxon	Functional group	Mean	SD	Mean	SD	Mean	SD	Mean	SD	Mean	SD	Mean	SD
ANNELIDA													
Arachnida													
Hydracarina	predator	0.00	0.00	0.00	0.00	0.01	0.04	0.00	0.00	0.04	0.05	0.01	0.04
CRUSTACEA													
Cladocera	scraper	0.00	0.00	0.00	0.00	0.00	0.00	0.00	0.00	0.02	0.06	0.00	0.00
Bosmina sp.													
Copepoda													
Cyclopoida	collector-gather	0.12	0.13	0.02	0.05	0.27	0.42	0.20	0.29	0.07	0.10	0.00	0.00
Calanoida	collector-filter	0.00	0.00	0.00	0.00	0.00	0.00	0.03	0.10	0.00	0.00	0.00	0.00
Harpacticoida	scraper	0.06	0.05	0.01	0.02	0.21	0.30	0.09	0.10	0.00	0.00	0.00	0.00
Ostracoda	collector-gather	0.58	0.75	0.22	0.43	1.44	2.00	1.08	1.09	2.09	2.84	0.16	0.28
Decapoda													
Cambaridae	omnivorous	0.00	0.00	0.00	0.00	0.00	0.00	22.50	63.64	502.40	1421.00	939.87	2486.67
INSECTA													
Coleoptera													
Dytisicdae (larvae)	predator	0.00	0.00	0.00	0.00	0.00	0.00	0.00	0.00	0.00	0.00	6.07	16.07
Elmidae (larvae)	scraper	0.00	0.00	0.00	0.00	0.00	0.00	0.00	0.00	7.63	21.59	0.00	0.00
(adult)	scraper	0.00	0.00	0.00	0.00	24.79	70.11	0.00	0.00	24.79	70.11	0.00	0.00

Diptera													
Chironomidae													
Non-Tanypodinae	collector-gather	72.57	40.53	47.72	42.83	1510.72	1404.93	298.81	243.11	1138.45	896.08	530.48	606.02
Tanypodinae	predator	8.64	11.93	0.18	0.52	0.51	1.44	13.67	21.40	13.89	25.30	3.78	6.43
Pupae		0.00	0.00	0.00	0.00	15.15	32.26	3.07	7.60	10.07	16.47	0.00	0.00
Psychodidae													
Pericoma	collector-gather	0.00	0.00	0.00	0.00	0.00	0.00	0.00	0.00	0.00	0.00	1.76	4.66
Stratiomyidae													
Caloparyphus	collector-gather	4.92	13.92	0.00	0.00	0.00	0.00	0.00	0.00	0.00	0.00	0.00	0.00
Ephemeroptera													
Heptageniidae													
Stenonema	scraper	12.10	13.28	7.82	5.54	49.21	81.85	27.96	45.16	3533.13	2136.21	4854.85	2867.25
Plecoptera													
Perlidae													
Perlesta	predator	0.00	0.00	0.00	0.00	0.00	0.00	0.00	0.00	40.20	113.69	0.00	0.00
Trichoptera													
Helicopsychidae													
Helicopsyche	scraper	0.00	0.00	0.00	0.00	0.00	0.00	0.00	0.00	0.15	0.43	0.00	0.00
Hydroptilidae	scraper	0.00	0.00	0.00	0.00	0.00	0.00	0.00	0.00	0.00	0.00	0.63	1.68
Polycentripodidae	predator	210.74	596.07	2.96	8.39	142.37	282.75	102.24	145.54	115.07	197.66	99.33	124.73
MOLLUSCA													
Gastropoda													
Physidae	scraper	0.00	0.00	0.00	0.00	0.00	0.00	0.00	0.00	78.42	160.21	346.48	880.93
Planorbidae	scraper	1.40	3.96	0.00	0.00	0.00	0.00	0.00	0.00	0.00	0.00	0.00	0.00

Table A-0-2 Macroinvertebrate mean biomass (mg dry mass m^{-2}) and standard deviations (SD) for the mesocosm drought experiment.

		Day 18				Day 42			
		Fish		No fish		Fish		No fish	
Taxon	Functional group	Mean	SD	Mean	SD	Mean	SD	Mean	SD
ANNELIDA									
Oligochaeta	collector-gather	0.02	0.05	0.01	0.02	8.44	15.51	4.11	3.34
ARACHNIDA									
Hydracarina	predator	0.01	0.03	0.00	0.00	0.00	0.00	0.05	0.11
COLLEMBOLA									
Sminthuridae	collector-gather	0.08	0.16	0.00	0.00	0.00	0.00	0.00	0.00
CRUSTACEA									
Cladocera									
Bosmina sp.	collector-filter	19.42	25.38	42.69	26.72	38.72	23.63	28.29	12.39
Copepoda	collector-gather	1.17	2.34	5.28	3.52	0.00	0.00	1.17	2.34
Ostracoda	collector-gather	196.24	125.27	113.76	36.34	505.61	152.24	702.80	238.94
INSECTA									
Anispotera									
Libellulidae	predator	6.94	8.51	8.93	7.13	55.01	66.70	131.44	190.52
Ephemeroptera									
Baetidae	scraper	1.12	1.91	40.03	80.06	28.16	48.05	3.25	6.50
Diptera									
Ceratopogonidae	predator	0.00	0.00	0.00	0.00	0.56	1.13	0.00	0.00
Chironomidae									
Non-Tanypodinae	collector-gather	255.74	216.79	932.91	421.65	515.58	317.22	967.01	408.94
Tanypodinae	predator	0.76	1.05	21.06	41.04	0.96	1.14	1.76	3.15
Pupae		0.07	0.15	7.72	7.82	0.37	0.74	1.68	1.14
MOLLUSCA									
Gastropoda									
Physidae	scraper	29.23	58.46	0.39	0.78	50.75	101.51	25.79	51.57

Appendix B - Permission to include Chapter 3

Figure B-0-1 Email correspondence with Blackwell Publishing to include a published manuscript (Chapter 3) in dissertation

Dear Justin Murdock,

Thank you for your email request. Permission is granted for you to use the material below for your thesis/dissertation subject to the usual acknowledgements and on the understanding that you will reapply for permission if you wish to distribute or publish your thesis/dissertation commercially.

Best wishes,

Lina Kopicaite
Permissions Assistant
Wiley-Blackwell
PO Box 805
9600 Garsington Road
Oxford OX4 2DQ
UK
Tel: +44 (0) 1865 476158
Fax: +44 (0) 1865 471158
Email: lkopicai@wiley.com

-----Original Message-----
From: Justin Murdock [mailto:murdockj@ksu.edu]
Sent: 16 July 2008 17:26
To: Journals Rights
Subject: permission to use article

July 16, 2008

Blackwell Publishing
9600 Garsington Road
Oxford OX4 2DQ
UK

To Whom It May Concern:

I am a doctoral student at Kansas State University and am writing for permission to include in my dissertation, all of the material from Journal of Phycology, LINKING BENTHIC ALGAL BIOMASS TO STREAM SUBSTRATUM TOPOGRAPHY by Justin N. Murdock and Walter K. Dodds. Issue 43, pages 449–460, 2007.

My dissertation will be made available online through the K-State Research Exchange (http://krex.ksu.edu). In addition, my dissertation will be microfilmed by UMI/ProQuest Information and Learning), and copies of the dissertation will be available for purchase.

Please supply a signed letter granting me permission to use the work.

You can email, mail or fax the permission to

murdockj@ksu.edu,

104 Ackert Hall
Division of Biology
Kansas State University
Manhattan, Kansas USA 66506

Fax- 785-532-6653

Thank you for your assistance.

Sincerely,

Justin N. Murdock

104 Ackert Hall
Division of Biology
Kansas State University
785-236-9651
murdockj@ksu.edu

Appendix C - Permission to include Chapter 4

Figure C-0-2 Email correspondence with Elsevier to include a published manuscript (Chapter 4) in dissertation

Dear Mr Murdock

We hereby grant you permission to reprint the material detailed below at no charge in your thesis, in print and on the K-State Research Exchange web site subject to the following conditions:

1. If any part of the material to be used (for example, figures) has appeared in our publication with credit or acknowledgement to another source, permission must also be sought from that source. If such permission is not obtained then that material may not be included in your publication/copies.

2. Suitable acknowledgment to the source must be made, either as a footnote or in a reference list at the end of your publication, as follows:

   "This article was published in Publication title, Vol number, Author(s), Title of article, Page Nos, Copyright Elsevier (or appropriate Society name) (Year)."

3. Your thesis may be submitted to your institution in either print or electronic form.

4. Reproduction of this material is confined to the purpose for which permission is hereby given.

5. This permission is granted for non-exclusive world English rights only. For other languages please reapply separately for each one required. Permission excludes use in an electronic form. Should you have a specific electronic project in mind please reapply for permission.

6. This includes permission for UMI to supply single copies, on demand, of the complete thesis. Should your thesis be published commercially, please reapply for permission.

Yours sincerely

Steph Smith
Rights Assistant, Elsevier Ltd
The Boulevard
Langford Lane
Kidlington Oxford
OX5 1GB

-----Original Message-----
From: murdockj@ksu.edu [mailto:murdockj@ksu.edu]
Sent: 16 July 2008 17:50
To: Rights and Permissions (ELS)
Subject: Obtain Permission

This Email was sent from the Elsevier Corporate Web Site and is related to Obtain Permission form:

Product: Customer Support
Component: Obtain Permission
Web server: http://www.elsevier.com
IP address: 195.212.150.72
Client: Mozilla/4.0 (compatible; MSIE 7.0; Windows NT 5.1; .NET CLR 1.1.4322; InfoPath.2)
Invoked from:
http://www.elsevier.com/wps/find/obtainpermissionform.cws_home?isSubmitted=yes&navigateXmlFileName=/store/scstargets/prd53/act/framework_support/obtainpermission.xml
Request From:
Graduate Research Assistant Justin N. Murdock Kansas State University
104 Ackert Hall, Division of Biology
66506
Manhattan, Kansas
United States
Contact Details:
Telephone: 785-236-9651
Fax: 785-532-6653
Email Address: murdockj@ksu.edu
To use the following material:
ISSN/ISBN:
Title: Vibrational Spectroscopy
Author(s): JN. Murdock, WK. Dodds, DL. Wetzel
Volume: in press
Issue: in press
Year: 2008
Pages: xxxx - xxxx
Article title: Subcellular localized chemical imaging of benthic
How much of the requested material is to be used: entire article will be used
Are you the author: Yes
Author at institute: Yes
How/where will the requested material be used:

I am a doctoral student at Kansas State University and am writing for permission to include in my dissertation, all of the material from the article Subcellular localized chemical imaging of benthic algal nutritional content via HgCdTe array FT-IR which is currently in press in the Journal Vibrational Spectroscopy.

My dissertation will be made available online through the K-State Research Exchange (http://krex.ksu.edu). In addition, my dissertation will be microfilmed by UMI/ProQuest Information and Learning), and copies of the dissertation will be available for purchase.

For further info regarding this automatic email, please contact:

WEB APPLICATIONS TEAM (esweb.admin@elsevier.co.uk)
This email is from Elsevier Limited, a company registered in England and Wales with company number 1982084, whose registered office is The Boulevard, Langford Lane, Kidlington, Oxford, OX5 1GB, United Kingdom.